



Title: Fatigue analysis of flexible pipes using alternative element types and bend stiffener data	Delivered: June 15ht, 2011
	Availability:
Student: Minghao Chen	Number of pages: 90

Abstract:

The flexible pipe is a vital part of a floating production system. The lifetime of a flexible riser system is crucial for the Health Safety and Environment (HSE) management. As a result of this, it is very necessary to carry out research on the lifetime of flexible pipe. In this thesis we formalized analysis on flexible pipes, utilizing the finite element analysis software BFLEX 2010, developed by MARINTEK.

Chapter 1 describes basic knowledge about flexible pipe and relevant facilities. Chapter 2 gives more information about failure mode of flexible pipe and flexible pipe system. The design criteria and design flow chart is included in this part. Chapter 3 demonstrates the concepts in BFLEX 2010 and its basic principles. For BFLEX 2010, different modeling methods are available for the flexible pipes.

In Chapter 4, the basic properties about the flexible pipe which is used in this thesis are introduced. The BFLEX model in this thesis is included in this chapter, too. In Chapter 5, two specified load cases are analyzed by BFLEX 2010 with different bending formulations for tendons. Fatigue damage on tensile armour layers and longitudinal stress in pressure armour is given. The fatigue damage is given in the form of Miner Sum. The comparison between different bending formulations is made. In Chapter 6, Comparison between calculation results and testing data is made. At the same time, correlation study about fatigue damage on tensile armour layer is finished. This thesis focuses on the effect of gap between flexible pipe and bending stiffener, and the influence of the E-modulus of bending stiffener.

Keyword:

Flexible pipe, BFLEX2010, Fenite Element Mechod, Fatige damage

Advisor:

Svein Sævik

THESIS WORK SPRING 2011

for

Stud. tech. Minghao Chen

Fatigue analysis of flexible pipes using alternative element types and bend stiffener data

Utmatningsanalyse av fleksible stigerør med bruk av alternative elementtyper og bøyestiverdata.

The flexible riser is a vital part of a floating production system. In order to predict the riser lifetime for given environmental conditions, different analysis procedures may be applied, however, in most cases including the three fundamental steps:

1. Global dynamic analysis of the riser system in order to find the global response quantities in the form of time series of tension, curvature and end angles. This is obtained by a global analysis software such as the Marintek software RIFLEX.
2. Transform the global response quantities into into time series of stresses using a local analysis tool such as the Marintek software BFLEX.
3. Group the time series of stress into classes of stress ranges and combine these with fatigue S-N data to obtain the Miner sum, i.e. the accumulated fatigue damage throughout the lifetime of the riser.

This project work focus on investigating the effect of applying different modelling assumptions with regard to the local stress models. The project work is to be carried out as follows:

- 1) Literature study, flexible riser technology in general, mechanical behaviour, failure modes and design criteria and methods for local stress analysis of flexible pipes including non-linear finite element techniques used to perform both global an local response analysis.
- 2) Familiarize with the Marintek software BFLEX.
- 3) For a given cross-section, establish two Bflex models, all representing the floater top connection point. The models are identical with respect to geometry and cross-section and shall include 10-15 m length and a bend stiffener section. The differences between them are:
 - i) Model 1 – the bi-linear moment behaviour is represented by beam elements.
 - ii) Model 2 – the bi-linear moment behaviour is represented by sandwich beam elements
- 4) For a case with given pressure and temperature and where the global responses are given in terms of classes of mean tension, tension range, mean end angle and end angle ranges, perform stress and fatigue analysis using the established models.
- 5) Based on measured stresses of the outer tensile armour perform correlation studies with respect to the static stress level as well as the friction, bending and total stress ranges.

- 6) Based on a given distribution of end angle and tension use the models to perform parameter studies of the fatigue damage by varying the following parameters: E-modulus/the stress strain curves at elevated temperatures and the size of the gap between the BS and the pipe.
- 7) Conclusions and recommendations for further work

The work scope may prove to be larger than initially anticipated. Subject to approval from the supervisors, topics may be deleted from the list above or reduced in extent.

In the thesis the candidate shall present his personal contribution to the resolution of problems within the scope of the thesis work

Theories and conclusions should be based on mathematical derivations and/or logic reasoning identifying the various steps in the deduction.

The candidate should utilise the existing possibilities for obtaining relevant literature.

Thesis format

The thesis should be organised in a rational manner to give a clear exposition of results, assessments, and conclusions. The text should be brief and to the point, with a clear language. Telegraphic language should be avoided.

The thesis shall contain the following elements: A text defining the scope, preface, list of contents, summary, main body of thesis, conclusions with recommendations for further work, list of symbols and acronyms, references and (optional) appendices. All figures, tables and equations shall be numerated.

The supervisors may require that the candidate, in an early stage of the work, presents a written plan for the completion of the work.

The original contribution of the candidate and material taken from other sources shall be clearly defined. Work from other sources shall be properly referenced using an acknowledged referencing system.

The report shall be submitted in two copies:

- Signed by the candidate
- The text defining the scope included
- In bound volume(s)
- Drawings and/or computer prints which cannot be bound should be organised in a separate folder.

Ownership

NTNU has according to the present rules the ownership of the thesis. Any use of the thesis has to be approved by NTNU (or external partner when this applies). The department has the right to use the thesis as if the work was carried out by a NTNU employee, if nothing else has been agreed in advance.

Thesis supervisors
Prof. Svein Sævik

Deadline: June 14th, 2011

Trondheim, January 20, 2011

Svein Sævik

Candidate - date and signature:

PREFACE

This thesis is for the Master of Science degree in Norwegian University of Science and Technology (NTNU). The Duration of thesis work is about 5 months.

Through this thesis work, basic concepts of flexible pipes are introduced. Plenty of Finite Element Analysis with BFLEX 2010 is finished. The thesis compares the calculated results by BFLEX with the testing data.

At the same time, this thesis focuses on the fatigue performance of tensile armour layer in flexible pipes. The correlation studies between fatigue damage on tensile armour layer and different parameters are finished in this thesis.

I would like to express my sincere gratitude to my supervisor Svein Sævik. Without his advice and unique support this thesis would never had become a reality. Further I would like to thank Naiquan Ye in MARINTEK for this help on BFLEX.

Minghao Chen

June 14th, 2011

Trondheim, Norway

ABSTRACT

The flexible pipe is a vital part of a floating production system. The lifetime of a flexible riser system is crucial for the Health Safety and Environment (HSE) management. As a result of this, it is very necessary to carry out research on the lifetime of flexible pipe. In this thesis we formalized analysis on flexible pipes, utilizing the finite element analysis software BFLEX 2010, developed by MARINTEK.

Chapter 1 describes basic knowledge about flexible pipe and relevant facilities. Chapter 2 gives more information about failure mode of flexible pipe and flexible pipe system. The design criteria and design flow chart is included in this part. Chapter 3 demonstrates the concepts in BFLEX 2010 and its basic principles. For BFLEX 2010, different modeling methods are available for the flexible pipes.

In Chapter 4, the basic properties about the flexible pipe which is used in this thesis are introduced. The BFLEX model in this thesis is included in this chapter, too. In Chapter 5, two specified load cases are analyzed by BFLEX 2010 with different bending formulations for tendons. Fatigue damage on tensile armour layers and longitudinal stress in pressure armour is given. The fatigue damage is given in the form of Miner Sum. The comparison between different bending formulations is made. In Chapter 6, Comparison between calculation results and testing data is made. At the same time, correlation study about fatigue damage on tensile armour layer is finished. This thesis focuses on the effect of gap between flexible pipe and bending stiffener, and the influence of the E-modulus of bending stiffener.

Figure list

- Figure 1.1, Floating Production Systems (FPS)
- Figure 1.2, typical cross section of an unbonded flexible pipe
- Figure 1.3, typical profile of the carcass
- Figure 1.4, cross section of Zeta- shaped pressure armour
- Figure 1.5, pipe wall structure, more details available
- Figure 1.6, the schematic and picture of bending stiffener
- Figure 1.7, the schematic of Bell Mouth
- Figure 2.1, main failure tree for flexible pipes
- Figure 2.2, Possible sequences of failure in case of erosion/corrosion of a Coflexip pipe, from FPS2000 Report 2.3-3.
- Figure 2.3, shear stress on the cross section of Zeta pressure armour (red part refers to areas with high shear stress)
- Figure 2.4, fixture for cross-wire fatigue testing of pressure armour.
- Figure 2.5, Fatigue strength criterion for tensile armour of nonbonded pipe, from Feret and Bournazel (1986)
- Figure 2.6, bending behaviour of nonbonded pipe
- Figure 2.7, fatigue design procedure for dynamic risers, about 20 year ago
- Figure 2.8, Schematic of Procedure for fatigue design of flexible pipes in 2000
- Figure 3.1, a BFLEX model. The white part is tensile armour
- Figure 3.2, the boundary model , which gives transverse cross sectional stress result
- Figure 3.3, the PFLEX model, which gives bending stress distribution of pressure armour
- Figure 3.4, BFLEX 2010 software system
- Figure 3.5, Loxodromic and Geodesic helical path along bent cylinder
- Figure 3.6, the two-bar systems
- Figure 3.7, Load-deflection characteristics of two-bar system
- Figure 4.1, shape of Zeta-pressure armour
- Figure 4.2, Shape of carcass (made from a thin steel plate with dimension of 1.4*55 mm)
- Figure 4.3, the Young's Modulus of polyurethane (PU) of bending stiffener
- Figure 4.4, testing facilities in laboratory
- Figure 4.5, the details about test facilities (test rig)
- Figure 4.6, model in BFLEX and the boundary conditions
- Figure 4.7, cross section for ITCODE0 and ITCODE31
- Figure 4.8, real flexible pipe and the model that is used in BFLEX 2010
- Figure 4.9, the model in BFLEX 2010
- Figure 5.1, transverse curvature bending and normal curvature bending
- Figure 5.2, the distribution of curvature at each load step, LC1, ITCODE0
- Figure 5.3, fatigue on the cross section of zeta pressure armour and flat spiral (LC1, ITCODE 0)
- Figure 5.4, distribution of total longitudinal stress, LC1, ITCODE 0
- Figure 5.5, Fatigue damage for 4 tensile armour layers, LC1, ITCODE 0
- Figure 5.6, the distribution of curvature at each load step, LC2, ITCODE0
- Figure 5.7, fatigue on the cross sections of zeta pressure armour and flat spiral (LC2, ITCODE 0)
- Figure 5.8, distribution of total longitudinal stress (LC2, ITCODE 0)

- Figure 5.9, Fatigue damage for 4 tensile armour layers, LC2, ITCODE 0
- Figure 5.10, the distribution of curvature at each load step, LC1, ITCODE31
- Figure 5.11, fatigue on the cross sections of zeta pressure armour & flat spiral (LC1, ITCODE 31)
- Figure 5.12, distribution of total longitudinal stress (LC1, ITCODE 31)
- Figure 5.13, Fatigue damage for 4 tensile armour layers, LC1, ITCODE 31
- Figure 5.14, the distribution of curvature at each load step, LC2, ITCODE31
- Figure 5.15, fatigue on the cross sections of zeta pressure armour & flat spiral (LC2, ITCODE 31)
- Figure 5.16, distribution of total longitudinal stress (LC2, ITCODE 31)
- Figure 5.17, Fatigue damage for 4 tensile armour layers, LC2, ITCODE 31
- Figure 5.18, fatigue damage, LC1+LC2
- Figure 6.1, the strain gauges mounted on flexible pipe.
- Figure 6.2, configuration of strain gauges
- Figure 6.3, the strain gauges on tensile tendons
- Figure 6.4, COMPARISION, LC1, ITCODE 0, stations 1-9
- Figure 6.5, COMPARISION, LC1, ITCODE 0, stations 10-20
- Figure 6.6, COMPARISION, LC1, ITCODE 31, stations 1-9
- Figure 6.7, COMPARISION, LC1, ITCODE 31, stations 10-20
- Figure 6.8, COMPARISION, LC3, ITCODE 0, stations 1-9
- Figure 6.9, COMPARISION, LC3, ITCODE 0, stations 10-20
- Figure 6.10, COMPARISION, LC3, ITCODE 31, stations 1-9
- Figure 6.11, COMPARISION, LC3, ITCODE 31, stations 10-20
- Figure 6.12, E-modulus for correlation studies
- Figure 6.13, correlation studies on E-modulus, LC1, ITCODE0
- Figure 6.14, correlation studies on E-modulus, LC2, ITCODE0
- Figure 6.15, correlation studies on E-modulus, LC1, ITCODE31
- Figure 6.16, correlation studies on E-modulus, LC2, ITCODE31
- Figure 6.17, correlation studies on RD, LC1
- Figure 6.18, the ideal relationship between fatigue damage and GAP



CONTENTS

Chapter 1. Flexible pipe technology in offshore industry	1
1.1 General remarks	1
1.2 Flexible Pipe Cross Section	3
1.2.1 Interlocked carcass	3
1.2.2 Internal pressure sheath.....	4
1.2.3 Zeta pressure spiral / flat spiral.....	5
1.2.4 Tensile armour.....	6
1.2.5 External thermal plastic layer / outer sheath.....	6
1.3 Other Layers and Configurations	7
1.3.1 End fitting facilities/ annulus venting facilities	7
1.3.2 Bending stiffener and bell mouth.....	7
1.3.3 Annulus Venting System	8
Chapter 2. Failure mode, Mechanical Properties and Design principles	10
2.1 Failure modes of flexible pipes.....	10
2.2 Failure Modes of layers	12
2.3 Service lifetime	15
2.4 Mechanical properties of bending.....	16
2.5 The design process of flexible pipes & recommendations	17
Chapter 3. BFLEX2010 and non-linear Finite Element Analysis	20
3.1 Introductions	20
3.2 The structure of BFLEX 2010 software.....	20
3.3 Formulations of tensile armour model.....	23
3.4 Non-linear Finite Element Method approach	25
Chapter 4. Fatigue assessment of flexible riser	28
4.1 Introductions	28
4.2 description of flexible pipe data.....	28
4.2.1 The pipe data sheet.....	28
4.2.2 Material properties	30
4.2.3 Mechanical properties and loading condition.....	31
4.2.4 Load cases	31
4.3 BFLEX Model	32
4.3.1 The test configuration	32
4.3.2 the Finite Element Model in BFLEX.....	33
4.3.3 Elements Distribution in ITCODE 0 case and ITCODE 31 case.	34
Chapter 5. BFLEX analysis	39
5.1 Introductions	39
5.2 ITCODE 0 CASE.....	41
5.2.1 Load Case 1, ITCODE 0.....	41
5.2.2 Load Case 2, ITCODE 0.....	45
5.3 ITCODE 31 CASE.....	48
5.3.1 Load Case 1, ITCODE 31	48



NTNU Trondheim

Norges teknisk-naturvitenskapelige universitet

Institutt for marin teknikk

5.3.2 Load Case 2, ITCODE 31	51
5.4 Combination of LC1 and LC 2	54
5.5 Comparison of fatigue damage on tensile armour	55
Chapter 6. Comparison between BFLEX and measured data / correlation studies	56
6.1 Comparison between BFLEX calculation and strain gauge measurement....	56
6.1.1 Configuration of strain gauges.....	56
6.1.2 Strain gauge test program	59
6.1.3 The comparison between BFLEX data and test results	60
6.2 Correlation studies	69
6.2.1 Correlation between E-modulus of bending stiffener and fatigue damage	69
6.2.2 Correlation studies between Gap and fatigue damage.....	72
6.3 Conclusions.....	74
Appendix1. BFLEX input file, ITCODE0, LC1.....	75
Appendix 2. BFLEX input file, LC1, ITCODE 31.....	83
Reference	90

Chapter 1. Flexible pipe technology in offshore industry

1.1 General remarks

Flexible pipes traces its origin to pioneering work carried out in the late 1970s. It was used in the relatively benign weather conditions in the beginning, such as the Far East, offshore fields in Brazil and the Mediterranean. But due to its rapid development, flexible pipe and risers are utilized in various fields in North Sea, and are also gaining popularity in the Gulf of Mexico.

Through 1990s, the concept of Floating Production Systems (FPS) was developed and implemented as a very cost effective way of exploiting offshore oil and gas resources. When the offshore industry approaches deeper water, most of time, there are no alternatives. For marginal fields, the engineering cost may be significantly reduced by using FPS instead of traditional fixed platforms. A floating production system with flexible pipe system is shown in figure 1.1.

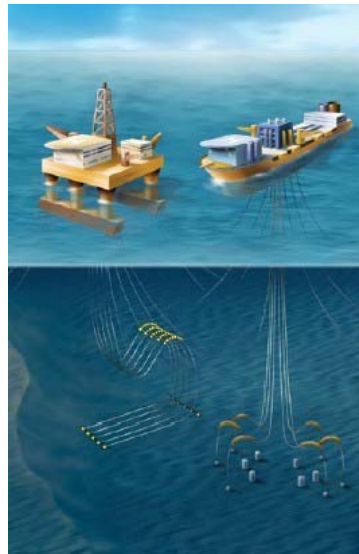


Figure 1.1, Floating Production Systems (FPS)

The flexible pipe system plays a very important and dominant role in FPS. If the flexible pipe fails, the whole system would fail. Flexible pipes connected to the top floater could allow large floater motions induced by wind, current and wave. For most of the cases, the flexible pipe in FPS is unbonded flexible pipe, which is a complex structure, made of a composite unbonded pipe wall that allows large variations in curvature.

Here are some of the advantages of flexible pipes:

- ◆ Purpose designed product optimized for each specific application
- ◆ A design that combines the flexibility of a polymer pipe with the strength and weight of a steel pipe
- ◆ Minimization of external corrosion effects owing to encapsulation of the steel armour inside a continuous polymer outer sheath
- ◆ Accommodate misalignments during installation and tie-in operations
- ◆ Diverless installation is possible - no metrology required
- ◆ Load-out and installation safer, faster and cheaper than any other pipe application
- ◆ Retrievability and reusability for alternative application thus enhancing the overall field development economics and preserving the environment
- ◆ Excellent inherent thermal insulation properties

The most significant difference between flexible pipe and other steel pipe is its low relative bending to axial stress. This is achieved through the use of a number of layers of different material in the pipe wall fabrication. These layers are capable of slipping past each other when they are under the influence of external and internal loads. Hence this characteristic gives a flexible pipe its property of a low bending stiffness.

In this chapter, the relevant knowledge about Floating Production Systems (FPS) and profile of flexible pipe is introduced, especially the layers in wall structure of flexible pipes.

1.2 Flexible Pipe Cross Section

We have two types of flexible pipes in offshore industry: one is bonded flexible pipe, the other one is unbonded flexible pipes. The first kind of flexible pipes are only used in short sections, such as the jumpers. In this thesis, we focus on the latter one, the unbonded flexible pipes. As mentioned, the flexible pipes have a low relative bending relative to axial stiffness. This is totally decided by its wall structures. Figure 1.2 shows the intact cross section of one flexible pipes.

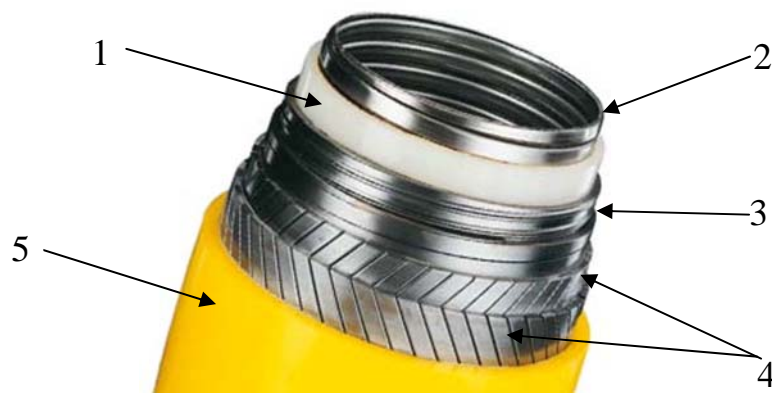


Figure 1.2, typical cross section of an unbonded flexible pipe

Figure 1.2 clearly identifies the main components of the flexible pipe cross section. The space between internal polymer sheath and the external polymer sheath is called pipe annulus.

The configuration of cross section for each flexible pipe may be a little different due to different working condition and operation requirements. Because flexible pipe is a purpose designed product, which could be optimized for each specific application. But they have some common properties and layers. The 5 layers shown in figure 1.2 are as follows:

1. Interlocked stainless steel carcass
2. Internal pressure sheath
3. Zeta spiral (pressure armour)
4. Tensile armour (double cross wound armours)
5. Outer thermoplastic sheath

1.2.1 Interlocked carcass

The carcass is the innermost layer of a flexible pipe, which is the only metallic

component that is in direct contact with the fluid in the bore. It is made of a stainless steel flat strip that is formed into an interlocking profile, which is shown in figure 1.3. The fluid in the bore is free to flow through the carcass. As a result of this, the material of carcass must be corrosion-resistant to the bore fluid.



Figure 1.3, typical profile of the carcass

The function of carcass layer is to provide resistance strength against the external hydrostatic pressure. The pressure of fluid in the bore do not have significant mechanical loading on the carcass, because the carcass structure is merged in the fluid. When there is a damage of the outer sheath, the external seawater will be acting directly on the layer. A basic design criterion is to make sure that the carcass is safe when it is subjected to the external pressure at maximum water depth.

At the same time, the carcass supplies the protection against pigging tools and abrasive particles. During the installation operations, the crushing loads could be resisted by carcass, too.

The collapse of carcass layer could also be caused by the release of gas in the liner. For the hydrocarbon-carrying flexible pipes, the gas may diffuse from the inner pipe bore into the annulus, and could be stored in the annulus of flexible pipes. In case of shut-down of well, the pressure of the gas in the annulus could cause the collapse of carcass, due to the subsequent depressurization of bore. The carcass is not designed for this emergency. So this must be avoided in design process and operation phase.

1.2.2 Internal pressure sheath

The pressure sheath layer is an extruded polymer layer which provides internal fluid integrity. So it is used as sealing component, made from a thermoplastic by extrusion over the carcass. The main function is to ensure integrity and sealing. The fluid temperature in the bore is guaranteed by this layer.

For some special applications, we could see a multi-layer liner is used here, with the sacrificial layers on the inside and/or the outside of the sealing layer. The motivation for the sacrificial layers is to supply protection against the metallic components.

The internal pressure is not made from metallic materials. There are three kind of materials that is used. They are as follows:

- ◆ Polyamide (nylon), PA11 or PA 22
- ◆ Poly vinylidene fluoride (PVDF)

- ◆ High density polyethylene (HDPE) and cross-linked polyethylene (XLPE)

The manufacturer of flexible pipes will not only use only one type of materials mentioned above, the final polymer sheath would be made from the combination of different materials. For example, the trademark of Rilsan® is the combination of PA11 and some plasticizer, owned by Atofina.

The polymer sheath layer thickness is decided by various parameters, such as the inner bore fluid temperature, composition and inner bore pressure. Most of the thicknesses are between 5- 8 mm, but flexible pipes with up to 13 mm of internal polymer sheath have been manufactured.

1.2.3 Zeta pressure spiral / flat spiral

The main role of pressure armour is to withstand the stress in the hoop direction which is caused by the internal fluid pressure.

The Zeta pressure armour is made of Z-shaped interlocking wires, which is shown in figure 1.4. These wire profiles allow bending flexibility and control the gap between the armour wires to prevent internal sheath extrusion through the armour layer.

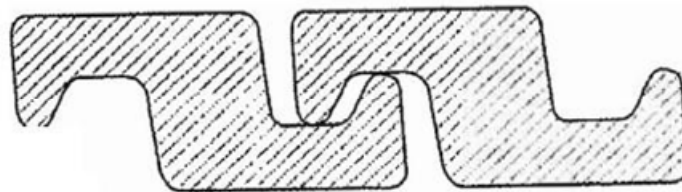


Figure 1.4, cross section of Zeta- shaped pressure armour

At the same time, it will also provide resistance against external pressure and crushing effects from the tensile armour. In order to best resist the hoop stress in the pipe wall, the pressure armour is wound at an angle of about 89 degree to the pipe longitudinal axis. The material of pressure armour is rolled carbon steel with tensile strength in the range of 700 – 900 Mpa. Other different profiles of pressure armour are also used in engineering, such as C-clip, Theta shaped pressure armour, X-LiNkt and K-LiNKt, etc.

In case of need, in order to satisfy certain operation requirements in engineering, the zeta layer may be reinforced by a flat steel spiral. This kind of cross-section is shown in figure 1.5. For this pipe wall structure, more details are available.

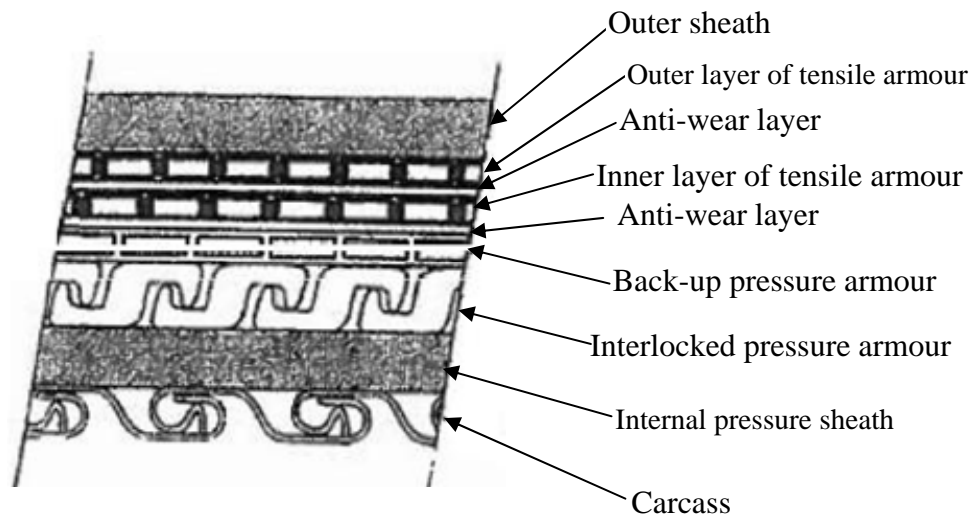


Figure 1.5, pipe wall structure, more details available

1.2.4 Tensile armour

The tensile armour layers are always cross-wound in pairs. As its names implies, the tensile armour layers provide resistance to axial loads and torsion. Most of time, the tensile armor layers are made of flat rectangular wires, which are laid at about 30° - 55° to the longitudinal axis along the flexible riser. At the connection point between flexible pipe and floating vessels, the whole weight of all pipe layers is supported by the tensile armour. This weight is transformed to the vessel or platform on the sea surface.

In order to reduce the friction and wear effect, lubrication or thermoplastic antifricition is also used between tensile armours. High tension in a deepwater riser may require the use of four tensile armor layers, rather than just two. In production of flexible risers, the tensile armour are usually made from high strength carbon steel.

In this thesis, we focus on the lifetime and fatigue damage of the tensile armour.

1.2.5 External thermal plastic layer / outer sheath

This is a layer that we could see directly from the outside of flexible riser. It is also called outer sheath. The function of the external thermoplastic layer is to protect the metallic layers against corrosion, abrasion and bind the underlying armour. Also it could separate the steel components and the sea water. It is totally made from non-metallic materials, could be made of the same materials as the internal polymer sheath. For this reason, we do not focus on the fatigue performance of this layer. In this thesis, we do not focus on the fatigue performance of this layer.

1.3 Other Layers and Configurations

The main components in a cross section of flexible pipes are mentioned from section 1.2.1 to section 1.2.5. But the flexible pipes could be different with each other, due to the different operation fields. There are still some other layers, just as figure 1.5 shows. We could see there are several anti-wear layers in figure 1.5, such as the anti-wear layer between two tensile armour layers, and the anti-wear layer between inner layer of tensile armour and back-up pressure armour.

The purpose of anti-wear layer is to reduce friction and hence wear of the wire layers when they rub past each other as the pipe flexes due to external loads. Anti-wear tapes can also be used to make sure that the armor layers maintain their wound shape. These tapes ensure that the wires do not twist out of their pre-set configuration.

But there exists no anti-wear layer between zeta pressure armour and back-up pressure armour (flat spiral). This is due to the large contact pressure and shear force between these two layers. The anti-wear material could not sustain such an interaction. In fact, if we put the anti-wear layers between them, it would crack very fast.

1.3.1 End fitting facilities/ annulus venting facilities

End fitting facilities is a very important component in the global flexible pipe design process. In this thesis, the research objective is one flexible pipe segment which is connected to the floating vessels/ platforms. This segment is subjected to much more loading than other ones at other locations. The most critical location for fatigue damage is usually at this location, it decides the lifetime of the whole flexible pipe.

The function of ending fitting facilities is to transfer the load sustained by the flexible pipe armour layers onto the floating vessels, also guarantee the sealing of the polymer fluid barrier layers.

1.3.2 Bending stiffener and bell mouth

The most severe location for fatigue damage in the flexible pipes is usually in the top hang off region. At this location, the flexible pipe is protected from over bending by either a bending stiffener or a bell mouth. The exact profiles of these two facilities are shown in figure 1.6 and figure 1.7.

Not only the bending stiffener could provide a better engineering performance under large motion conditions, but also it is able to provide a moment distribution transition between flexible riser and its connection point to the platform. In figure 6, in this operation condition, the flexible riser is connected to the platform by a segment of bending stiffener with length about 10 meters.

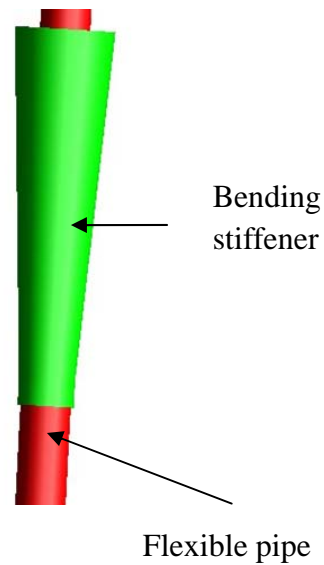
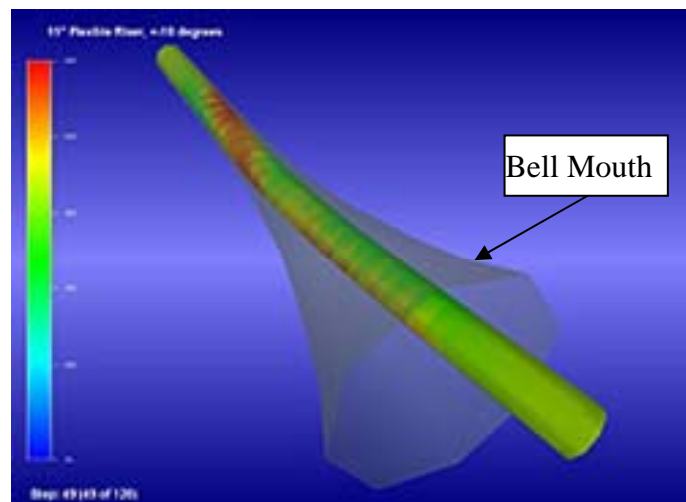


Figure 1.6, the schematic and picture of bending stiffener



. Figure 1.7, the schematic of Bell Mouth

1.3.3 Annulus Venting System

As we have mentioned, the space between internal polymer sheath and the external polymer sheath is called pipe annulus. Through the operation in offshore engineering, the fluid transported in bore will diffuse through the internal polymer sheath into the annulus. There gas which diffuse into the annulus include water, CO₂ and H₂S, they all have the negative influence on the steel components in the annulus.

At the same time, the build-up of pressure in the annulus due to the presence of gas could cause the collapse of the internal polymer sheath of the pipe, especially in case of a sudden pressure loss in the bore of the flexible pipe.



NTNU Trondheim
Norges teknisk-naturvitenskapelige universitet
Institutt for marin teknikk

In order to prevent the occurrence of build-up of gas in the annulus of flexible pipe due to diffusion, we need the venting system. A venting system is incorporated into the pipe structure to make the gas be vented out to outer environment. Generally there exist three vent valves which are incorporated into both end fittings of a flexible pipe.

Chapter 2. Failure mode, Mechanical Properties and Design principles

It is very important to have a deep understanding on the flexible pipe performance characteristics and failure modes, if we want to carry out a reliable design of flexible pipe systems. Generally, the analytical methods and experimental testing are the main methods that are available in nowadays.

The difference on structural complexity from rigid pipelines makes it more difficult to calculate the force and moment on the flexible pipes. The mechanical properties of flexible pipes are really different from others.

In this chapter, the failure modes of flexible pipes and mechanical properties are included. At the same time, the fatigue damage mechanism is introduced briefly. Finally, the design process of flexible pipes is also involved.

It should be noted, in the design process, the load cases should reflect both operational and extreme load conditions, as well as loads imposed on flexible pipes during transient conditions such as storage, handling, transportation and installation. Accidental load conditions should also be considered.

2.1 Failure modes of flexible pipes

In this part, failure modes as known from service experience and full- scale tests are described. The study of failure modes and failure causes for flexible pipes is usually based on the evaluation of pipe structure integrity, function of each layer, interface between pipe and end fitting, etc.

There are only two main failure modes that can impede fluid transportation through a flexible pipe:

- ◆ Leakage
- ◆ Reduction of internal cross section

The main failure tree for flexible pipes is shown in figure 2.1, as it illustrated, we could find leakage can be caused by the following failure modes:

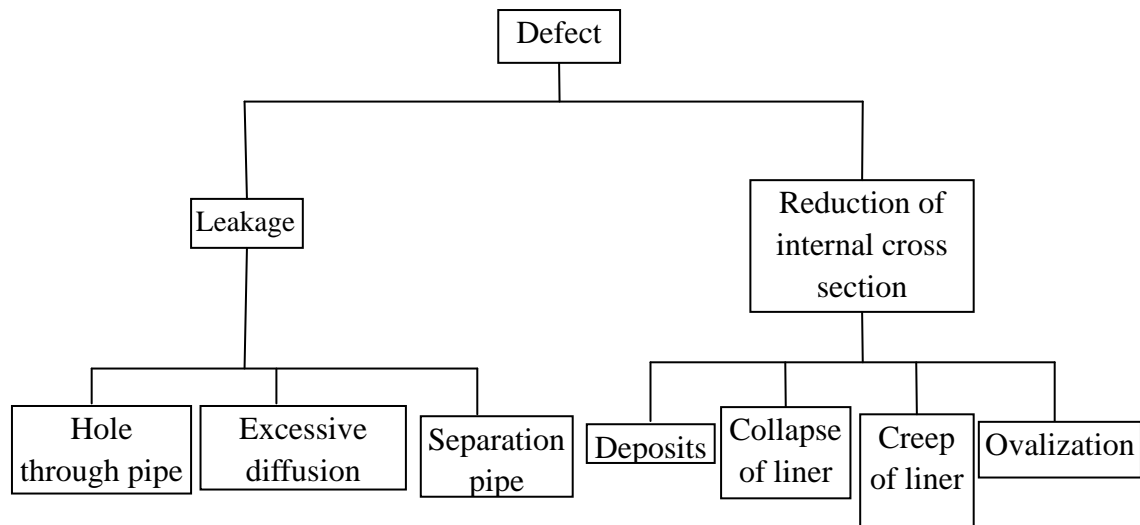


Figure 2.1, main failure tree for flexible pipes

- ◆ Hole through pipe wall
- ◆ Excessive diffusion
- ◆ Separation pipe/nipple

Reduction of internal cross section can be caused by:

- ◆ Ovalization / flattening of pipe
- ◆ Collapse of liner
- ◆ Deposits
- ◆ Creep of liner

As we have already mentioned, because of the complexity of the flexible pipe structure, the failure modes listed above are often results of a sequence of events or partial failures.

Most of the time, the initial failure or degradation mechanism will not be serious enough to cause complete failure. The initial partial failure will cause a condition that was not intended in the original design, and then the degradation leads to full failure finally. This is illustrated in figure 2.2. Figure 2.2 demonstrates the possible results of partial failures for a segment of unbonded flexible pipe, when erosion/ corrosion is the initial degradation mechanism.

These diagrams, which may be established for different initial degradation mechanisms and/or conditions causing a failure, are useful when devising inspection strategies for flexible pipes.

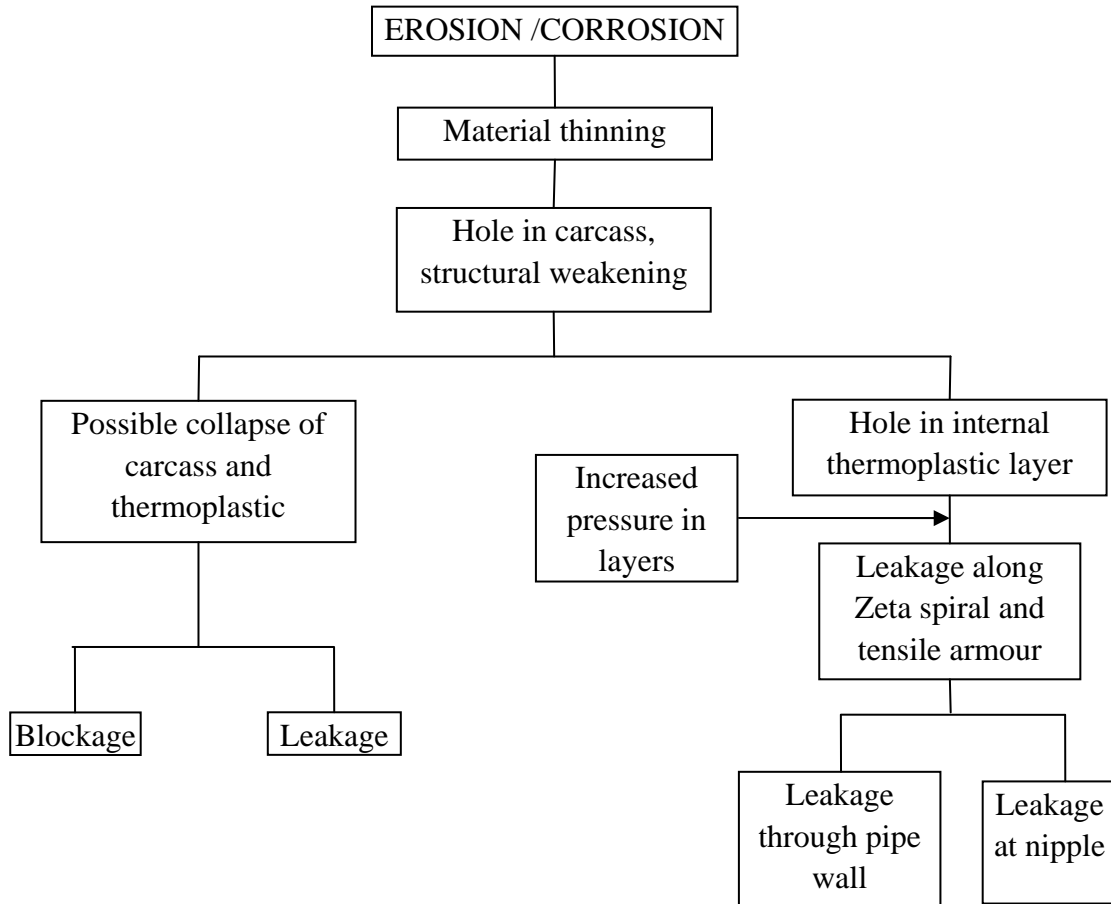


Figure 2.2, Possible sequences of failure in case of erosion/corrosion of a Coflexip pipe, from FPS2000 Report 2.3-3.

The mechanism behind the failure mode of flexible risers is affected by many factors. For example, the “hole through pipe wall” phenomenon could be due to excessive straining, accidental loads, tensile failure, corrosion and fatigue/ wear, etc.

All of these factors need to be considered in the design procedure of the whole project. These factors could be grouped into two main categories:

- ◆ Service life consideration
- ◆ Initial strength consideration

Service life consideration includes two parts, mechanical deterioration and material degradation. Each single layer in the cross section of flexible pipe resist to different loading modes. As a result of this, they would have their own failure modes.

2.2 Failure Modes of layers

- ◆ For interlocked carcass layer



The carcass layer structure may be subjected to a large number of failure modes, such as radial collapse, wear, erosion, corrosion and the damage from pigging and other relevant operations.

Radial collapse has been reported in several engineering production cases. This is frequently mentioned in relevant documents on carcass. Gas in the bore will diffuse into the internal pressure sheath. For flexible pipes with multiple liners, pressure will build up between liners and create a pressurized gap when the bore pressure is reduced. This would add an additional pressure on the carcass layer.

For some gas condensate fields with sand production, the erosion and corrosion could be observed. Also the full scale tests have shown that the corrosive environment with CO₂ will give enhanced erosion rate.

◆ Failure modes for pressure armour

The pressure armour in flexible pipes works as a little machine. With the curvature of the whole pipe is changing, the windings of pressure armour is sliding with each other. This results in considerable contact stress at contact points, as figure 2.3 shows. This is a problem particularly for the Zeta pressure spiral. The sliding may thus results in significant cyclic stress in the cross-wire direction. Subsequently, the fatigue crack growing in the hoop direction (longitudinal to the wires) is indispensable. In testing laboratory, this loading is simulated by a bi-axial test fixture, just as figure 2.4 shows.

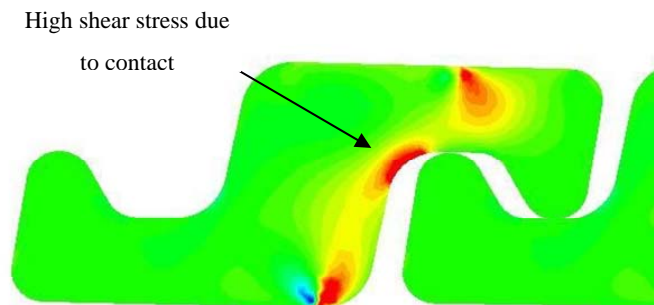


Figure 2.3, shear stress on the cross section of Zeta pressure armour (red part refers to areas with high shear stress)

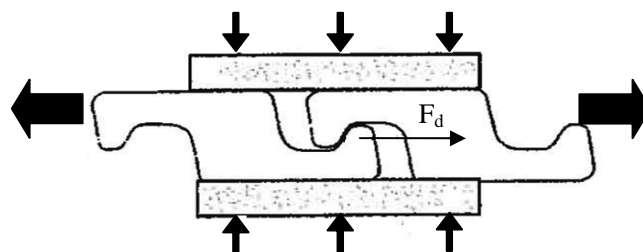


Figure 2.4, fixture for cross-wire fatigue testing of pressure armour.

The pressure armour in figure 2.4 is Zeta-profile armour. This applies for the testing of C-clip and Theta profiles. The direction of dynamic loading is in horizontal direction. Proving ring provides the static contact pressure.

The ovalisation of the pipe due to curvature variations and possible side loads from a bending stiffener or a bellmouth will give cyclic stresses longitudinal to the armour profile. The subsequent fatigue crack increases in the direction which is normal to the axis of pressure armour.

These two failure modes due to fatigue have already been observed from full scale fatigue testing of flexible pipes with Zeta profiles. Theta and C-clip profiles demonstrate better fatigue properties.

◆ Failure modes of tensile armour layers

In this thesis, the emphasis is put on the fatigue performance of tensile armour layers. There are so many possible failure modes for tensile armour layers. Such as:

- Overload in bending or compression causing wire disarray or birdcaging
- Overload in tension, in combination with internal pressure
- Overload in torsion, causing unwinding of armour or birdcaging
- Fatigue
- Wear or corrosion
- Fretting fatigue
- Hydrogen induced cracks

The fatigue properties of tensile armour may be critical w.r.t design life of the whole flexible pipe system. We must be aware of the importance of bore fluid. In the as fabricated state, void space in the annulus is filled with air. For this reason fatigue strength criteria have been derived on the basis of fatigue tests in air, assuming the environment in pipe annulus to be benign. But in the operation phase, the chemical composition of the annulus could be corrosive easily.

It is very easy to explain this phenomenon. Firstly the bore fluid could diffuse and permeate through the internal pressure sheath. Secondly, the outer pressure sheath may be damaged during the process of installation and operation. This would lead the flooding of seawater in the annulus. Finally, the sea water would be combined with sulphide (H₂S) and/or carbon dioxide (CO₂). This combination has negative influence on the tensile armour layers. The fatigue failure will be introduced in section 2.3.

2.3 Service lifetime

Flexible pipes are complicated structures, particularly from a fatigue point of view. In this thesis, we focus on the fatigue performance/ service lifetime, especially for the service life of tensile armour layer. Three major source of damage have the influence on the service life of flexible pipes. They are cumulative damage effects due to flexure, erosion and material degradation. Here only the cumulative damage effect is taken into account.

Not only the pressure armour, but also the tensile armour will be sliding against each other, when the flexible pipe is subjected to oscillatory bending. The contact pressure exists between different layers.

Two stages of deterioration are assumed. The first stage refers the wear which is caused by reciprocating sliding, followed by the decrease in the cross section of the tensile armour. The second one is reached when the stresses in the tensile armour have increased above the fatigue limit. The fatigue limit was assessed on the basis of uniaxial fatigue tests of individual wires of armour, from which a Haigh diagram was constructed, in figure 2.5.

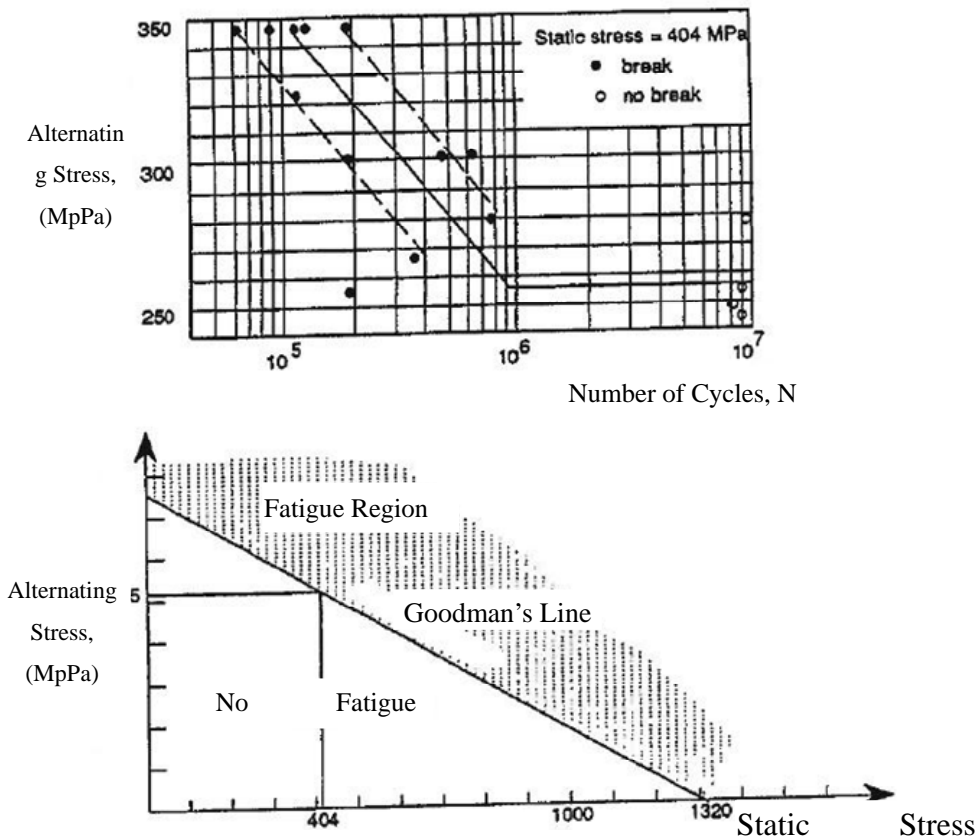


Figure 2.5, Fatigue strength criterion for tensile armour of nonbonded pipe, from Feret and Bournazel (1986)



Tensile layer wire is subjected to a combination of axial stress and bending dynamic stress. Axial testing compared to bending testing of the same wire may not necessarily yield the same SN curve. Here are several reasons for this.

1. The tensile layer tendon should be straightened before the testing, no matter whether it is taken from a pipe or as-delivered on a reel. Otherwise, the residual out-of-straightness will produce secondary bending effect in axial testing.
2. In order to avoid failures in the grip area, the axial testing specimens must be machined to a reduced cross section over a certain length. This process may have the influence on the fatigue life of the testing specimens. As a result of this, the care on the specimen must be taken.
3. Most of the time, the specimen testing is in the form of bending testing. While the tensile armour is produced by rolling, and large residual stresses are likely to be present. Due to the shake-down of residual stress, the relationship between loading and displacement during fatigue loading history could be changed. Unless care is taken to compensate for this effect, errors will be introduced when data from displacement controlled tests are interpreted in terms of stress range.

2.4 Mechanical properties of bending

Mechanical properties of flexible risers means how the riser response to different loading modes, when the flexible riser is subjected to axial loads, internal pressure and external pressure, torsion and bending. Also the combined loading condition of these effects is important for design. But in this section only the bending properties of flexible pipes is introduced here.

The bending response of one segment of flexible pipe shows a pronounced hysteretic behaviour. We could observe this phenomenon in figure 2.6. The horizontal axis corresponds to the curvature of flexible pipes, while the vertical axis demonstrates the moment applied. This hysteretic behaviour of nonbonded pipes may be explained by the internal slip mechanism.

There are several helical reinforcing layers in the cross section of flexible pipe, for example the two cross-wound tensile layers. These tensile layers would slip relative to each other when the pipe is under bending loads. At the beginning of bending, the curvature of flexible riser is relatively small, so the slip is strongly restricted by the internal friction between different layers. That is why we have a high initial tangent bending stiffness. But we have to be aware of that, when the curvature reaches a certain value, the slip is indispensable. This curvature correspondent to a friction forces, M_f , is called the friction moment. In fact, this M_f is crucial for nonlinear Finite



Element Analysis, since it is the symbol of geometrical non-linearization.

M_f depends on the contact pressure between pipe layers, and consequently on the loads applied on the pipe. When the friction moment is exceeded, the curvature varies linearly with the moment variation. The stiffness in full slip phase is rather lower and the main part of it is due to the stiffness of the plastic sheaths. It should also be noted that when the direction of the curvature is changed, the change in moment has to exceed twice the friction moment before elastic behaviour occurs.

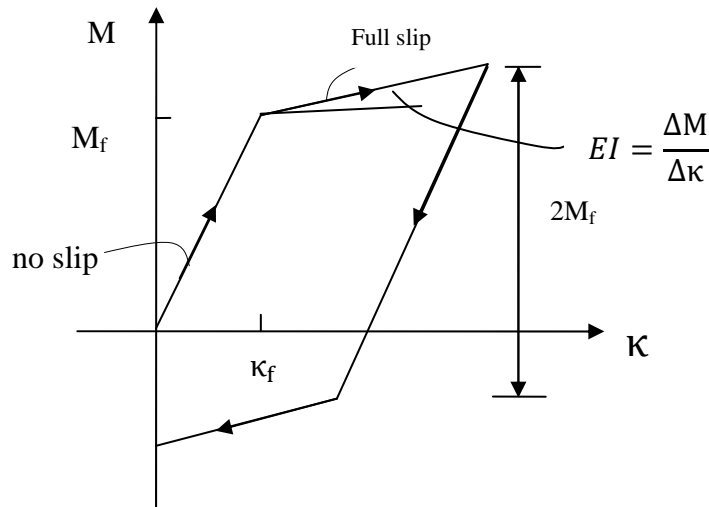


Figure 2.6, bending behaviour of nonbonded pipe

In the analysis and design of flexible pipes, the quantity of curvature is a very crucial value. The curvature decides the relative location between each single layer. The slip is associated with curvature, too. In fact, when it is needed to decide the most critical load case and most critical location on the one segment of flexible pipe, the value of curvature is absolutely one crucial reference. This is reflected in Chapter 5. In this section, we have to carry our detail analysis on the cross-sectional structures. Because the detail analysis on the whole flexible pipe is very time-consuming, so we have to only focus on some critical segments along the flexible pipe. In this process, the curvature decides the location on which we shall carry out the detailed analysis.

2.5 The design process of flexible pipes & recommendations

About twenty years ago, most of the design process of flexible pipes is finished by full scale dynamic testing of prototype pipes. That is because at that time, there are not so many effective approaches on the analysis of flexible pipes. The procedure for design verification which was generally around 1990 is shown schematically in figure 2.7. Through the full scale testing, the response of flexible pipe and the fatigue



damage is available. But it very obvious to know, this testing process is rather time-consuming. The flexible pipe specimen must be bending several million times.

In order to improve the efficiency of engineering design, significant developments have taken place after 1990s. Validated computational tools have been developed, for calculation of stress, displacement, frictional static, dynamic and thermal loads. At the same time, complimentary experimental techniques were developed, for assessment of input data and validation of analysis results, using small scale, mid scale and full scale test models.

The current situation (2000) with regard to design verification is shown schematically in figure 2.8.

- Recommendations for the design of flexible pipes

In the design process, the design of flexible pipe system should be treated as a primary element of production system. In the concept design stage, the reliability and robustness of flexible pipe system must be involved.

Flexible pipe technology is a new developing technology; the relevant engineering operation experience is too short to assess the reliability and robustness of flexible pipes in demanding applications. Although we have developed some software to verify the stress distribution of flexible pipes, we still need the testing result and data to support our research.

Through the last few years, the experience on the operation of flexible pipes has been accumulated. These experiences show that flexible pipes will fail due to new and unexpected failure modes, even if the flexible pipe design has been fully qualified. This indicates that the behavior of the materials and in particular the interaction between the different materials in a pipe wall is not fully understood. Further research is needed.

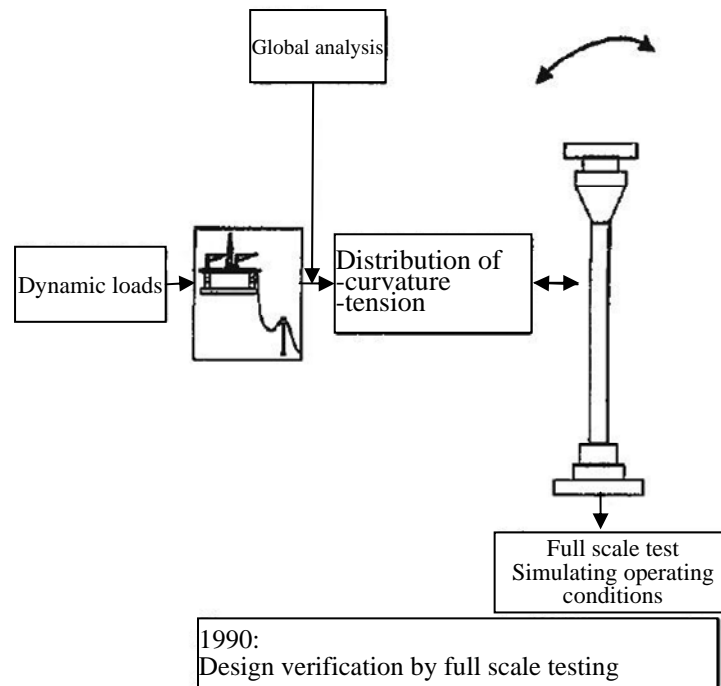


Figure 2.7, fatigue design procedure for dynamic risers, about 20 year ago

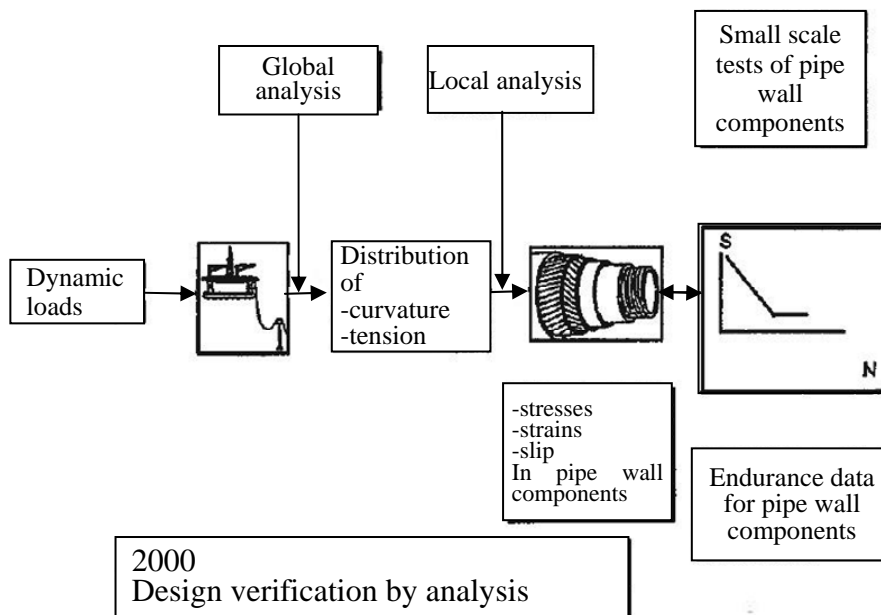


Figure 2.8, Schematic of Procedure for fatigue design of flexible pipes in 2000

Chapter 3. BFLEX2010 and non-linear Finite Element Analysis

3.1 Introductions

As we mentioned in Chapter 2, full scale testing of flexible pipes is very time consuming. This results in the development of calculation software. BFLEX 2010 is one of these software packages which focus on the local analysis and fatigue assessment of flexible pipes, developed by MARINTEK, SINTEF.

BFLEX 2010 is part of the solution of flexible pipe design. It focuses on the local analysis of flexible risers. With the help of BFLEX 2010, we are capable of concluding the information of stress/strain distribution, displacements, and fatigue damage of each layer in the cross section of flexible riser. Especially, the stress data on the cross section of pressure spiral is even available by the specific modules in BFLEX 2010.

The algorithm of BFLEX is based on Finite Element Analysis (FEA) method. With the development of engineering calculation, more and more structural engineering problems could be solved or simulated by FEA Method with the development of computer system. But as we have already mentioned, the most special properties of flexible pipe is its complex structure. Then it is really a challenge to take into account of this characteristic. In BFLEX 2010, the structural response of flexible pipes is solved by non-linear FEA approach. As a result of this, the non-linear FEA method is introduced here, too.

3.2 The structure of BFLEX 2010 software

When we are carrying out design work with BFLEX, our research objective is not the whole segment of flexible pipe. On the contrary, the analysis objective is part of the whole flexible pipe. The loading and displacement data is from the global analysis, which comes from other global analysis software such as RIFLEX. In this thesis, the length on which the BFLEX analysis is done has the length of 15 meter. The BFLEX 2010 gives out the stress distribution of tensile armour layer, pressure armour layer and the carcass. It is not a single FEM analysis tool, on the contrary, it consists several modules. Each of them plays one single analysis role in BFLEX 2010. Through these modules, the fatigue damage of each layer is available.

A summary of the available modules is given below:

- The BFLEX 2010 module.
This module reads all the command in the input file and generates the .raf file which contains all the data of analysis. At the same time, the global analysis of riser segment and tensile armour stress analysis is finished in this module. A BFLEX 2010 model is shown in figure 3.1. We could see the white tensile armour in this model.

- The BFLEX 2010 POST module
This module plays a role of post-processing of database file generated by BFLEX 2010. POST module could generate ASCII files that can be plotted by the plotting program Matrixplot. This ASCII file gives the information about the location at which the maximum curvature occurs during the whole calculation process. Utilizing BOUNDARY and PFLEX module, the boundary model and PFLEX windings are positioned at the location with maximum curvature. And then the LIFETIME module is used.

The analysis on each part in the cross section could be done with the following sub modules:

1. The BPOST module. This module could post process the local results data, and then the ASCII files will be available, which could be plotted by Matrixplot.
2. The BOUNDARY module. It will perform transverse cross-sectional stress analysis.
3. The PFLEX module. It will carry our pressure spiral bending stress analysis.
4. The LIFETIME module, this module will perform fatigue analysis of tensile armour, pressure spiral and boundary model.

The difference between transverse cross-sectional stress analysis and pressure spiral bending stress analysis is shown in figure 3.2 and figure 3.3. Transverse cross-sectional stress means the stress distribution on the cross section of pressure armour / flat spiral, or the carcass, not the cross section which is normal to the axis of whole flexible riser. It is easy to find that the BOUNDARY module focuses on the cross section.

BFLEX2010-ITCODE0 LC1G1, by Minghao Chen

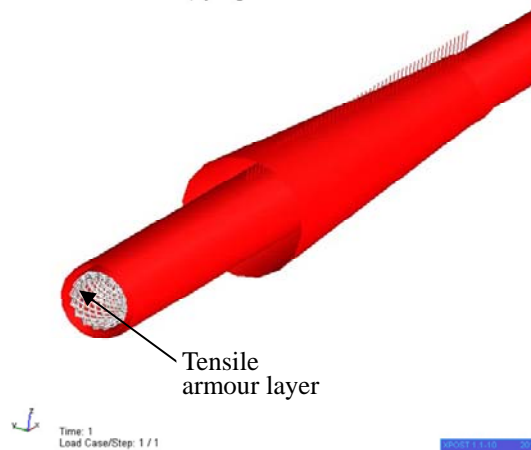


Figure 3.1, a BFLEX model. The white part is tensile armour

BFLEX2010-ITCODE0 LC1, by Minghao Chen

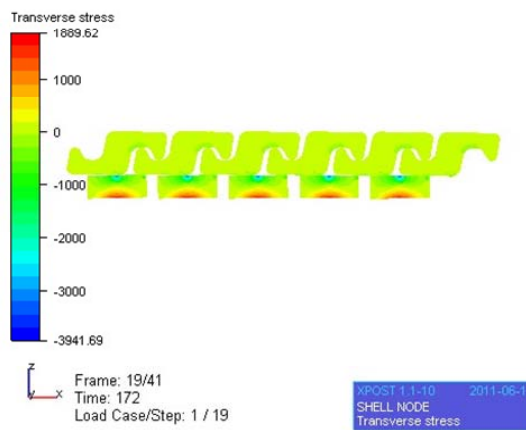


Figure 3.2, the boundary model, which gives transverse cross sectional stress result

BFLEX2010 - test - real nonlinear bs - depend node sys. -itcode 31 -2

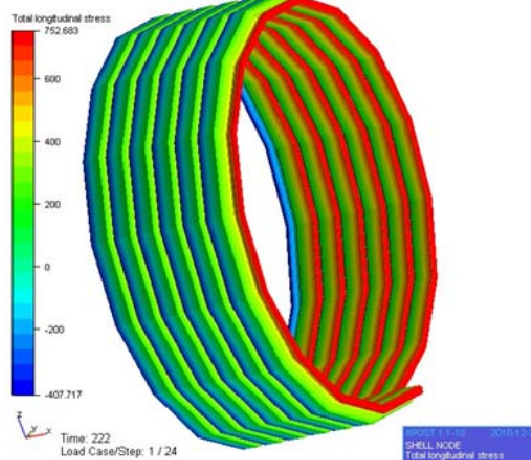


Figure 3.3, the PFLEX model, which gives bending stress distribution of pressure armour

In fact, each module in BFLEX 2010 is not independent with others. For example, in order to assess fatigue damage of tensile armour, and pressure spiral, the BFLEX2010 POST module and BFLEX 2010 must be run without any error. The system architecture of BFLEX 2010 system is shown in figure 3.4.

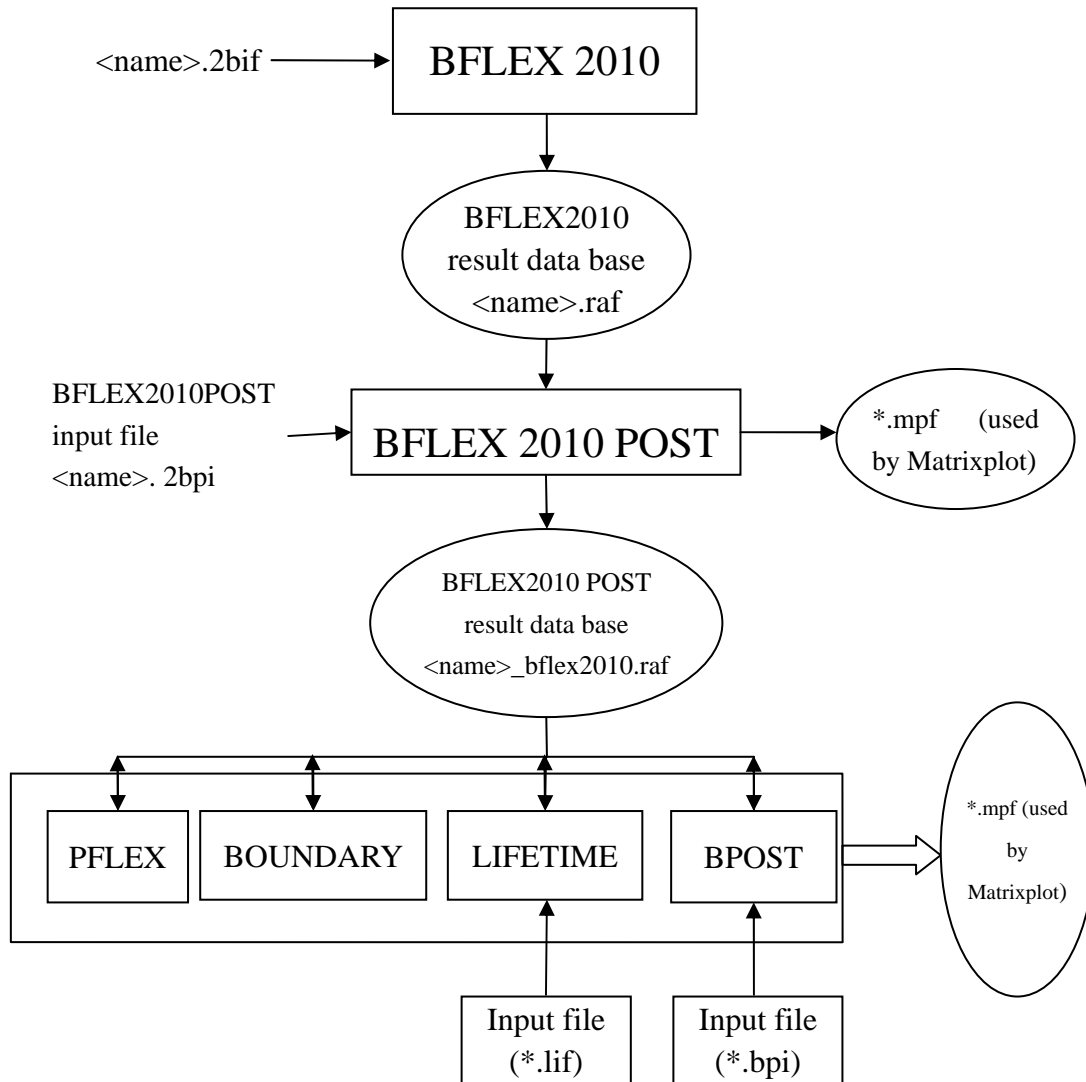


Figure 3.4, BFLEX 2010 software system

In fact, the *.mpf file could be read directly by Matrixplot, through which we are able to plot the information and data of the flexible riser.

3.3 Formulations of tensile armour model

Tendons in tensile armour layer supplies resistance to the tension along the axis of flexible pipe. In BFLEX, we have different formulations of the tensile armour models. Here are two important factors that we should mention in BFLEX 2010. They are:

- ◆ Number of degrees of freedom (NDOF)
- ◆ Contact/friction algorithm

In order to simplify the calculation and save more iteration time, some assumptions must be made:

- ◆ BFLEX neglects the transverse slip of the tensile armour. This means the tensile armour is assumed to follow a loxodromic surface curve. This is demonstrated in figure 3.5.
- ◆ The cross section maintains its form sufficiently to allow all local bending and torsion effects of the tensile armour to be calculated analytically
- ◆ Only in the condition of bending deformation, the shear stress between tensile armour tendons and supporting layers will be introduced. This means axisymmetric strains and bending strains are not coupled.

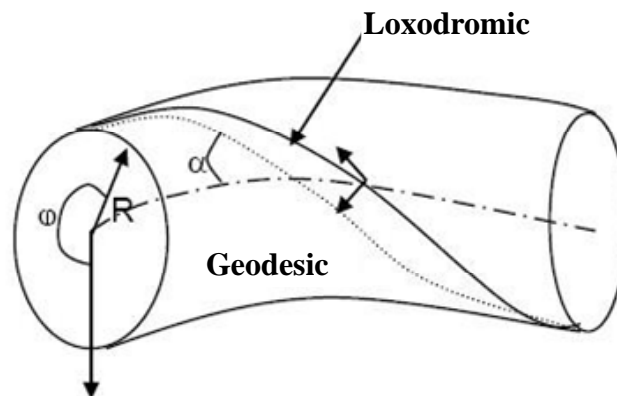


Figure 3.5, Loxodromic and Geodesic helical path along bent cylinder

There are three alternative bending formulations that have been included in the BFLEX tensile armour model. They are as follows:

1. ITCODE 0

In this bending formulation, the equilibrium equation of each individual tensile tendon is considered by taking into account of the shear interaction between tendon and the core pipe layer. In this process, the Sandwich Beam formulation (SBM) is applied.

In the iteration calculations, full equilibrium iteration of the entire cross section at each load step is achieved. The slip value is found from the inner layer. If we use ITCODE 1 bending formulation in calculation, then the slip value is found for each layer.

2. ITCODE21



A moment based model (MM), considering the friction moment contribution from all layers. The stresses are calculated by iteration with respect to moment balance.

Only one moment-curvature curve is used, and the slip curvature is based on the inner layer only (because it is the inner layer that is of concern for fatigue calculations).

3. ITCODE 31

The moment contribution from the tendons is taken into account by a friction moment approach as for ITCODE 21. So this is also a moment based model (MM). But in this model, each layer has its own moment – curvature curve. The slip property of each layer is considered, too. Under this method, the slip process is more correctly modeled. The stresses are calculated by iteration with respect to moment balance. It has already been proven that ITCODE 31 formulation gives less stress in extreme cases than ITCODE 0.

In this way, a four layer pipe will have four moment-curvature curves with different slip levels. And in the calculation, all these four moment – curvature will be added together to get the final correct result. When the calculation result is compared with the full scale test result, the ITCODE 31 formulation shows a best fit with respect to the fatigue damage of tensile armour layer.

3.4 Non-linear Finite Element Method approach

Flexible pipes are characterized by its complexity in cross section. The different layer may slip with respect to each other when the pipe is subjected to bending. At the same time, the material for each layer is not ideal elastic materials, such as the material for internal and external pressure sheath. For the tensile layer armour, when the bending curvature of flexible is sufficiently large, it will yield, because the stress has exceeded the yielding stress. And there exists the friction and relative motion between different windings for the pressure armour and the flat spirals. This increases the difficulties when we are trying to solve the response of flexible pipe with Finite Element Analysis Method. In fact, for these problems, the linear theory is nor any longer valid, the non-linear effect could not be neglected. And the non-linear approach is needed.

There exists three kinds of nonlinear effects it structural analysis, they are geometrical non-linearity, material non-linearity and boundary condition non-linearity. In this section, the geometrical non-linearity is introduced briefly.

Geometrical nonlinearity may be illustrated by a two bar system, shown in figure 3.6. In this case, two bars are jointed together by a pin-point. When the joint point is



subjected to a concentration force R , the joint point would move downward. This system could be simplified into a stiffness system, in which R is the resistance, and r is the displacement. α_0 is the original angle before deformation, and α is the angle after deformation.

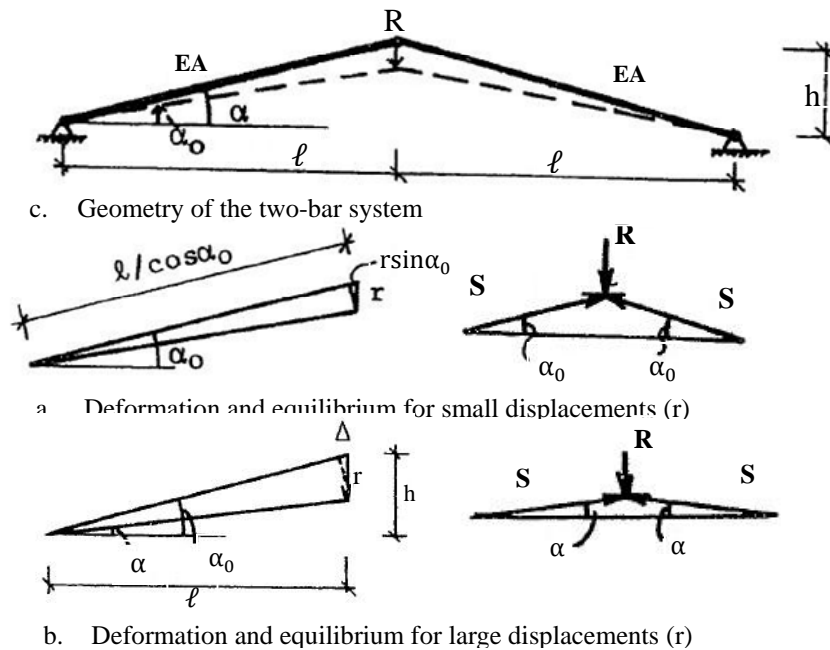


Figure 3.6, the two-bar systems

But the stiffness of this two-bar system is different for the small displacement case and the large displacement case. This demonstrates a Geometrical Non-linearity.

When the displacement is small as shown in figure 6b, the axial shortening of each bar is $r \cdot \sin \alpha_0$, the final stiffness relationship between R and r reads

$$R = \frac{2EA}{\ell} \sin^2 \alpha_0 \cos \alpha_0 \cdot r \quad (3.1)$$

$$\text{Or } R = Kr, \quad (3.2)$$

$$\text{where } K = \frac{2EA}{\ell} \sin^2 \alpha_0 \cos \alpha_0 \quad (3.3)$$

for this case, the stiffness K is constant, implying a linear relationship between R and r if the angle α_0 is small ($\alpha_0 \ll 1$), which means $\sin \alpha_0 \approx \alpha_0$, $\cos \alpha_0 \approx 1$, and then the stiffness relationship has changed to:

$$R = \frac{2EA\alpha_0^2}{\ell} r \quad (3.4)$$

Equation (3.3) is based on the assumption that the displacement is small. When the displacement is increasing gradually, the axial shortening of the bar is not $r \cdot \sin \alpha_0$ any longer. For this case, the true axial shortening Δ has changed to:

$$\Delta = \frac{\ell}{\cos \alpha_0} - \frac{\ell}{\cos \alpha} \quad (3.5)$$

Then the stiffness relationship between R and r is as follows:

$$R = \frac{2EA}{\ell} \left(\frac{h}{r} - 1 \right) \left(\frac{\ell}{\sqrt{\ell^2 + (h-r)^2}} - \frac{\ell}{\sqrt{\ell^2 + h^2}} \right) r \quad (3.6)$$

Here, $\sin\alpha = \frac{h-r}{\sqrt{\ell^2 + (h-r)^2}}$, $\cos\alpha = \frac{\ell}{\sqrt{\ell^2 + (h-r)^2}}$, $\cos\alpha_0 = \frac{\ell}{\sqrt{\ell^2 + h^2}}$

Equation (3.2) may be written as $R = K(r) \cdot r$

For small angles α and α_0 ,

$$\sin\alpha \approx \alpha \approx \tan\alpha = \frac{h-r}{\ell} \quad (3.7)$$

$$\cos\alpha \approx 1 - \frac{1}{2}\alpha^2 \approx 1 - \frac{1}{2}\left(\frac{h-r}{\ell}\right)^2 \quad (3.8)$$

$$\cos\alpha_0 \approx 1 - \frac{1}{2}\alpha_0^2 \approx 1 - \frac{1}{2}\left(\frac{h}{\ell}\right)^2 \quad (3.9)$$

then Equation (3.6) yields

$$R = \frac{2EA}{\ell} \frac{\left(\frac{h-r}{\ell}\right)\left(\frac{h}{\ell} - \frac{1r}{2\ell}\right)}{1 - \frac{1}{2}\left(\frac{h}{\ell}\right)^2} r \approx \frac{2EA}{\ell} \left(\frac{h}{\ell} - \frac{r}{\ell}\right) \left(\frac{h}{\ell} - \frac{1r}{2\ell}\right) r \quad (3.10)$$

After assuming $\left(\frac{h}{\ell}\right)^2 \ll 1$, $\frac{h}{\ell} \approx \alpha_0$

The final stiffness relationship and the stiffness of two-bar system yields:

$$R = \frac{2EA}{\ell} \alpha_0^2 \left(1 - \frac{r}{h}\right) \left(1 - \frac{r}{2h}\right) r = K(r) \cdot r \quad (3.11)$$

The stiffness for two-bar system when the displacement is large is:

$$K(r) = \frac{2EA}{\ell} \alpha_0^2 \left(1 - \frac{r}{h}\right) \left(1 - \frac{r}{2h}\right) \quad (3.12)$$

$$= \frac{2EA}{\ell} \alpha_0^2 + \frac{EA}{\ell} \alpha_0^2 \left(\frac{r}{h} - 3\right) \frac{r}{h} \quad (3.13)$$

$$K(r) = K_0 + K_g \quad (3.12)$$

In Equation(3.12), K_0 is the linear stiffness, and the K_g is the geometrical stiffness.

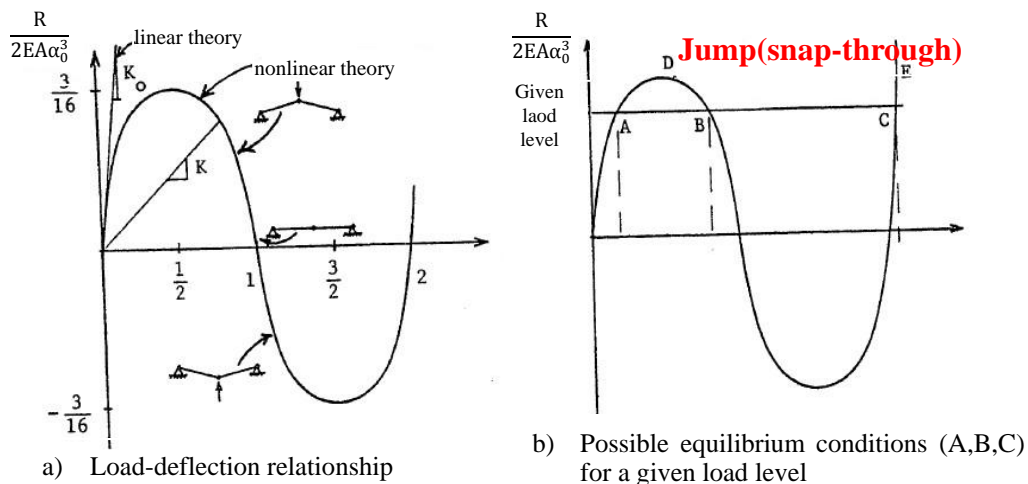


Figure 3.7, Load-deflection characteristics of two-bar system

Chater 4. Fatigue assessment of flexible riser

4.1 Introductions

In this project, one segment of flexible riser with length about 15 meters is modeled and analyzed. In fact, this BFLEX analysis is based on the test which is held by MARINTEK, SINTEF. In the testing, a segment of flexible pipe was installed on the test rig, and then was subjected to the rotation at the ending. We must make the BFLEX analysis model as identical to real test as possible. Two load cases are finished with BFLEX 2010 in this thesis with different cycle numbers, with bending formulation of ITCODE 0 and ITCODE 31 respectively. The final stress result and fatigue result are compared.

4.2 description of flexible pipe data

4.2.1 The pipe data sheet

The pipe data sheet is presented in table 4.1. In this table, the data of the geometrical shape and the service environment of flexible pipe are given.

Table 4.1, pipe data sheet

Inside diameter: 228.6 mm		Service: sour dynamic		Max fluid temperature: 130°C		
Design pressure: 50.07 MPa		Conveyed fluid: Oil		Water depth: 300 m		
Layer	Material	Strength (MPa)	I.D. (mm)	Thick (mm)	O.D. (mm)	Weight (kg/m)
Carcass	Steel	689	228.6	7	242.6	23.786
Antiwear	PVDF	-	242.6	3.99	248.6	4.097
Barrier	PVDF	-	248.6	12	272.6	17.389
Antiwear	PVDFc	-	272.6	1.02	274.63	0.873
Z-spiral	Carbon Steel	758	274.63	12	298.63	68.762
Flat spiral	Carbon Steel	758	298.63	5.99	310.62	40.835
Antiwear	PA11 (nylon)	-	310.62	1.52	313.67	1.569
Tensile_armour_1	Carbon Steel	758	313.67	5.99	325.66	43.049
Antiwear	PA11(nylon)	-	325.66	0.41	326.47	0.425
Antiwear	PA11(nylon)	-	326.47	1.52	329.52	1.649
Tensile_armour_2	Carbon Steel	758	329.52	5.99	341.51	45.4

Table 4.1

Antiwear	PA11(nylon)	-	341.51	0.41	342.32	0.445
Antiwear	PA11(nylon)	-	342.32	1.52	345.37	1.729
Tensile_armour_ 3	Carbon Steel	758	345.37	5.99	357.36	46.991
Antiwear	PA11(nylon)	-	357.36	0.41	358.17	0.466
Antiwear	PA11(nylon)	-	358.17	1.52	361.22	1.808
Tensile_armour_ 4	Carbon Steel	758	361.22	5.99	373.21	49.265
Antiwear	PA11(nylon)	-	373.21	0.41	374.02	0.487
Antiwear	PA11(nylon)	-	374.02	0.41	374.83	0.319
Protective sheath	PA11(nylon)	-	374.83	12	398.83	15.312

The steel tendon cross-section details are summarized in table 4.2. For this case, a rectangular flat spiral layer is installed in order to reinforce the flexible pipe.

Table 4.2, profile of steel tendon

Layer	Dimension (mm)	Pitch (mm)	Wires	Angle (°)	Filled (%)
Carcass	55×1.4	-	-	-	-
Z-spiral	26.8×12	-	-	-	-
Flat spiral	16×6	-	1	-	-
Tensile_armour_ 1	12×6	1039.9	54	44	91.3
Tensile_armour_ 2	12×6	1091.5	57	44	91.8
Tensile_armour_ 3	12×6	1225.9	61	42	90.7
Tensile_armour_ 4	12×6	1281.2	64	42	91

The cross-sectional profile of Zeta-pressure armour is shown in Figure4.1.

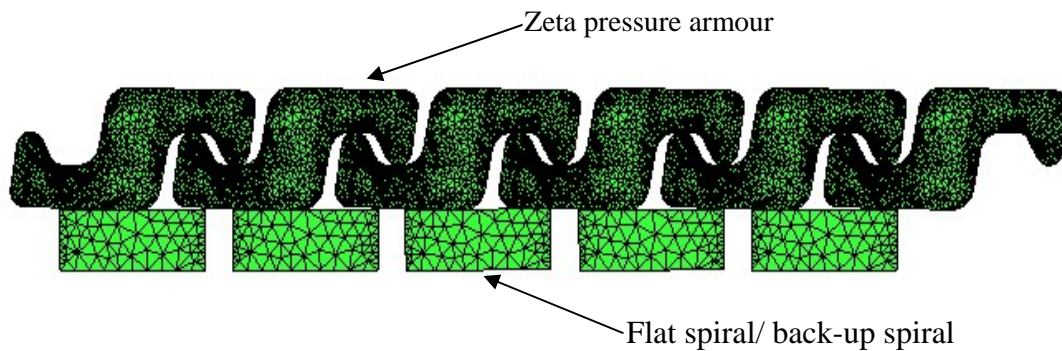


Figure 4.1, shape of Zeta-pressure armour

The geometry of the carcass is outlined in figure 4.2. It is made from a thin steel plate with dimension 1.4*55 mm.

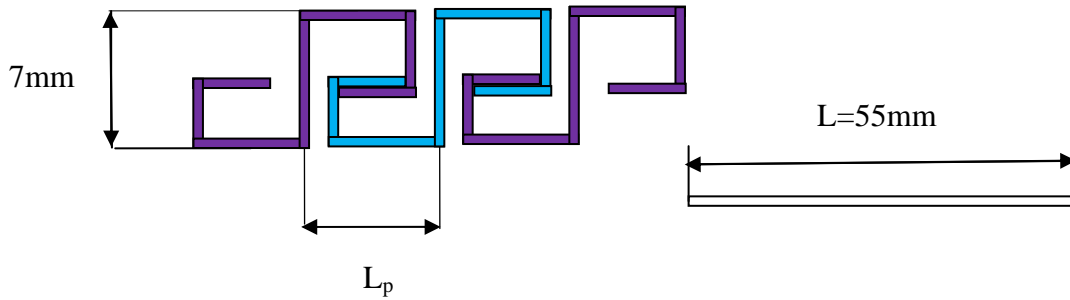


Figure 4.2, Shape of carcass (made from a thin steel plate with dimension of 1.4*55 mm)

In figure 4.2, L_p denotes the horizontal distance between two carcass cross sections.

Here, $L_p = \frac{2\pi R}{\tan \alpha}$, R is the radius to the center of the layer, α refers to the layering angle with respect to the longitudinal axis of flexible pipe.

4.2.2 Material properties

Material of each layer component of this segment of flexible risers is shown in table 4.3.

Table 4.3, material properties of each layer components

	Poisson's ratio	Density(kg/mm ³)	Young's modulus (MPa)	Shear modulus (MPa)	Transverse Young's modulus(MPa)
PVDF	0.45	1.76998e-6	1516.9	523.07	1516.9
PVDFc	0.45	1.01e-6	1516.9	523.07	1516.9
PA 11	0.45	1.03809e-6	55.2	19.03	55.2
Steel	0.3	7.82874e-6	2.1e5	80769	2.1e5
Carbon Steel	0.3	7.82874e-6	2.1e5	80769	2.1e5

The pipe bending stiffener is normally made from polyurethane (PU). The Young's modulus of elasticity during operation is taken to be 68.5 MPa. During testing at room temperature (23°C), we have got the following stress-strain curve, which is shown in figure 4.3, and summarized in table 4.4.

Table 4.4, material of bending stiffener

Strain (%)	Stress (MPa)
1	2
2	4
3	5.2
4	6.4
5	7.2

Table 4.4 material of bending stiffener

Strain (%)	Stress (MPa)
6	8
7	8.6
8	9.2
9	9.7
10	10.2

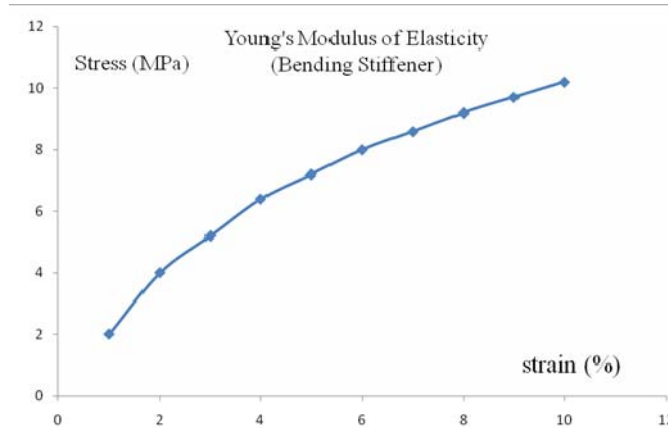


Figure 4.3, the Young's Modulus of polyurethane (PU) of bending stiffener

4.2.3 Mechanical properties and loading condition

◆ Fatigue data

As mentioned in Chapter 2, fatigue damage is one of the important failure modes of flexible pipes. In this thesis, it is fatigue performance that we are strongly interested in. Fatigue analysis is finished by LIFETIME module. The fatigue analysis on tensile armour and pressure armour is finished in this thesis.

The fatigue data for tensile armour is:

$$\begin{aligned}\log N &= \log a - n \log a - m \log(\Delta\sigma) \\ &= 23.89 - 6.53 \log(\Delta\sigma)\end{aligned}$$

For the Zeta spiral, the fatigue data is:

$$\begin{aligned}\log N &= \log a - n \log a - m \log(\Delta\sigma) \\ &= 12.5 - 3 \log(\Delta\sigma)\end{aligned}$$

Here, the unit of $\Delta\sigma$ is MPa.

◆ Operational internal pressure is about 50.07 MPa

◆ Friction coefficient

Between steel and plastic it is 0.15. Between steel and steel (for Z-spiral) it is 0.25

4.2.4 Load cases

Because this BFELX analysis is based on the testing in laboratory, we have to



utilize the same loading parameter as we used in the test. Two loading cases are simulated by BFLEX 2010 this thesis. The flexible pipe is subjected to different rocking angles, different tension and different cycle numbers. This is summarized in table 4.5.

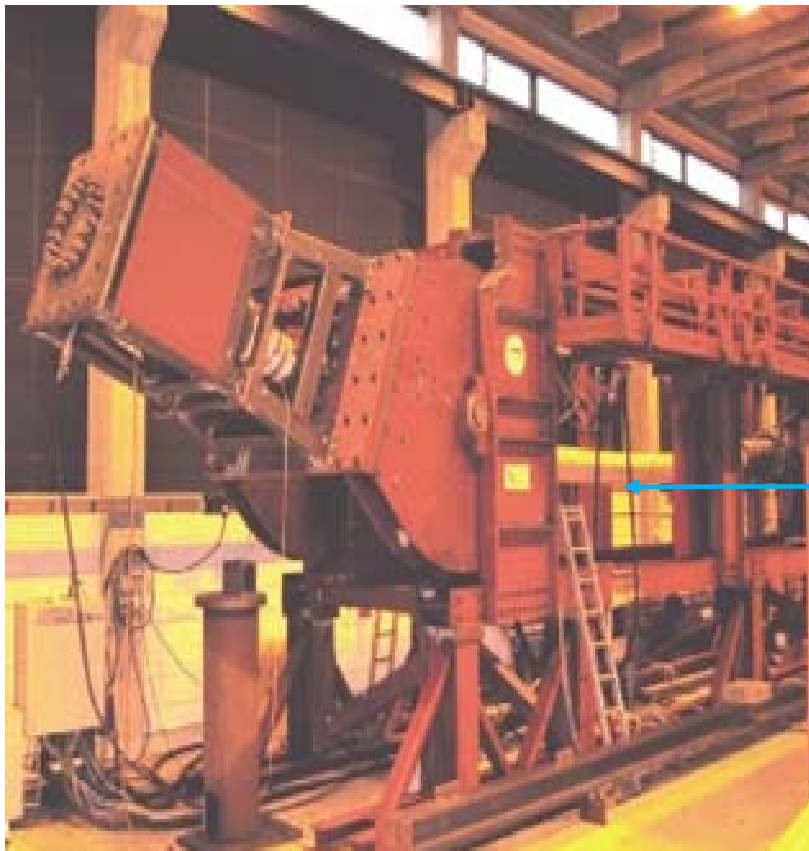
Table 4.5, Loading case 1 and loading case 2

No. of Load Case	Tension (kN)	Rocking angle (degree)	Number of cycles
LC1	725	+/- 7.5	400 000
LC2	750	+/- 12.5	200 000

4.3 BFLEX Model

4.3.1 The test configuration

The testing facilities which are usually used in flexible riser testing are illustrated in figure 4.4. This is a rocking machine in laboratory. In figure 4.4, the flexible pipe is visible with yellow color, and is connect to the left ending of the test rig. The details about the test rig are illustrated in figure 4.5.



Flexible pipe

Figure 4.4, testing facilities in laboratory

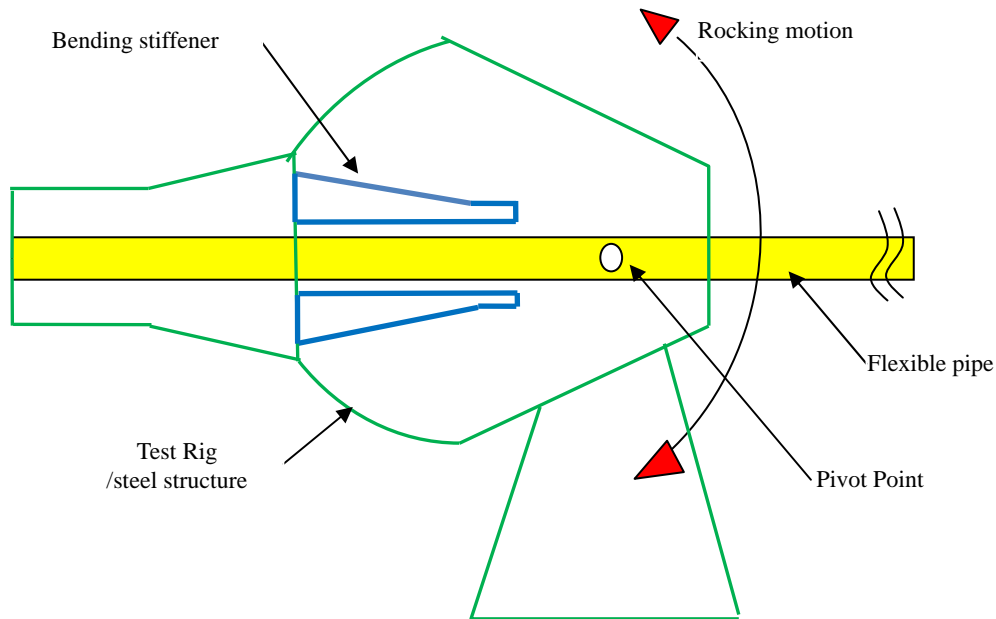


Figure 4.5, the details about test facilities (test rig)

Yellow part in figure 4.5 refers to the flexible pipe under testing, while the green part means test rig structure. Bending stiffener is denoted by the blue part. Head of test rig could rotate along the pivot point.

According to the description in figure 4.4 and figure 4.5, it is very easy to find that, one end of test flexible riser is connected to rocking head, and the other end is attached to the machine which supplied constant tension along the whole pipe. Both the flexible pipe and bending stiffener are connected to rocking head. The bending stiffener does not have direct contact with the flexible pipe, when the rocking head is horizontally located.

The configuration of testing decides the BFLEX model used in this thesis and other relevant Finite Elements Analysis (FEA) parameters, such as the boundary conditions. They are introduced in section 4.3.2.

4.3.2 the Finite Element Model in BFLEX

The length of each part of flexible pipe is shown in figure 4.8. The original length of flexible pipe is 16 900 mm, shown in figure 4.8a. The length of the tensioner in the right end is 1 180mm, which is used to supply tension along the longitudinal axis of flexible pipe. In order to simplify the calculation model and save calculation time, there are some changes in the BFLEX model, as shown in figure 4.8b. In the BFLEX model we are using, the total length is still 16 900 mm, the length of flexible pipe has changed to 14 950 mm. The tensioner has length 1 950 mm. After this simplification,

the flexible pipe, bending stiffener and the tensioner could be meshed with the element length of 50 mm. Plenty of calculation time has been saved.

According to the description in 4.3.1, the flexible pipe is different from the simply supported beam. The real trace of left end of flexible pipe is a circle. Center of this circle is the pivot point. In this thesis, two rigid pipe part are introduced, in order to model the tensioner and to simulate the circular motion of left end of flexible pipe. Figure 4.6 shows the details about the model that is used in this BFLEX 2010 analysis

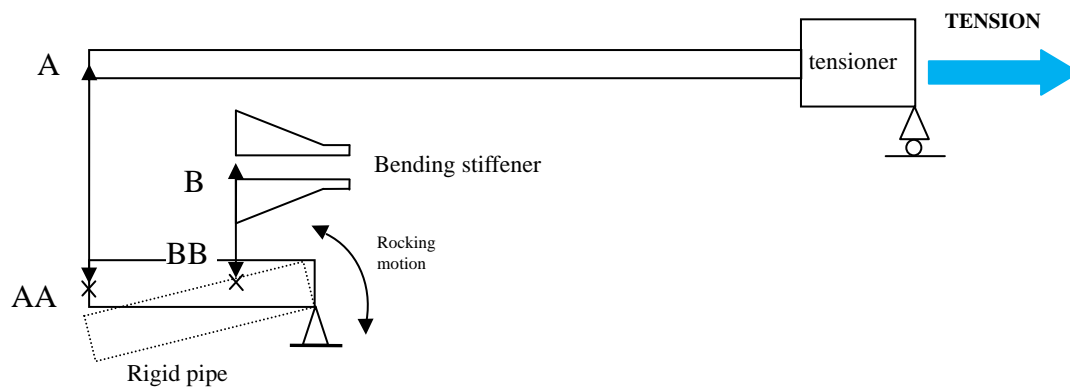


Figure 4.6, model in BFLEX and the boundary conditions

In figure 4.8, four parts are modelled with BFLEX 2010, flexible pipe, bending stiffener, tensioner and rigid pipe. The tensioner part and the rigid pipe part are both modelled with PIPE 31 element, with a very large axial stiffness compare with flxible pipe. Then the right end of rigid pipe is subjected to a rotaional motion.

The left end of flexible pipe will follow the motion of righ end of rigid pipe. This is shown in figure 4.6, in which the motion of end A follows the motion of end AA of rigid pipe. For the bending stiffener, the motion of left side of bending stiffener B follows BB point on rigid pipe. BB point corespondents the location where the bending stiffener is fixed together with rocking rig. With this approach, the motion of BFLEX FEA model is identical to that of test. The model in BFLEX 2010 is shown in figure 4.9.

The tension is applied at the right end of tensioner. The tensioner is also modelled by PIPE 31element with large axial stiffness.

4.3.3 Elements Distribution in ITCODE 0 case and ITCODE 31 case.

Two bending formulations are utilized here, in order to make the comparison. They



are ITCODE 0 and ITCODE 31. We have different models for these two ITCODEs. Table 4.6 and table 4.7 supplies the information about elements distribution in ITCODE0 case and ITCODE 31 case.

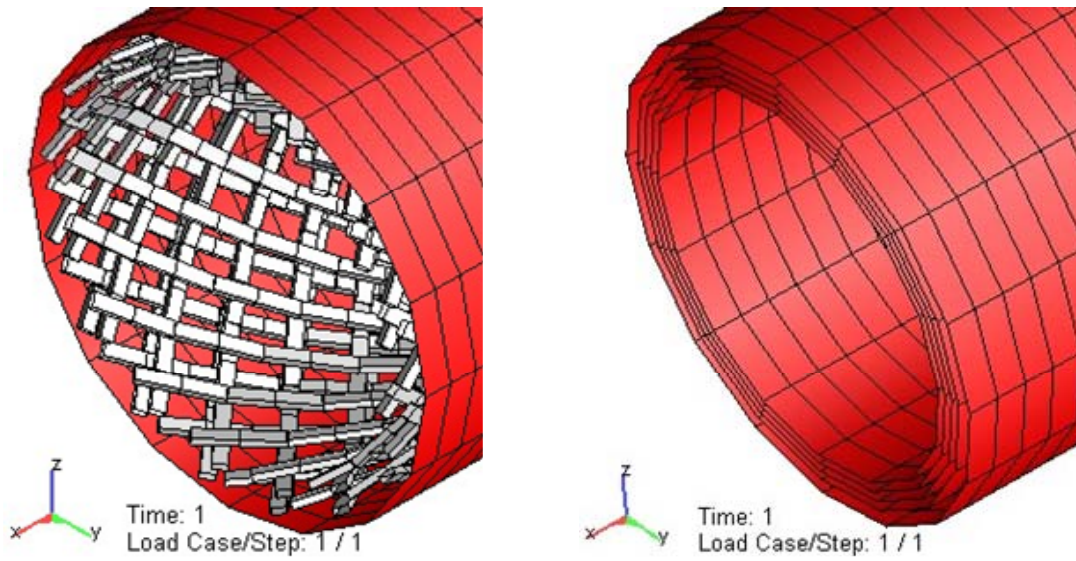
Table 4.6, Element distribution for ITCODE 0 case

	Element type	Number of Elements	explanation
core	pipe52	299	core element group
bendstiffener	pipe52	55	bending stiffener
bscontact	cont130	55	contact between bending stiffener and core
rigidpipe	pipe31	59	rigid pipe (rocking head)
rightpipe	pipe31	39	rigid pipe(tensioner at right side)
tenslayer1	hshear352	4784	tensile armour layer (inner most)
tenslayer2	hshear352	4784	-
tenslayer3	hshear352	4784	-
tenslayer4	hshear352	4784	tensile armour layer (outmost)

Table 4.7, Element distribution for ITCODE 31 case

	Element type	Number of Elements	explanation
core	pipe52	299	core element group
bendstiffener	pipe52	55	bending stiffener
bscontact	cont130	55	contact between bending stiffener and core
rigidpipe	pipe31	59	rigid pipe (rocking head)
rightpipe	pipe31	39	rigid pipe(tensioner at right side)
tenslayer1	pipe52	299	tensile armour layer (inner most)
tenslayer2	pipe52	299	-
tenslayer3	pipe52	299	-
tenslayer4	pipe52	299	tensile armour layer (outmost)

For ITCODE0 case, the cross section of tensile armour layer is modeled completely. The element type HSHEAR352 is applied for tensile armour. In this thesis, the tensile armour layer is represented by 16 tendons, shown in figure 4.7a. For ITCODE 31 case, the cross section of flexible pipe is shown in figure 4.7b.



a, cross section for ITCODE0

b, cross section for ITCODE31

Figure 4.7, cross section for ITCODE0 and ITCODE31

Two load cases are analyzed by utilization of BFLEX 2010, with both ITCODE 0 formulation and ITCODE 31 formulation respectively. The results are available in Chapter 5. The input file for LC1 and LC2 with ITCODE0 and ITCODE 31 bending formulation are in the appendix.

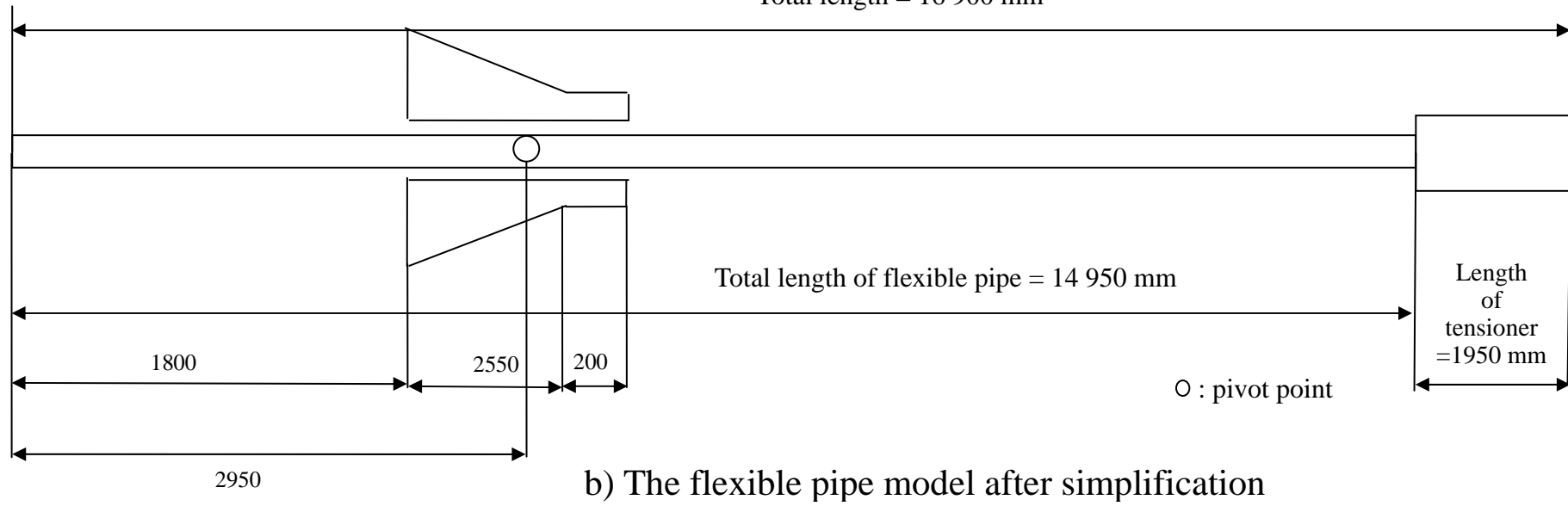
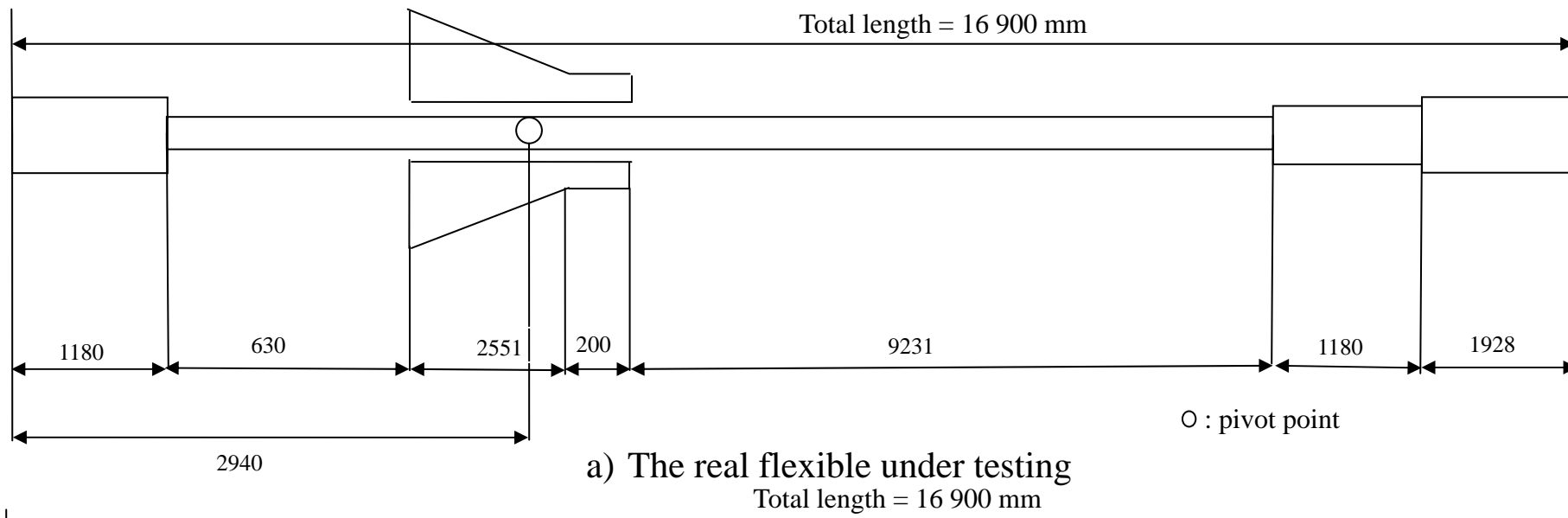


Figure 4.8, real flexible pipe and the model that is used in BFLEX 2010

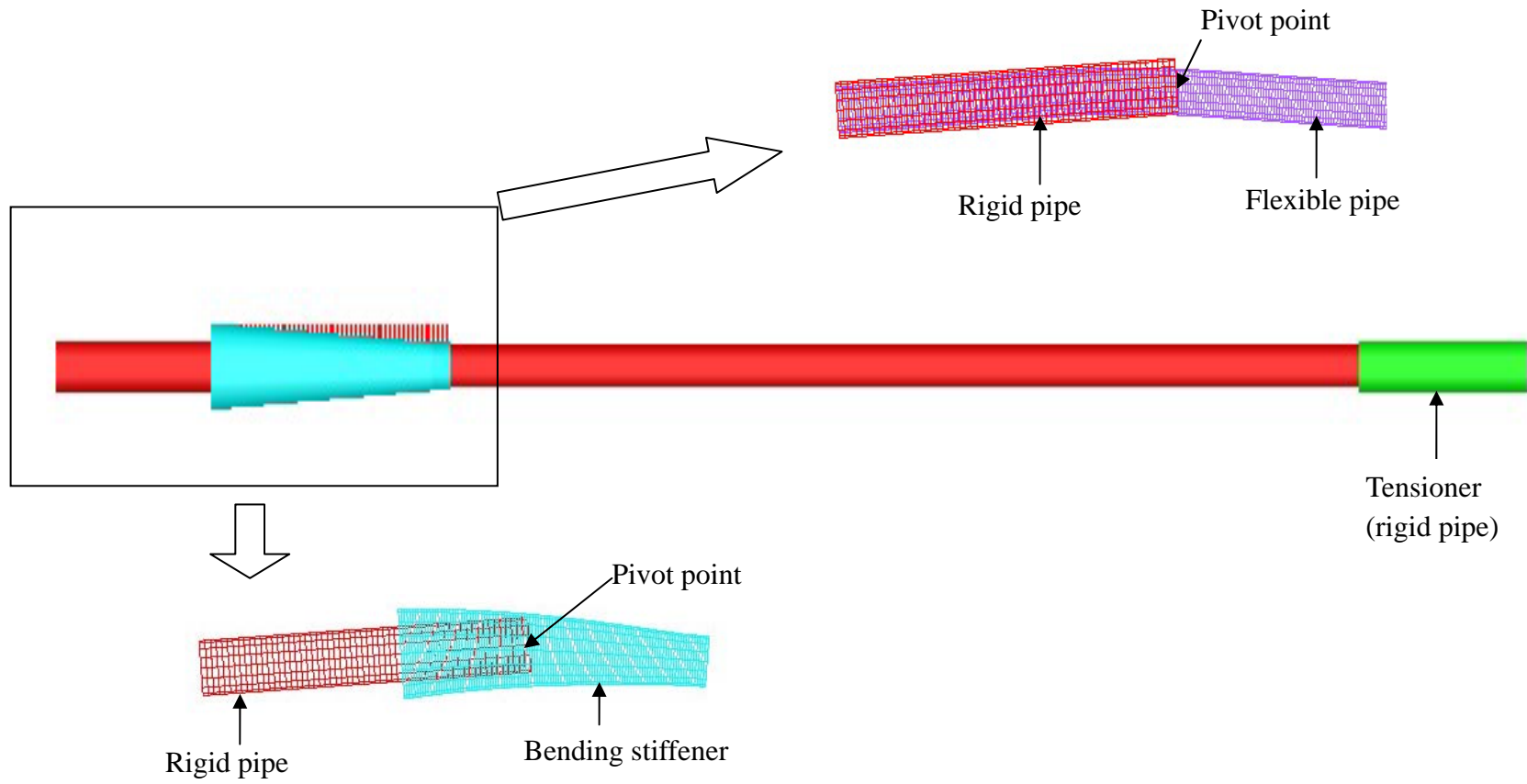


Figure 4.9, the model in BFLEX 2010

Chapter 5. BFLEX analysis

5.1 Introductions

In this chapter, the BFLEX analysis result is summarized. As we mentioned in section 4.2.4, two load cases LC1 and LC2 are analyzed by BFLEX. For each load case, the BFLEX analysis with bending formulation ITCODE 0 and ITCODE 31 is carried out. In this thesis, we focus on the fatigue damage of tensile armour layer. Also the fatigue damages on the Zeta-pressure armour and flat spiral are available.

The loading parameters in each load case are as follows:

- ◆ Load Case 1: 725 kN tension, 400 000 cycles, rocking angle ± 7.5 degree
- ◆ Load Case 2: 750 kN tension, 200 000 cycles, rocking angle ± 12.5 degree

After the post-processing is finished by BFLEX2010POST module, the BOUNDARY and PFLEX modules will process the data. The BOUNDARY program could put 6 cross section models at the location where the maximum curvature occurs. And then the stress components on the cross section of zeta pressure armour and flat spiral are calculated by the boundary element method. The Pflex program would put 6 windings of zeta pressure armour and 6 windings of flat spiral at the location where the maximum curvature occurs. Through the process of Pflex model, the beam bending stress components are available.

The cumulative fatigue damage is concluded by the LIFETIME module. After processing of LIFETIME module, the fatigue damage results are available, for tensile armour layer, boundary model of zeta-spiral and flat pressure spiral. Fatigue damage is given in the form of Miner Sum. This is the fatigue form which is frequently used for the assessment of cumulative damage in offshore industry engineering.

Pflex module performs bending stress analysis on the pressure armour. There are transverse curvature bending stress and normal curvature bending stress components on the cross section of pressure armour. The transverse curvature bending is about the vertical axis on the cross section, while the normal curvature bending is about the horizontal axis on the cross section, as shown in figure 5.1.

The total beam stress on the cross section is the sum of axial stress, normal curvature bending stress and the transverse bending stress. In Pflex, this total beam stress refers to total longitudinal stress.

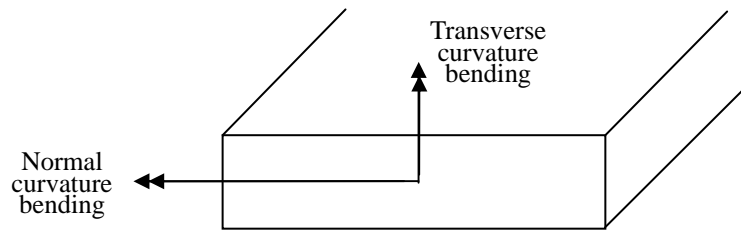


Figure 5.1, transverse curvature bending and normal curvature bending

5.2 ITCODE 0 CASE

5.2.1 Load Case 1, ITCODE 0

The curvature distribution at each load step along the longitudinal stress of flexible pipe is shown in figure 5.2.

Maximum curvature occurs at the location of 2700 mm along the flexible pipe, with the value of 0.0583

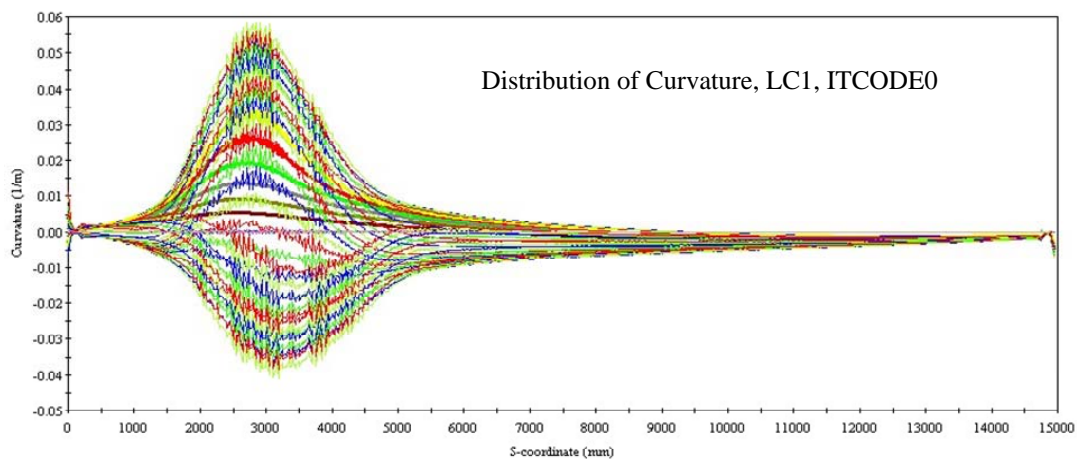


Figure 5.2, the distribution of curvature at each load step, LC1, ITCODE0

◆ Fatigue damage of tensile armour layer

The fatigue damage of 4 tensile armour layers is shown in figure 5.5.

The maximum fatigue damage for each tensile armour layer is shown in table 5.1.

Table 5.1, Maximum fatigue damage for tensile layer, LC1, ITCODE 0

	Tensile layer 1	Tensile layer 2	Tensile layer 3	Tensile layer 4
Miner Sum	0.54069	0.0665754	0.0063712	0.000142453

◆ Fatigue damage in BOUNDARY model

Fatigue damage for pressure armour is shown in figure 5.3. In figure 5.3, red parts denote the area in which the value of Miner sum exceeds 1.0.

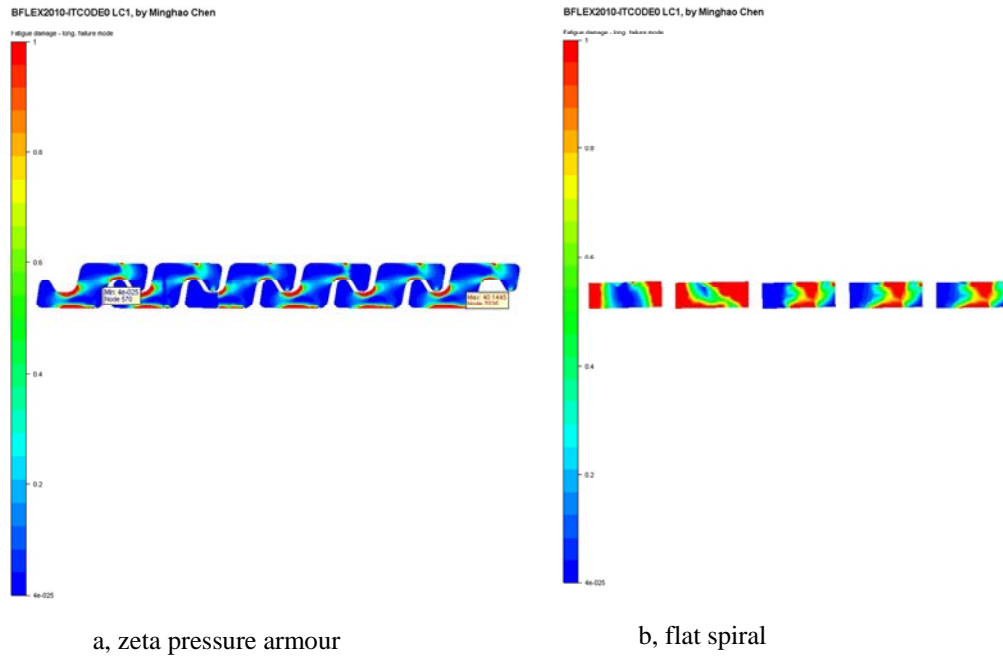


Figure 5.3, fatigue on the cross section of zeta pressure armour and flat spiral (LC1, ITCODE 0)

◆ Pflex analysis

The Pflex result is shown in figure. The distribution of total longitudinal stress is shown in figure 5.4.

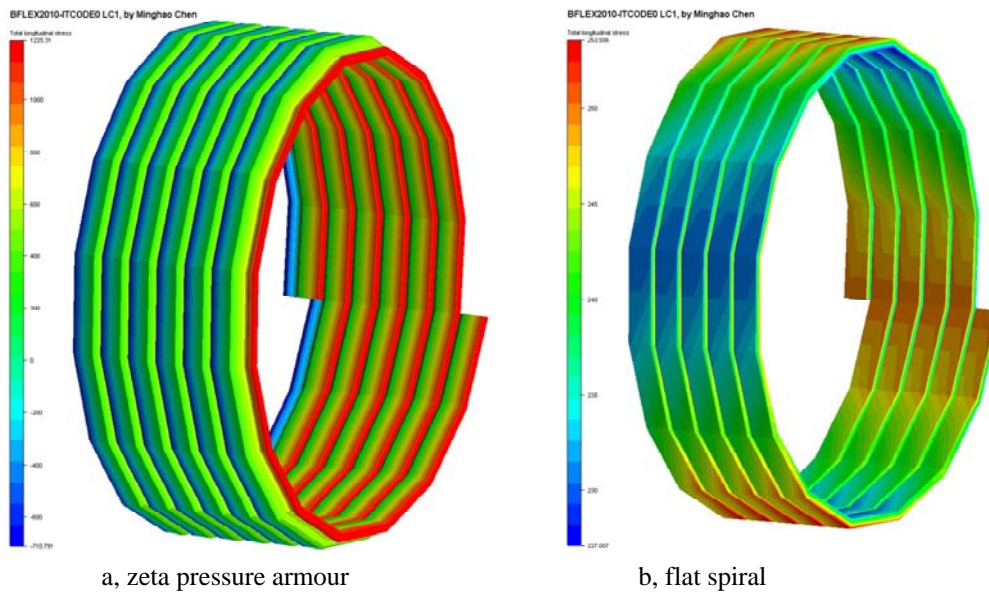


Figure 5.4, distribution of total longitudinal stress, LC1, ITCODE 0

Results of Pflex analysis is summarized in table 5.2.

Table5.2, Pflex results- LC1- ITCODE0

	zeta pressure amour	flat spiral
Max. of axial stress (MPa)	257.1	240.7
Max of normal curvature bending stress (MPa)	51.2	9.8
Max of transverse curvature bending stress (MPa)	969.9	3.5
Max of total longitudinal stress (MPa)	1226.1	253.6

The maximum value of total longitudinal stress is 1226 MPa. The maximum value of transverse curvature bending stress is 969 MPa, which is much larger than that of normal curvature bending stress. The transverse curvature bending stress is about the strong axis of spiral's cross section. This is very typical for the Zeta pressure armour profile. For the flat spiral, this conclusion applies, too.

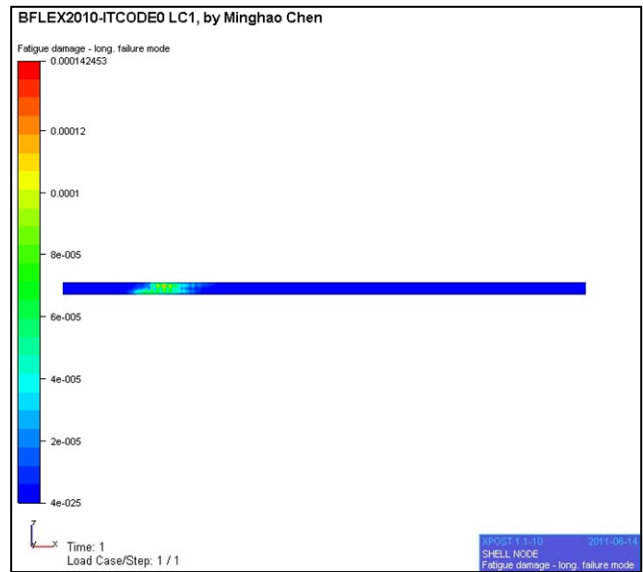
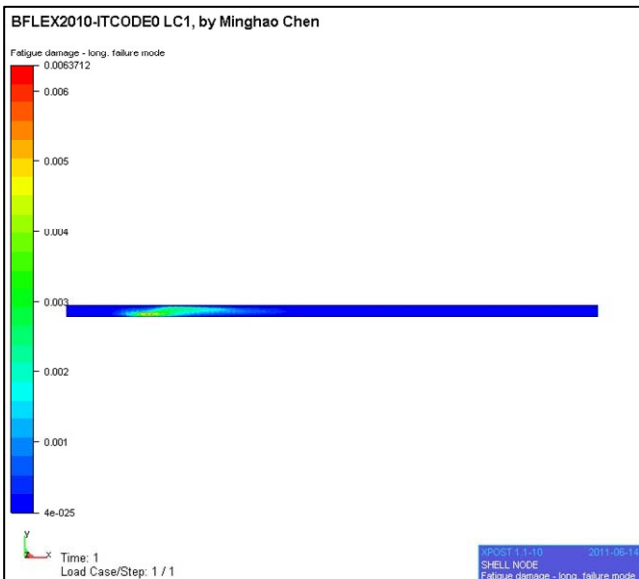
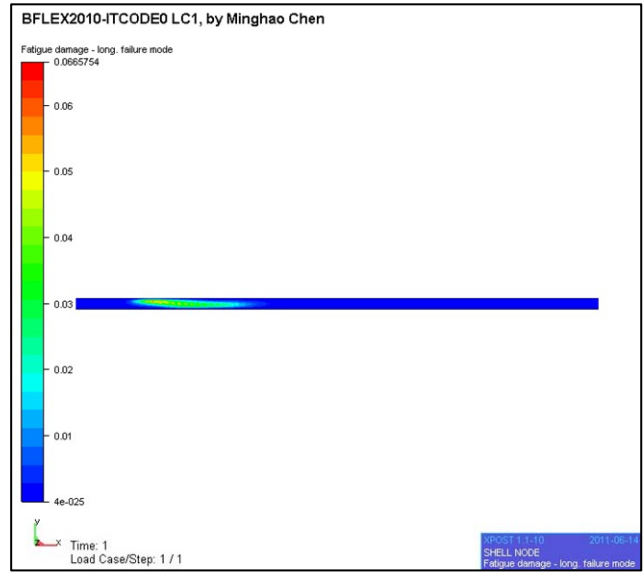
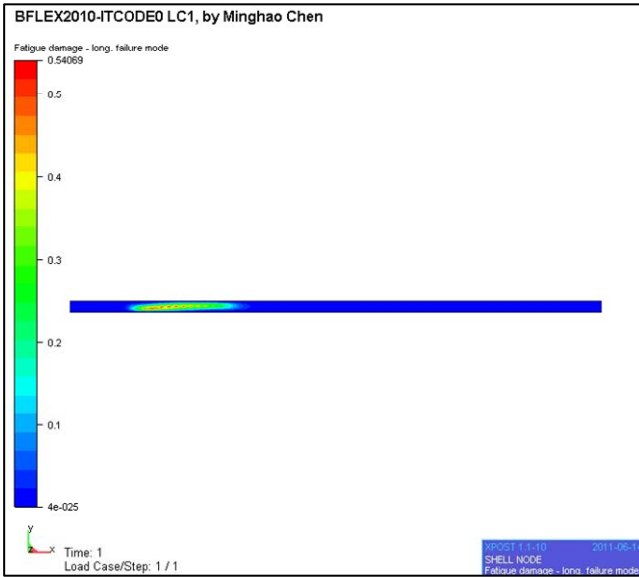


Figure 5.5, Fatigue damage for 4 tensile armour layers, LC1, ITCODE 0

5.2.2 Load Case 2, ITCODE 0

The distribution of curvature is shown in figure 5.6. Location of maximum curvature is 2850, with maximum value of 0.0939.

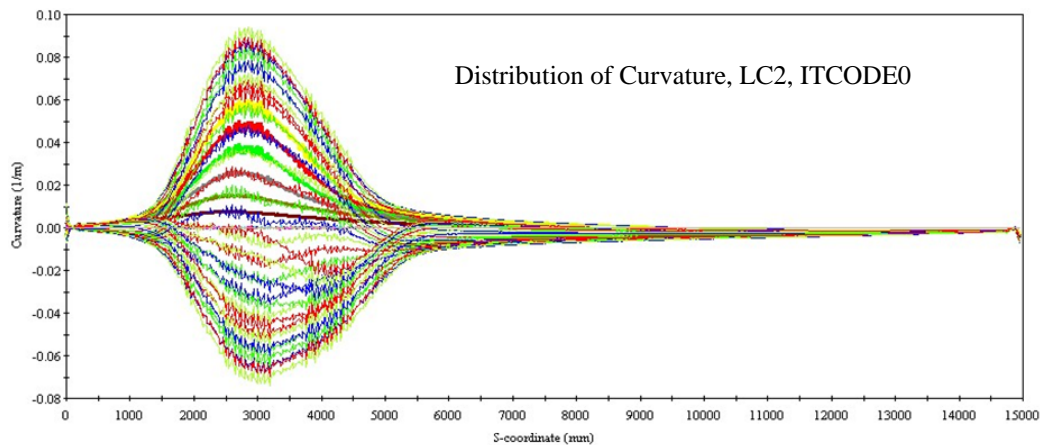


Figure 5.6, the distribution of curvature at each load step, LC2, ITCODE0

◆ Fatigue damage of tensile armour layer

The fatigue damage of 4 tensile armour layers is shown in figure 5.9.

The maximum fatigue damage for each tensile armour layer is shown in table 5.3.

Table 5.3, Maximum fatigue damage for tensile layer, LC2, ITCODE 0

	Tensile layer 1	Tensile layer 2	Tensile layer 3	Tensile layer 4
Miner Sum	0.423154	0.0564425	0.0076588	0.00128088

◆ Fatigue damage in BOUNDARY model

Fatigue damage for pressure armour is shown in figure 5.7. Red parts denote the area in which the value of Miner sum exceeds 1.0.

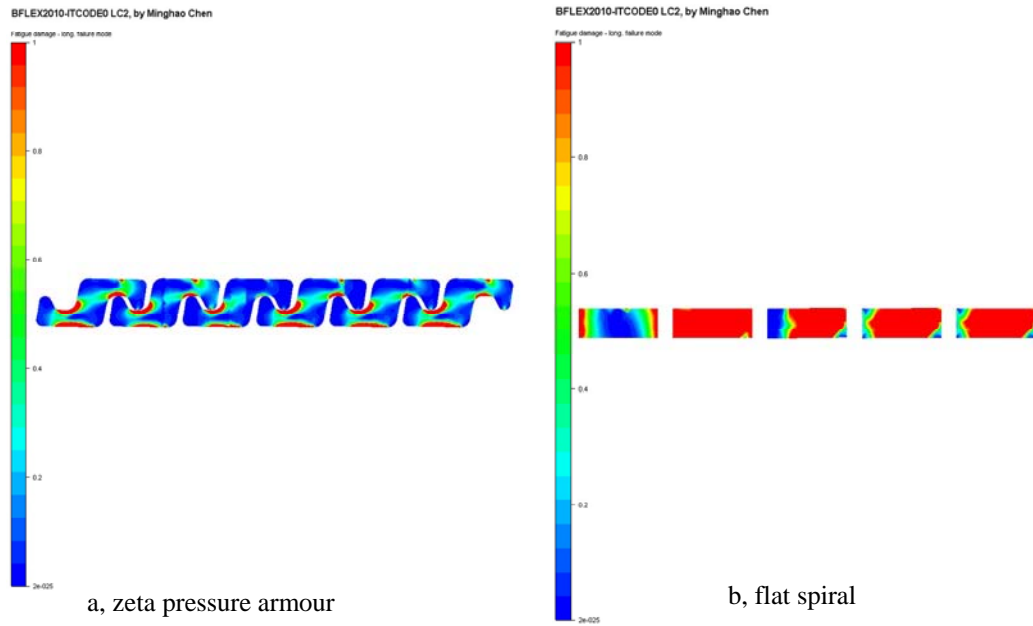


Figure 5.7, fatigue on the cross sections of zeta pressure armour and flat spiral (LC2, ITCODE 0)

◆ Pflex analysis

The distribution of total longitudinal stress is shown in figure 5.8.

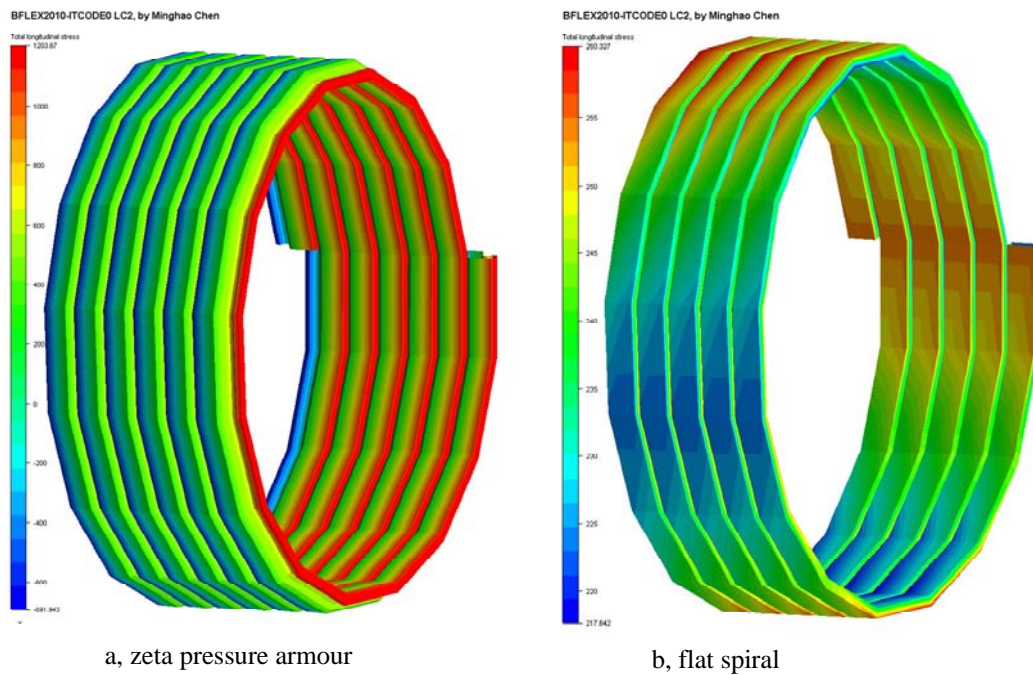


Figure 5.8, distribution of total longitudinal stress (LC2, ITCODE 0)

Results of Pflex analysis is summarized in table 5.4.

Table 5.4, Pflex results- LC2- ITCODE0

	zeta pressure amour	flat spiral
Max. of axial stress (MPa)	255.9	239.6
Max of normal curvature bending stress (MPa)	68.0	15.4
Max of transverse curvature bending stress (MPa)	974.1	5.9
Max of total longitudinal stress (MPa)	1236.9	260.3

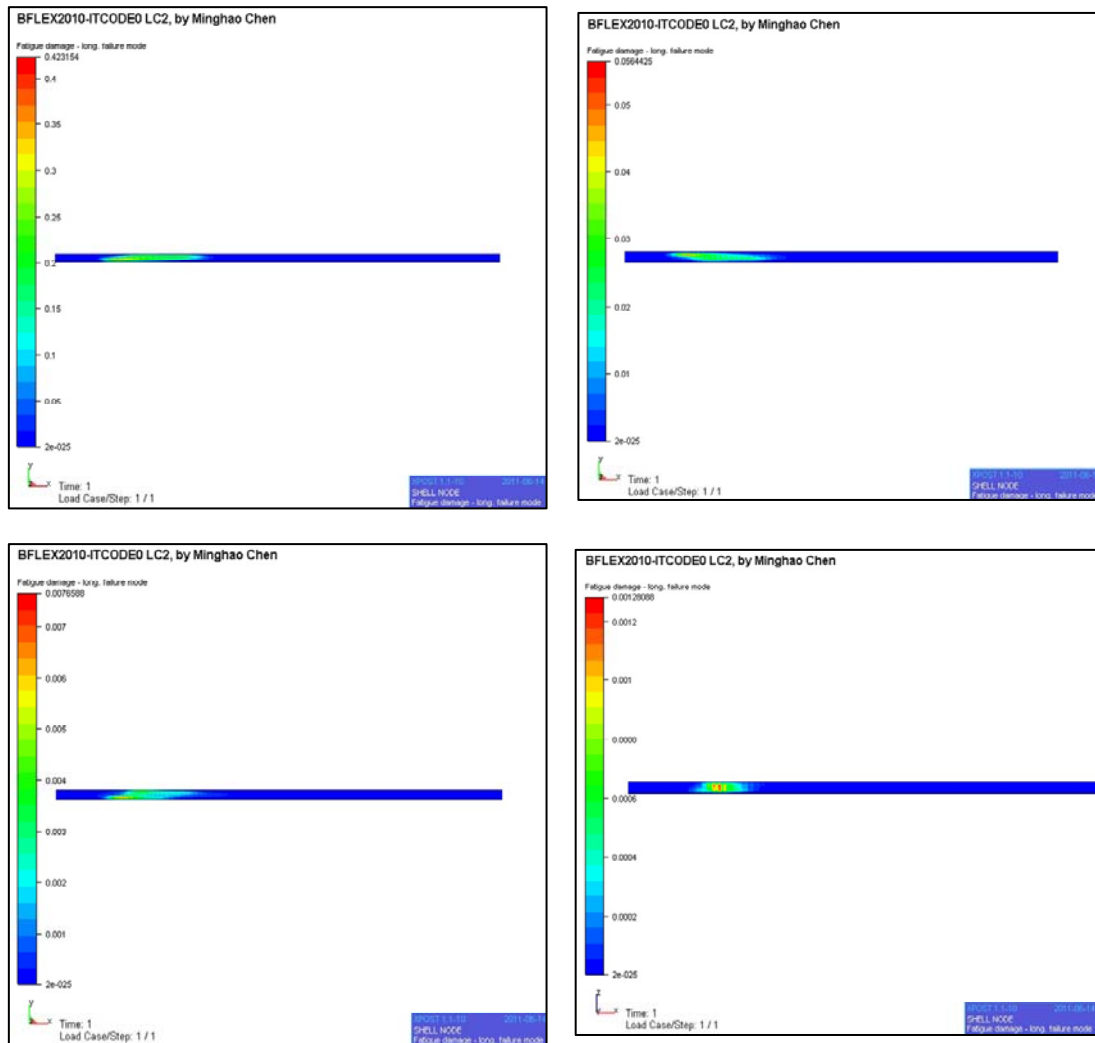


Figure 5.9, Fatigue damage for 4 tensile armour layers, LC2, ITCODE 0

5.3 ITCODE 31 CASE

5.3.1 Load Case 1, ITCODE 31

LC1- tension 725 kN, 400 000 cycles, with rocking angle ± 7.5 degree

The curvature distribution at each load step along the longitudinal stress of flexible pipe is shown in figure 5.10. Location of maximum curvature is 2550 mm, with maximum value of 0.0552.

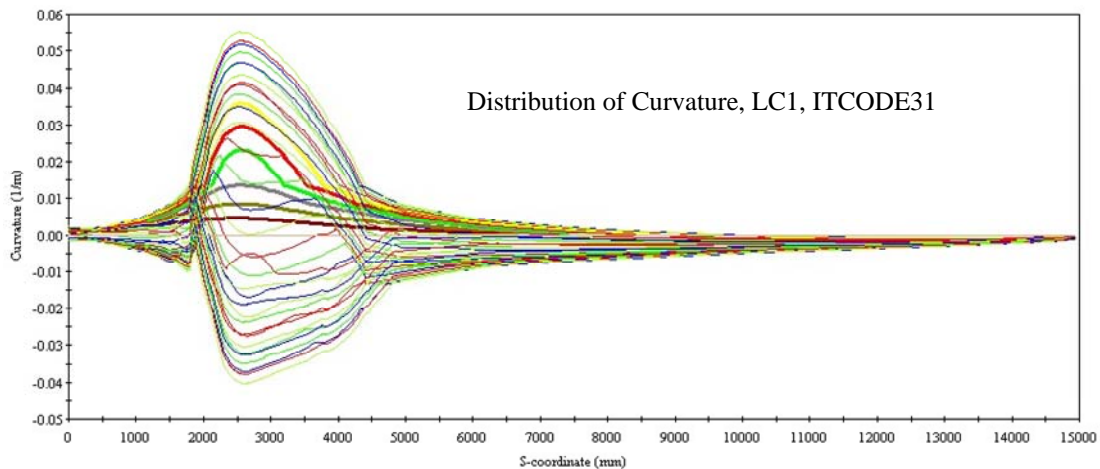


Figure 5.10, the distribution of curvature at each load step, LC1, ITCODE31

The fatigue damage of 4 tensile armour layers is shown in figure 5.13.

The maximum fatigue damage for each tensile armour layer is shown in table 5.5.

Table 5.5, Maximum fatigue damage for tensile layer, LC1, ITCODE 31

	Tensile layer 1	Tensile layer 2	Tensile layer 3	Tensile layer 4
Miner Sum	0.315207	0.038403	0.00437152	0.000121658

◆ Fatigue damage in BOUNDARY model

Fatigue damage for pressure armour is shown in figure 5.11. Red parts denote the area in which the value of Miner sum exceeds 1.0.

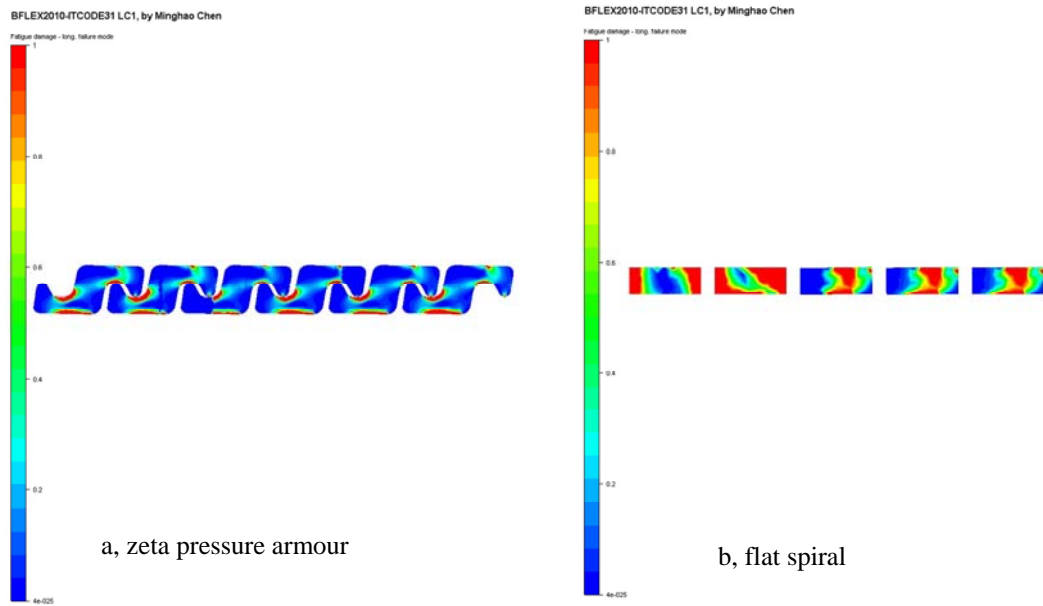


Figure 5.11, fatigue on the cross sections of zeta pressure armour & flat spiral (LC1, ITCODE 31)

◆ Pflex analysis

The distribution of total longitudinal stress is shown in figure 5.12.

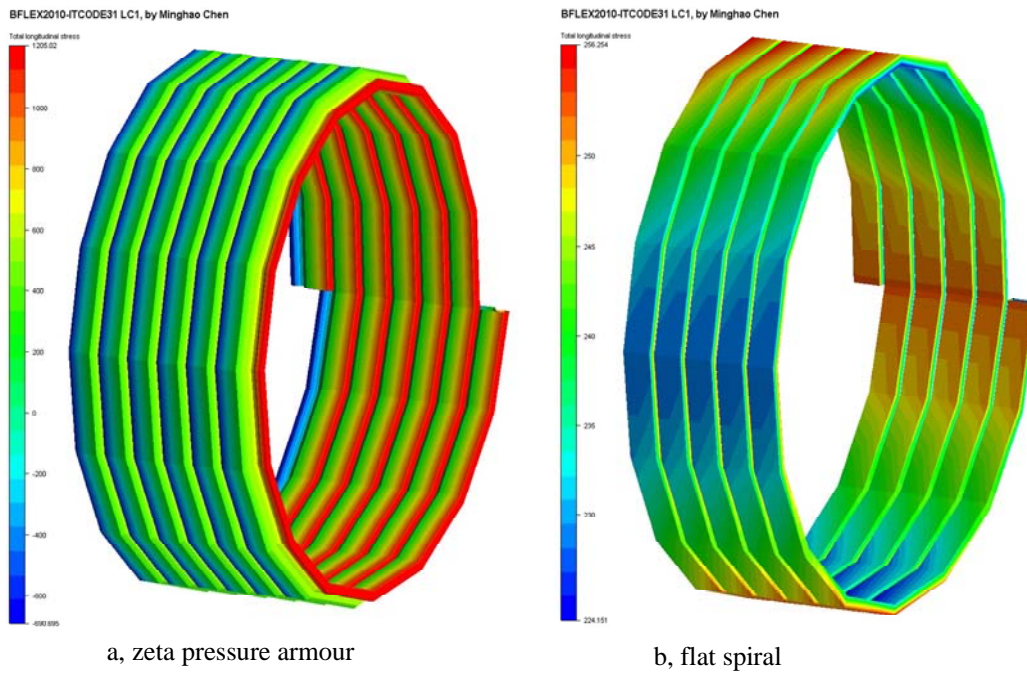


Figure 5.12, distribution of total longitudinal stress (LC1, ITCODE 31)

Results of Pflex analysis is summarized in table 5.6.

Table 5.6, Pflex results- LC2- ITCODE0

	zeta pressure amour	flat spiral
Max. of axial stress (MPa)	257.2	240.8
Max of normal curvature bending stress (MPa)	59.1	12.5
Max of transverse curvature bending stress (MPa)	970.1	3.7
Max of total longitudinal stress (MPa)	1231.6	256.3

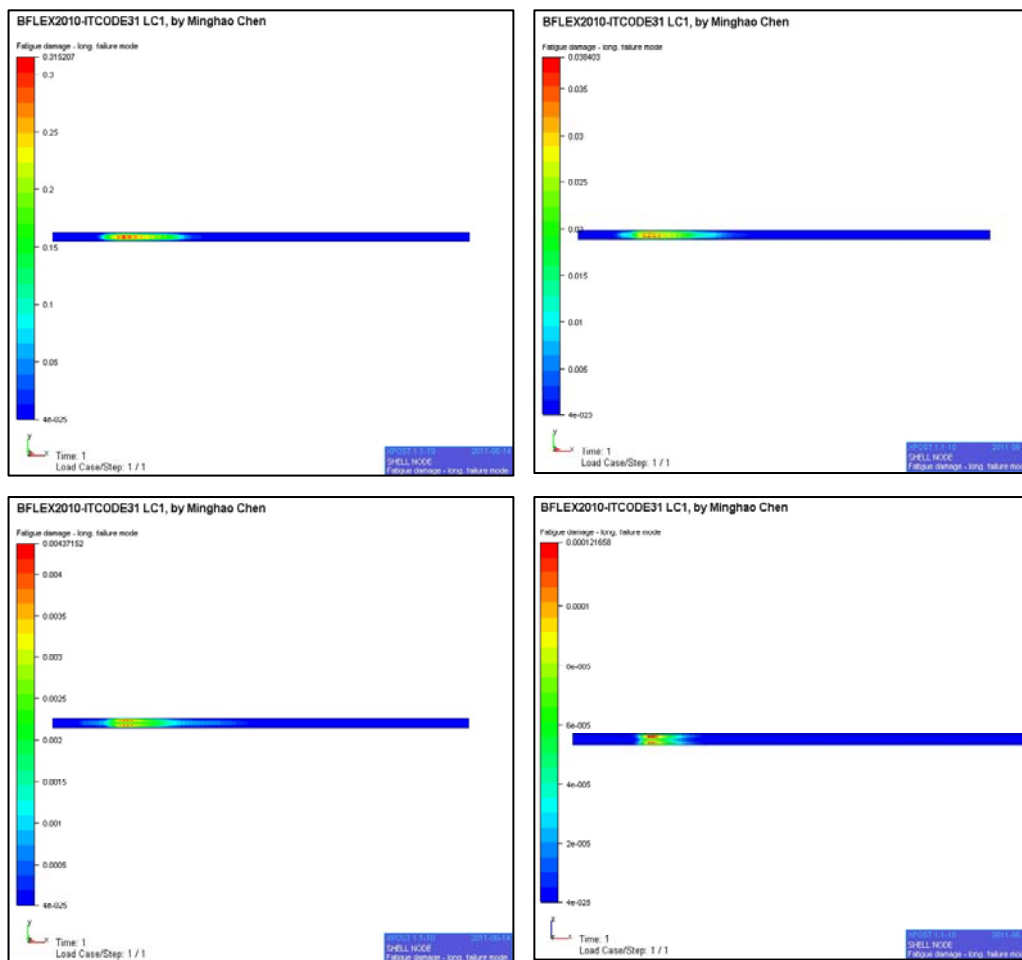


Figure 5.13, Fatigue damage for 4 tensile armour layers, LC1, ITCODE 31

5.3.2 Load Case 2, ITCODE 31

LC2- tension 750 kN, 200 000 cycles, with rocking angle ± 7.5 degree

The curvature distribution at each load step along the longitudinal stress of flexible pipe is shown in figure 5.14. Location of maximum curvature is 2550 mm, with maximum value of 0.0896.

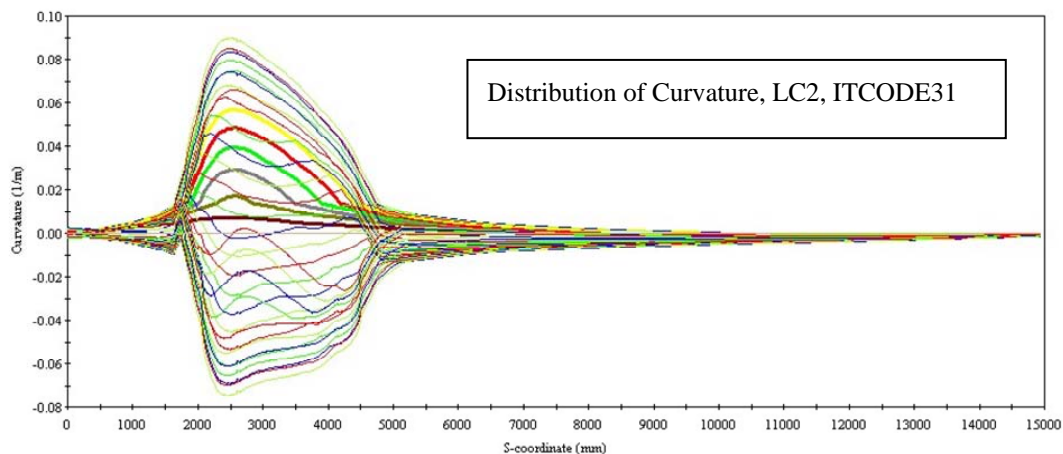


Figure 5.14, the distribution of curvature at each load step, LC2, ITCODE31

The fatigue damage of 4 tensile armour layers is shown in figure 5.17.

The maximum fatigue damage for each tensile armour layer is shown in table 5.7.

Table 5.7, Maximum fatigue damage for tensile layer, LC1, ITCODE 31

	Tensile layer 1	Tensile layer 2	Tensile layer 3	Tensile layer 4
Miner Sum	0.268044	0.0377718	0.0074873	0.00109364

◆ Fatigue damage in BOUNDARY model

Fatigue damage for pressure armour is shown in figure 5.15 Red parts denote the area in which the value of Miner sum exceeds 1.0.

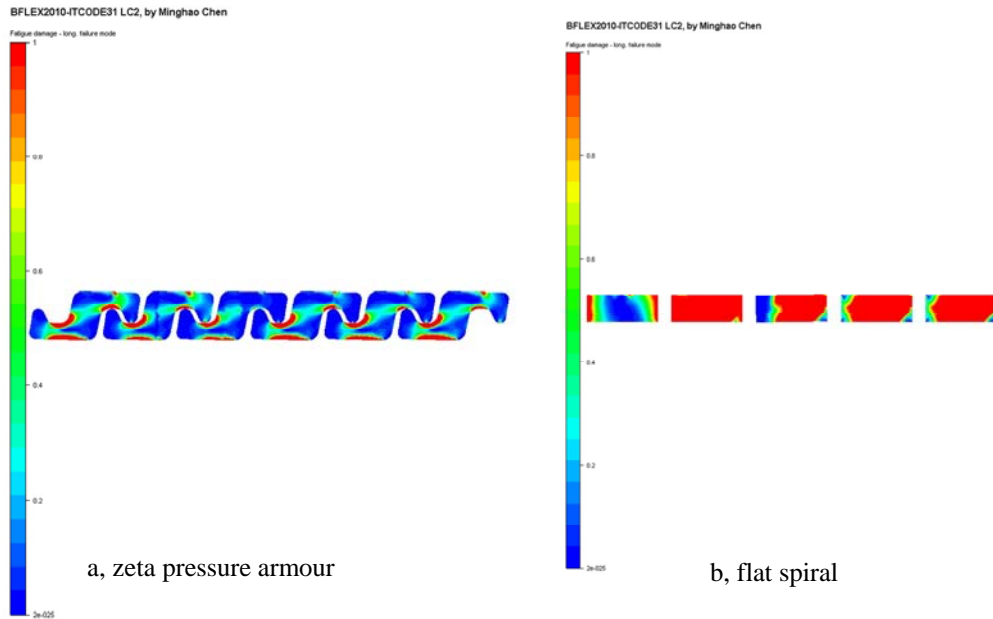


Figure 5.15, fatigue on the cross sections of zeta pressure armour & flat spiral (LC2, ITCODE 31)

◆ Pflex analysis

The distribution of total longitudinal stress is shown in figure 5.16.

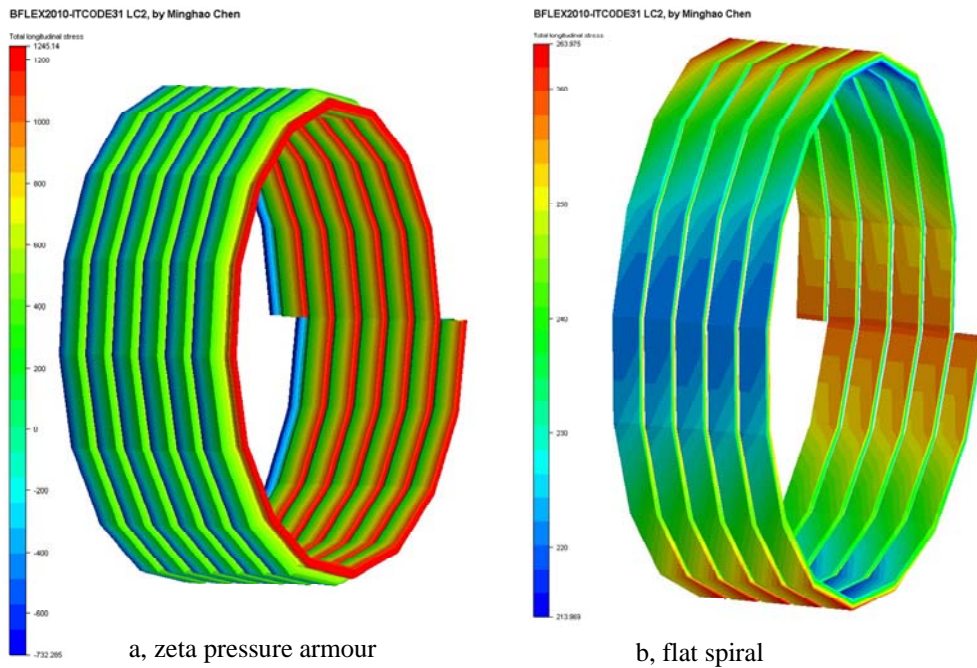


Figure 5.16, distribution of total longitudinal stress (LC2, ITCODE 31)

Results of Pflex analysis is summarized in table 5.8.

Table 5.8, Pflex results- LC2- ITCODE0

	zeta pressure amour	flat spiral
Max. of axial stress (MPa)	256.3	239.9
Max of normal curvature bending stress (MPa)	79.4	19.2
Max of transverse curvature bending stress (MPa)	974.3	6.0
Max of total longitudinal stress (MPa)	1245.1	263.9

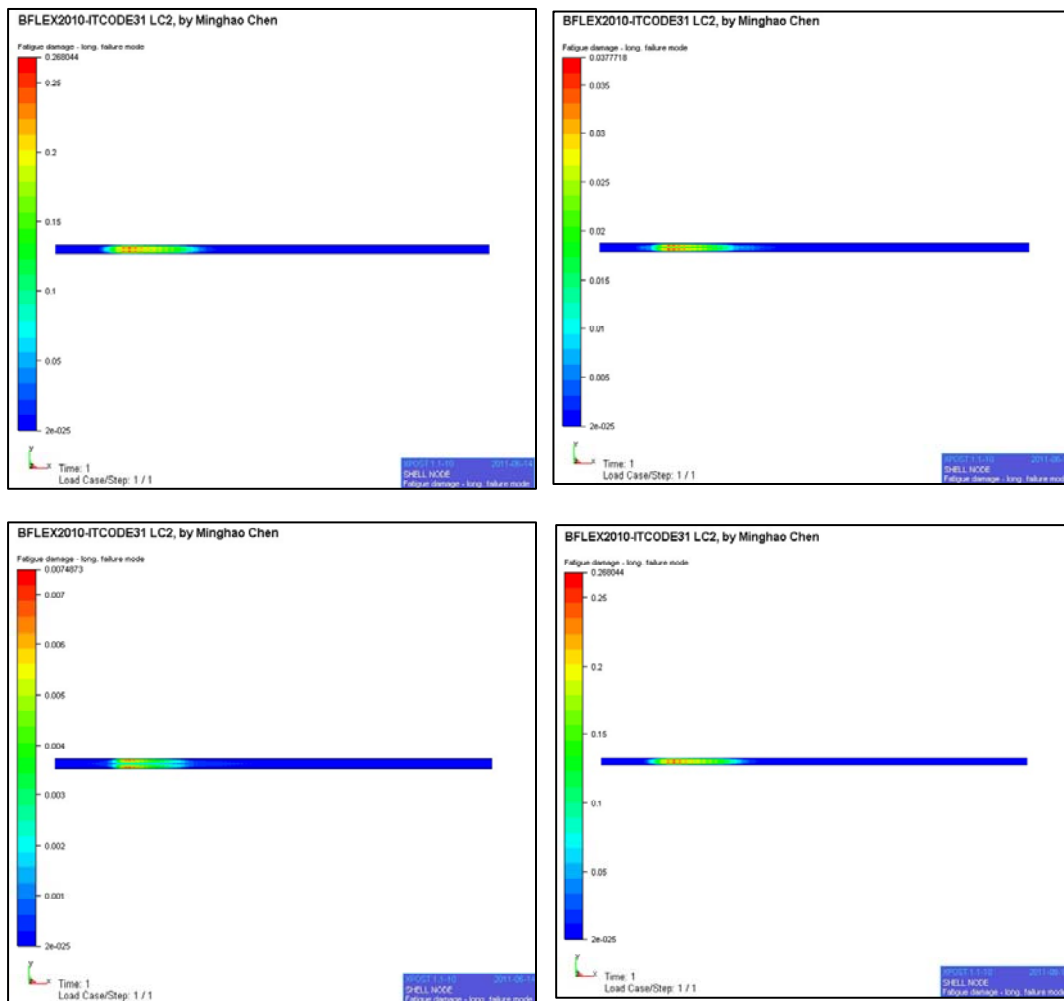


Figure 5.17, Fatigue damage for 4 tensile armour layers, LC2, ITCODE 31

5.4 Combination of LC1 and LC 2

In the real testing, LC2 follows LC2. The BFLEX analysis on the combination of LC1 and LC 2 is also carried out, utilizing ICODE 31 and ITCODE0 bending formulation respectively. The fatigue damage of the innermost tensile armour layer is shown in figure 5.18.

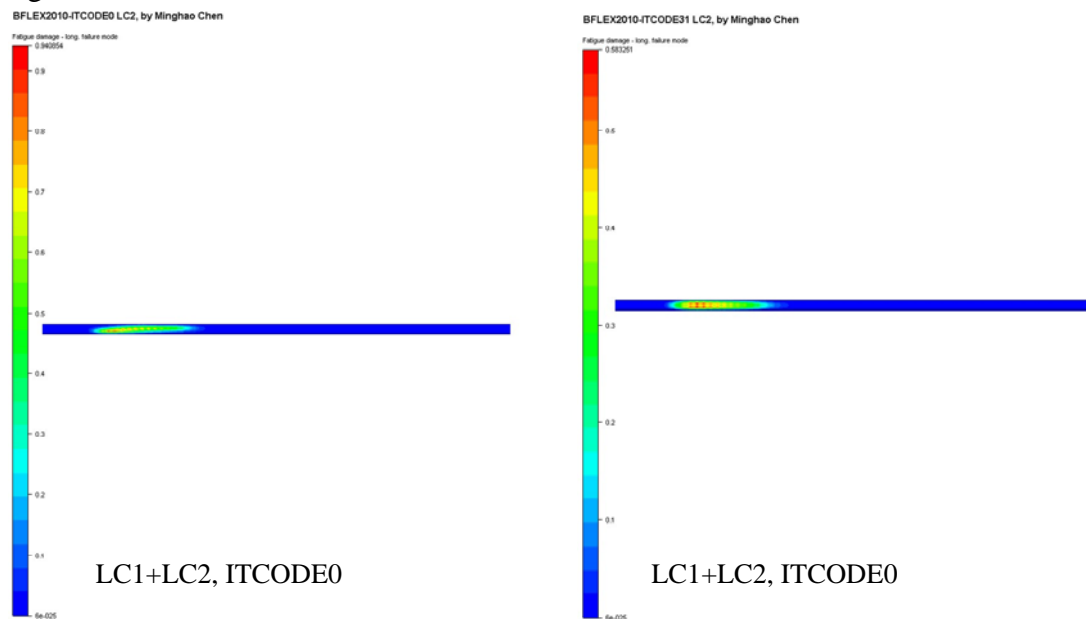


Figure 5.18, fatigue damage, LC1+LC2

The fatigue damage for each tensile armour layer is summarized in table 5.9.

Table 5.9, fatigue damage on tensile armour layer, LC1+LC2

	ITCODE 0	ITCODE 31
tensile armour layer 1	0.940854	0.583152
tensile armour layer 2	0.123018	0.0761748
tensile armour layer 3	0.01403	0.0109038
tensile armour layer 4	0.00142334	0.00121199

5.5 Comparison of fatigue damage on tensile armour

For a same load case, the fatigue damage on tensile armour is different, when we are utilizing different ICODE in the BFLEX analysis. This is due to the principle which defines the bending formulation of the cross section.

Table 5.10, comparison of fatigue damage between ITCODE0 and ITCODE31

	load case 1		load case 2		LC1+LC2	
	itcode 0	itcode 31	itcode 0	itcode 31	itcode 0	itcode 31
tensile layer 1	0.54069	0.315207	0.423154	0.268044	0.940854	0.583152
tensile layer 2	0.0665754	0.038403	0.0564425	0.0377718	0.123018	0.0761748
tensile layer 3	0.0063712	0.00437152	0.0076588	0.0074873	0.01403	0.0109038
tensile layer 4	0.000142453	0.000121658	0.00128088	0.00109364	0.00142334	0.00121199

According to the data in table, it is obvious to see that the bending formulation ITCODE 0 gives a larger value of fatigue damage than ITCODE 31. This applies for each tensile armour layer. At the same time, the fatigue damage of innermost tensile armour layer is larger than that of other tensile armour layers. This demonstrates that the innermost tensile armour layer is subjected to the most severe fatigue damage. In the practical engineering design, the fatigue integrity of innermost tensile armour layer must be guaranteed first.

As described in section 3.3, the ITCODE 31 formulation shows a best fit with respect to the fatigue damage of tensile armour layer. So the fatigue damage of the innermost tensile armour layer 0.315207 and 0.268044 are more acceptable.

It is obvious to see that the materials at the contact point on the cross section of zeta pressure armour, are subjected to more fatigue loading. For other parts at the cross section of zeta pressure armour, the fatigue damage is not as significant as the contact locations. There exists a very significant interaction between flat spiral and innermost tensile armour layer, and between the flat spiral and zeta pressure armour layer. The flat spiral is subjected to lots of fatigue damage. In fact, the failure of zeta pressure armour and that of flat spiral is observed in the real testing held in MARINTEK.

Chapter 6. Comparison between BFLEX and measured data / correlation studies

6.1 Comparison between BFLEX calculation and strain gauge measurement

The BFLEX model in this thesis is based on the test in MARINTEK. In fact, the relevant stress data are available after the testing is over. Plenty of strain gauges are mounted on the flexible in order to get the strain data when the flexible pipe is under testing. The main purpose of the strain gauge is to measure the variation in axial and bending stress in the outer tensile armour layer. That is because the range of stress is crucial for the fatigue life of structures. In this section, the BFLEX calculation data and the strain gauge data will be compared. Through this way, the BFLEX stress model for bending stiffener cases would be calibrated.

6.1.1 Configuration of strain gauges

The strain gauges are installed on the outer tensile armour layer tendons. This is shown in figure 1 . The configuration of strain gauges is shown in figure 2. Strain gauges were mounted along two armour tendons with 90 degree phase difference throughout one pitch of each tendon. For each tendon, nine regularly spaced stations were made in the pipe, corresponding to an angular spacing between each station of 45 degree. In order to deviated between components, two strain gauges were mounted at each station, which gave altogether 36 strain gauges (station 1-18 in figure). In addition, two strain gauges were positioned at the neutral axis of pipe along the bending stiffener in order to measure the curvature gradient (station 19 and 20 in figure). the position of strain gauges are summarized in table 1. At each station, two strain gauges were mounted. They were mounted symmetric to the middle axis of tensile armour's tendon, and the transverse distance between these two stain gauges is 6 mm. This is shown in figure 3.



Figure 6.1, the strain gauges mounted on flexible pipe.

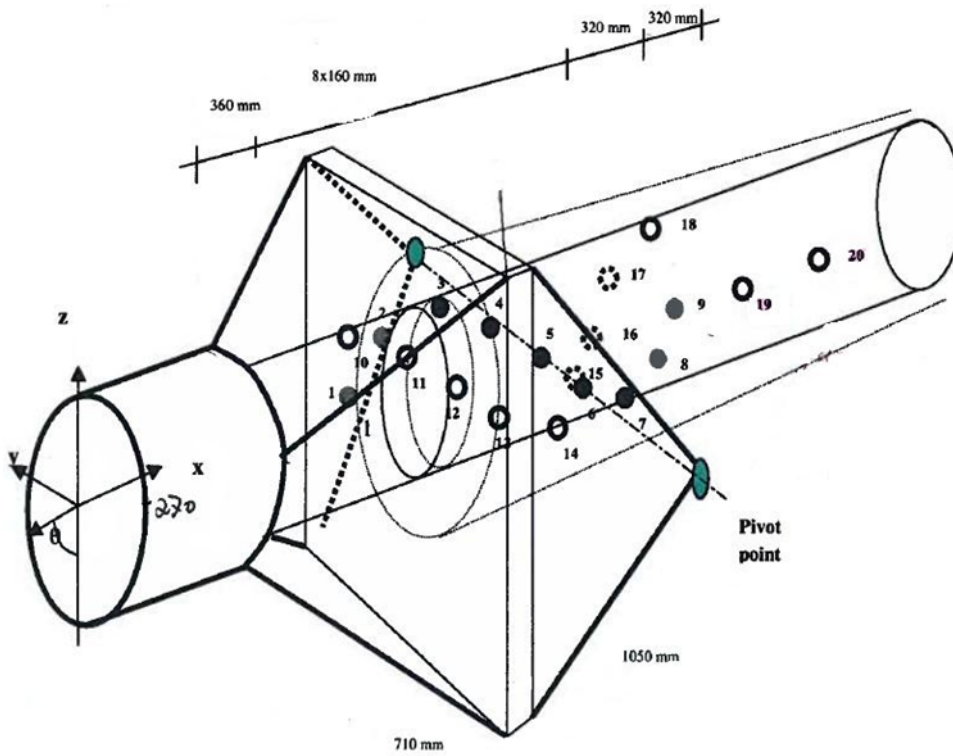


Figure 6.2, configuration of strain gauges

Table 6.1, positions of strain gauges

Station No.	Length from left end fitting (mm)	Angular position (degree)
1	360	90
2	520	135
3	680	180
4	840	225
5	1000	270
6	1160	315
7	1320	0
8	1480	45
9	1640	90
10	360	180
11	520	225
12	680	270
13	840	315
14	1000	0
15	1160	45
16	1320	90
17	1480	135
18	1640	180
19	1960	270
20	2280	270

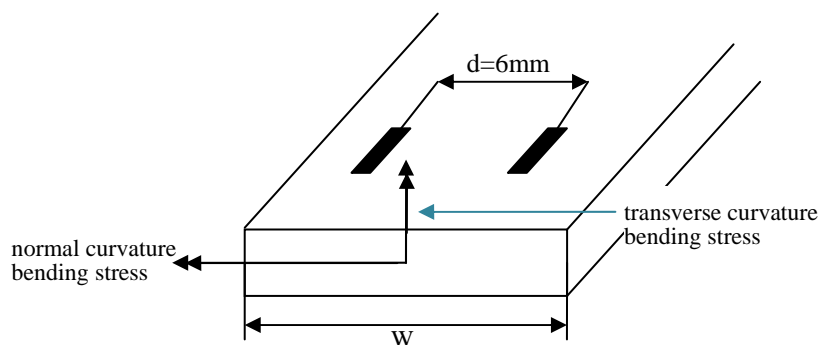


Figure 6.3, the strain gauges on tensile tendons

In figure 3, the black parts denote the strain gauges. The distance between them is 6 mm.

Let ε_1 and ε_2 denote the strain quantities from the two strain gauges in a same station. Then following expression could be concluded.

For the axial stress component:

$$\sigma_{\text{axial}} = E \cdot \frac{1}{2} \cdot (\varepsilon_1 + \varepsilon_2)$$

where E is the Young's modulus of tensile armour.

For the bending stress component

$$\sigma_{\text{bending}} = E \cdot \frac{1}{2} \cdot (\varepsilon_1 - \varepsilon_2) \cdot \frac{w}{d}$$

Where w is the distance between two strain gauges, and d denotes the thickness of tendon.

It is noted that there exists normal curvature bending stress at the outer surface of tendon. By this procedure, the σ_{axial} is not the real axial stress. In fact, the σ_{axial} here is the sum of real axial stress and the normal curvature stress component at the outer surface of tendon. However, since the tendon follows the loxodromic surface curve, the normal curvature stress component at surface is small compared with the transverse curvature stress and axial stress.

6.1.2 Strain gauge test program

The loading procedure was as follows:

1. zero strain gauge reading
2. apply international pressure
3. apply tension
4. apply the end angle cycles from zero to the maximum and minimum values throughout the prescribed number of cycles.

Here, two load cases are analyzed here, which is shown in table 2.

Table 6.2, the load cases in dynamic testing program

	Internal pressure (bar)	Tension (kN)	Cycling speed (Hz)	Max. angle (deg.)	Min. angle (deg.)	Number of bend cycles
LC1	475	725	0.01	8.5	-6.5	3
LC1	475	725	0.05	8.5	-6.5	3
LC3	475	1000	0.05	8.5	-6.5	3

Two LC1 cases are induced here. LC1 was carried out twice with different cycling speed. But what we care about in this chapter is the stress range at different strain gauges, so this does not have any kind of influence on our stress range values. In section 6.1.3, you will see we have two groups of data titled with LC1. The data of these two groups is very similar.

6.1.3 The comparison between BFLEX data and test results

The results in terms of measured and calculated dynamic stresses ranges are presented in figure 6.4 – figure 6.11. The results include axial stress, bending stress and total stresses. Here, the axial stress is not only the axial stress components on the cross section of tendon. It is the sum of axial stress and the normal curvature stress at the outer surface of tendon. The bending stress here refers to the transverse curvature bending stress. The stress quantities mean the stress range during the whole process of simulation.

M.Stress refers to the measured stress range, and C.Stress refers to the calculation stress range by BFLEX2010.



LC1—ITCODE 0—station 1-9

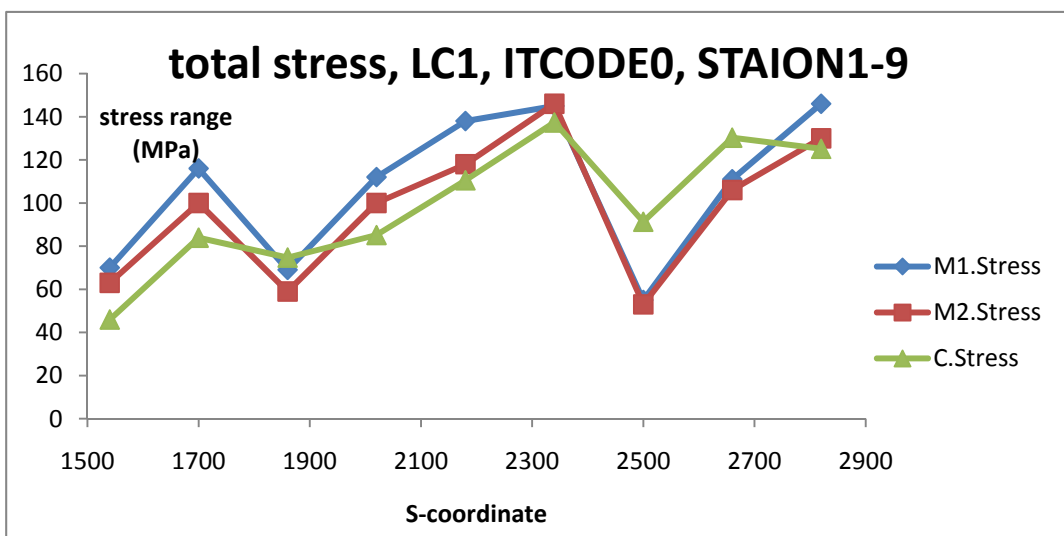
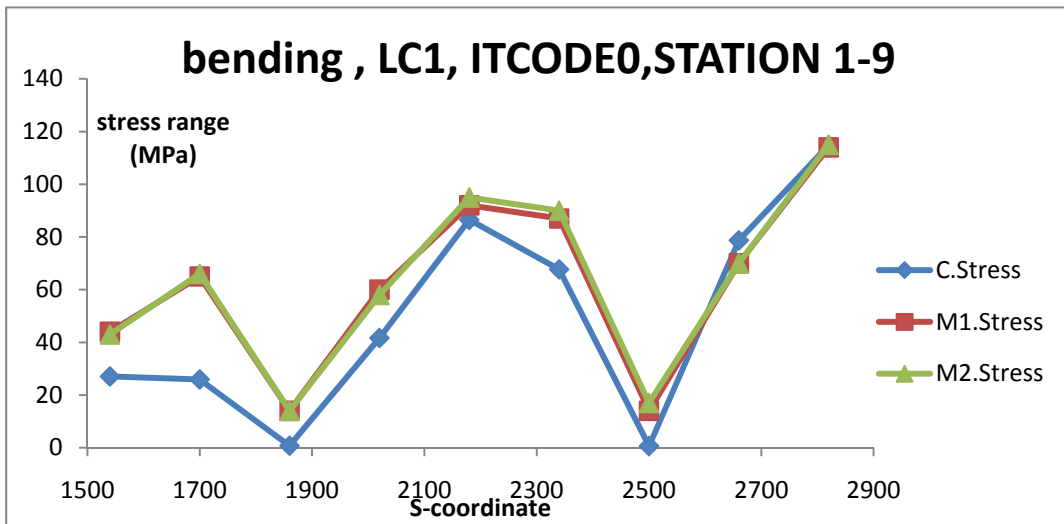
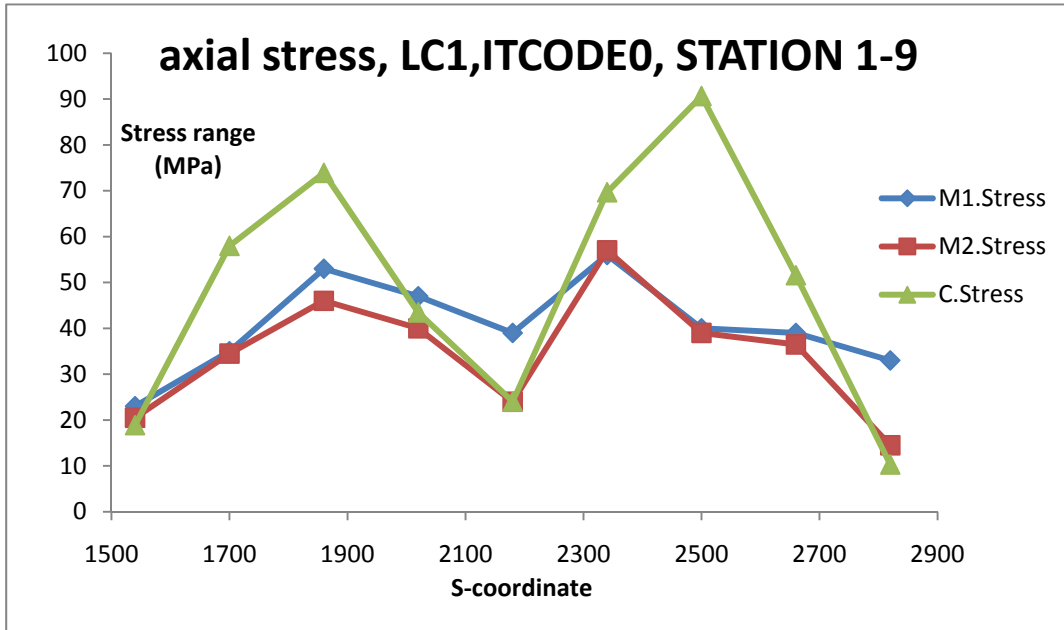


Figure 6.4, COMPARISON, LC1, ITCODE 0, stations 1-9



LC1—ITCODE 0—station 10-20

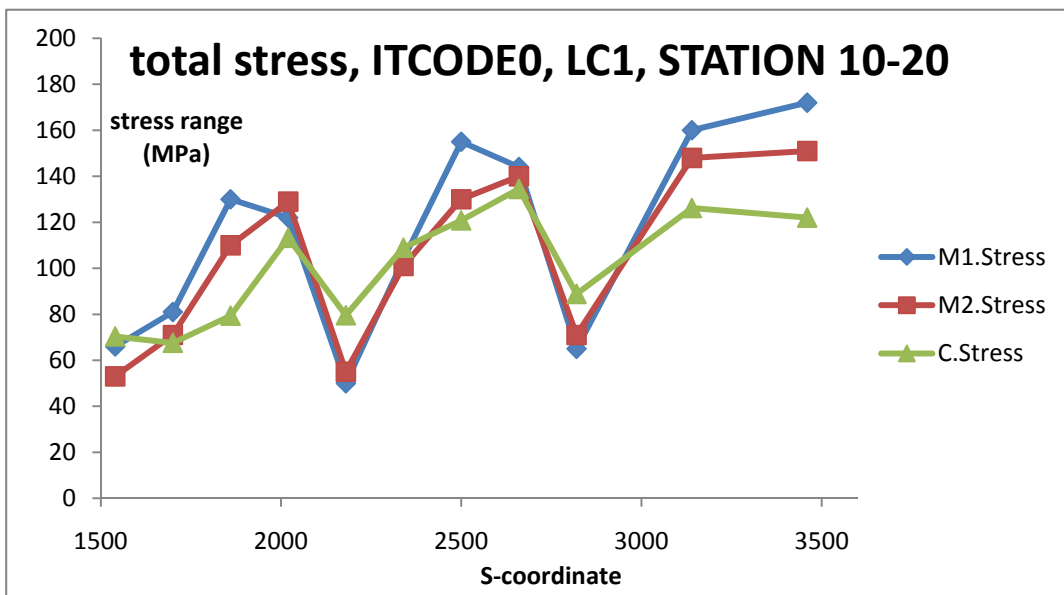
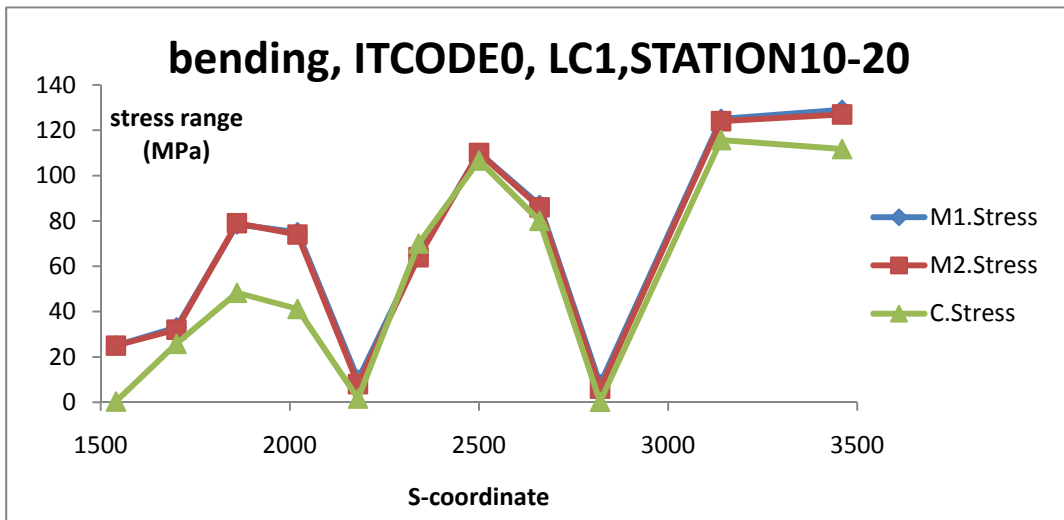
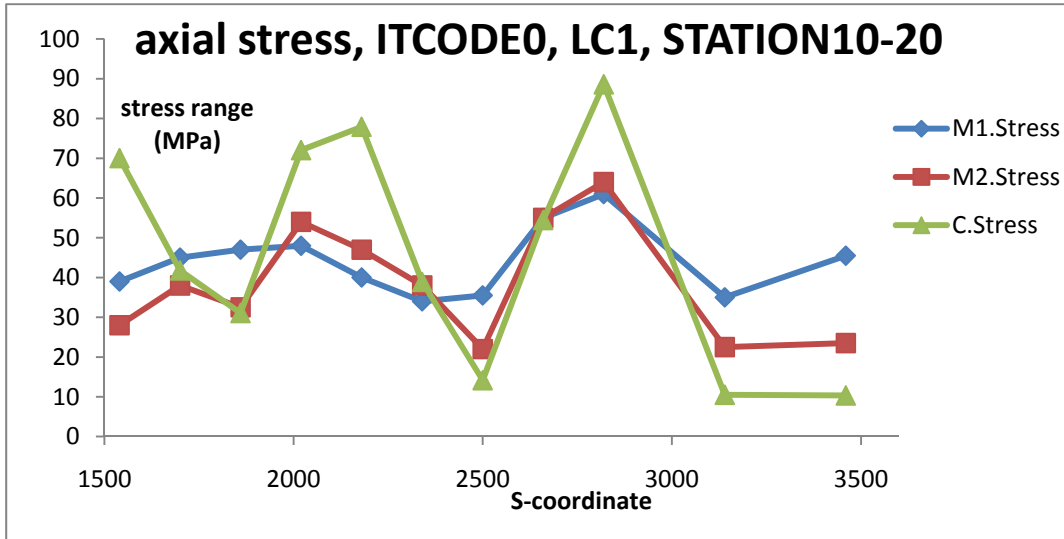


Figure6.5, COMPARISION, LC1, ITCODE 0, stations 10-20



LC1—ITCODE 31—station 1-9

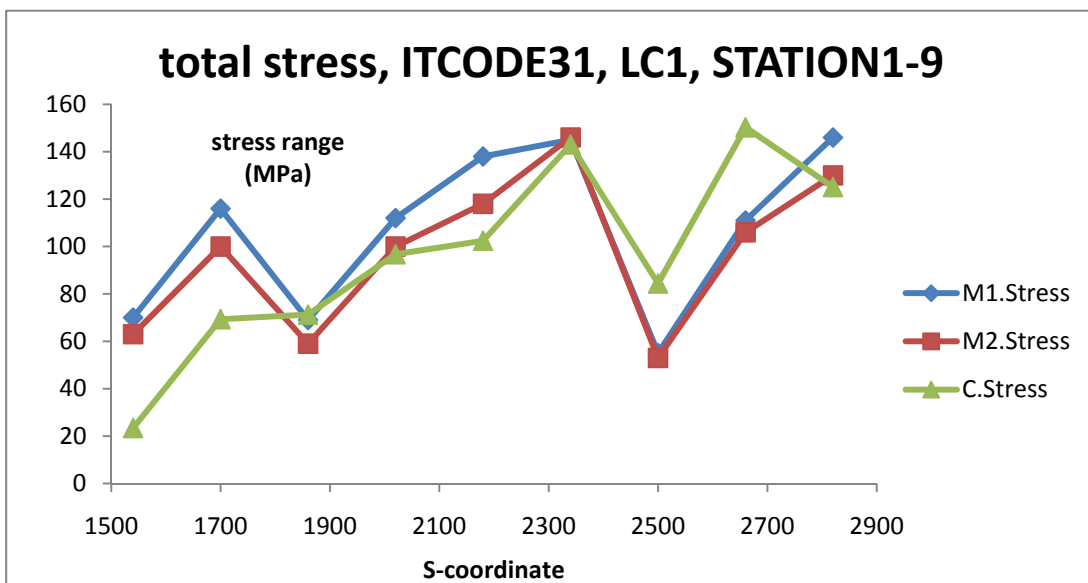
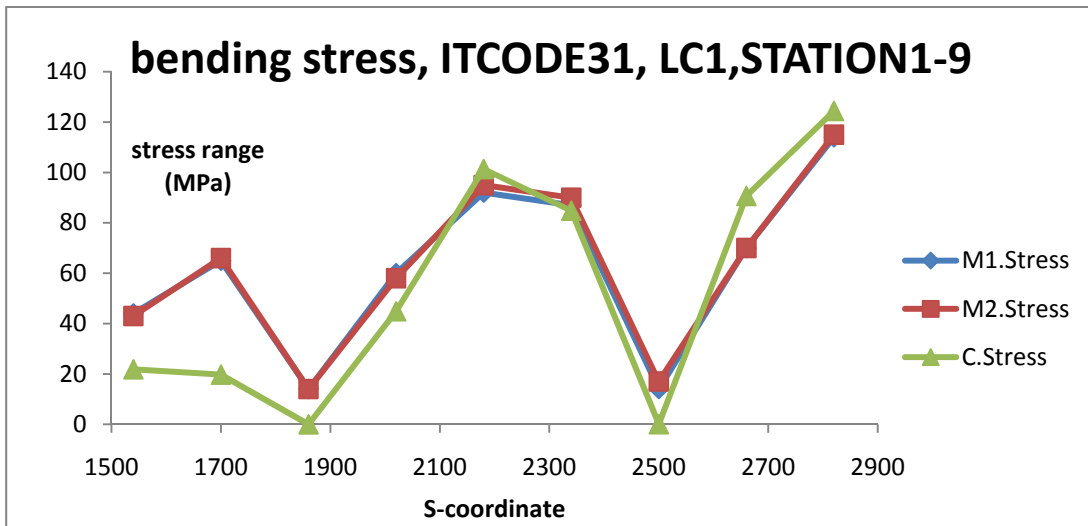
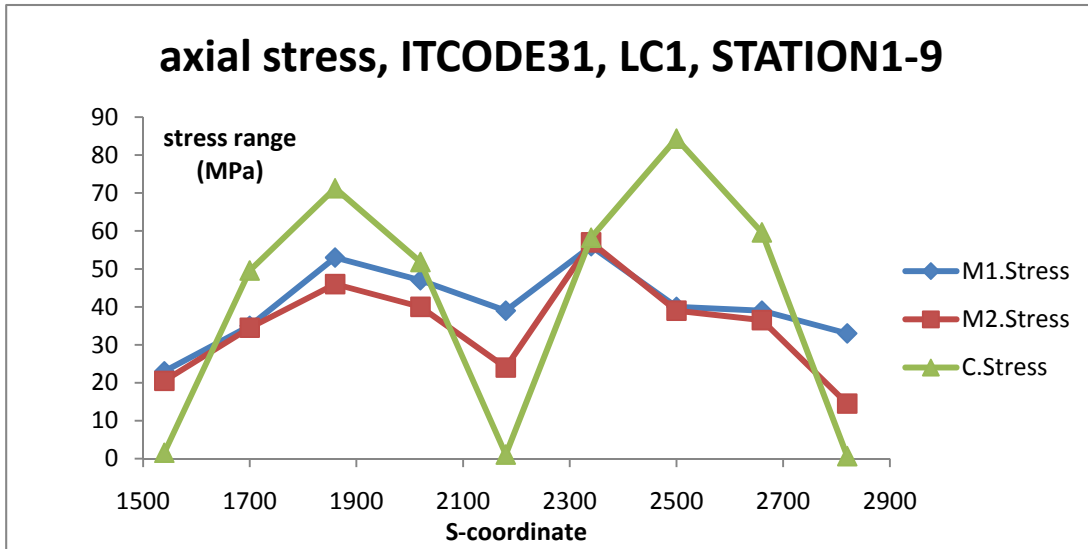


Figure 6.6, COMPARISION, LC1, ITCODE 31, stations 1-9



LC1—ITCODE 31—station 10-20

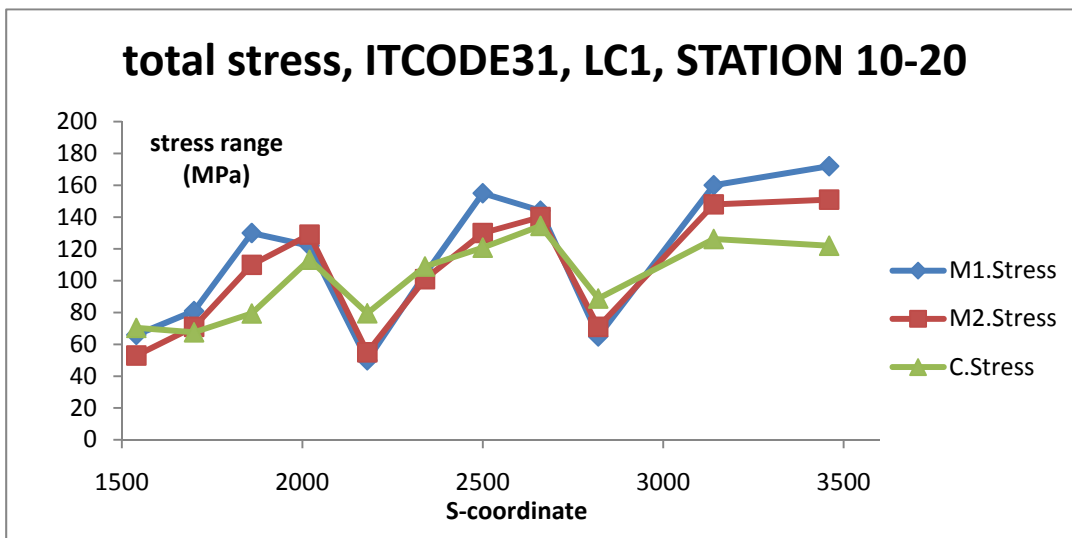
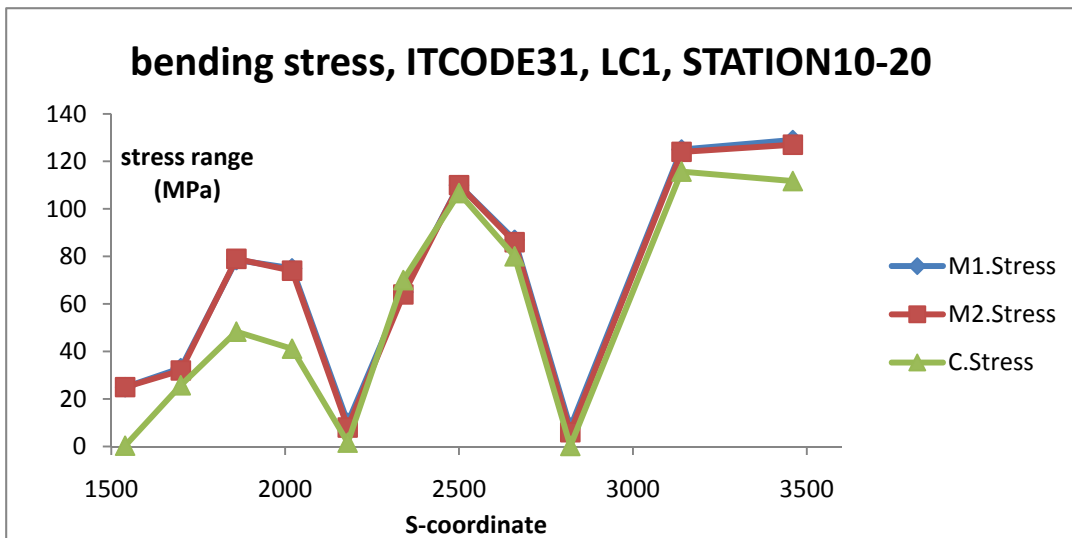
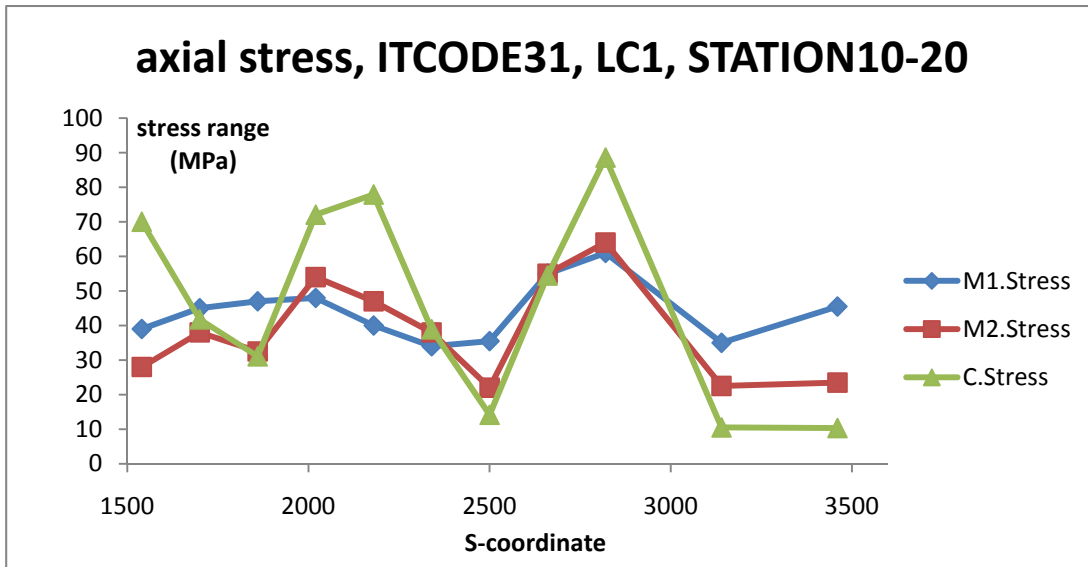


Figure 6.7, COMPARISON, LC1, ITCODE 31, stations 10-20



LC3—ITCODE 0—staion 1-9

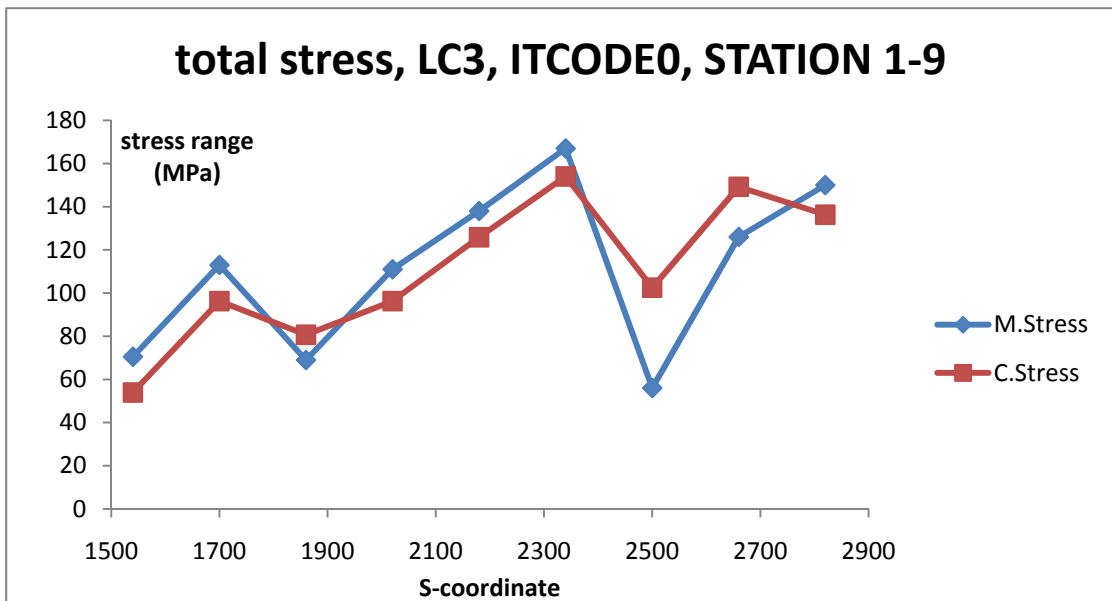
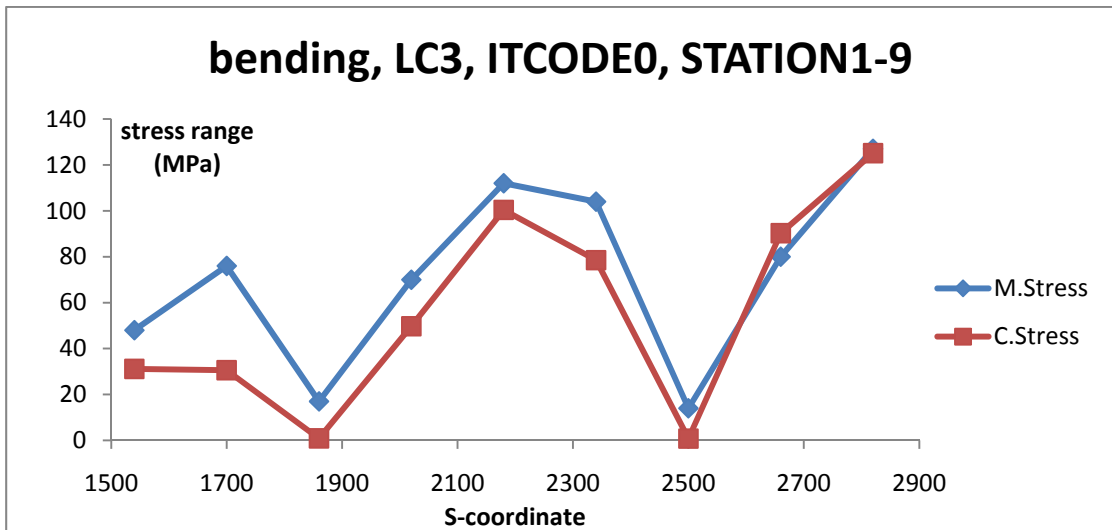
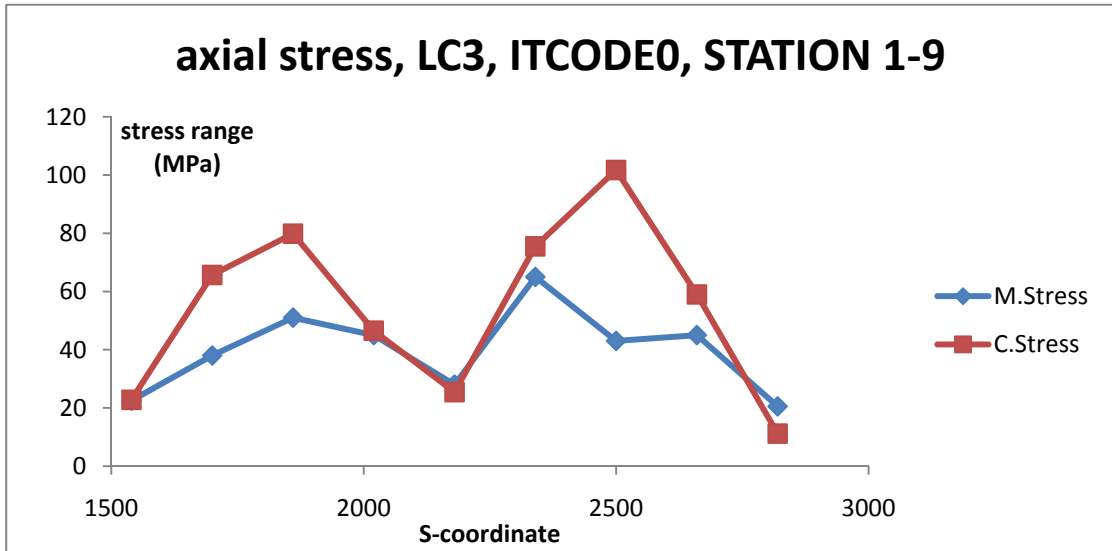


Figure 6.8, COMPARISON, LC3, ITCODE 0, stations 1-9



LC3—ITCODE 0—station 10-20

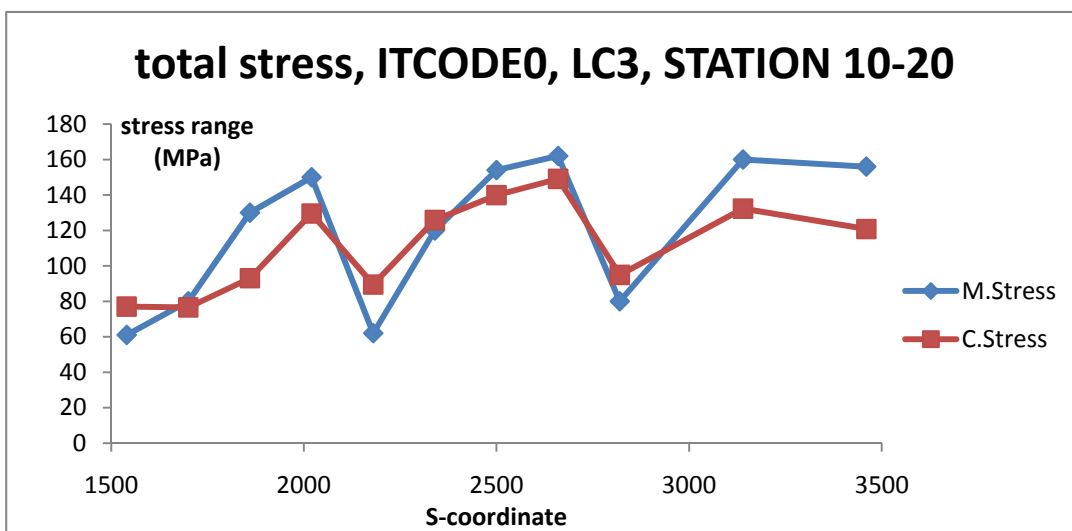
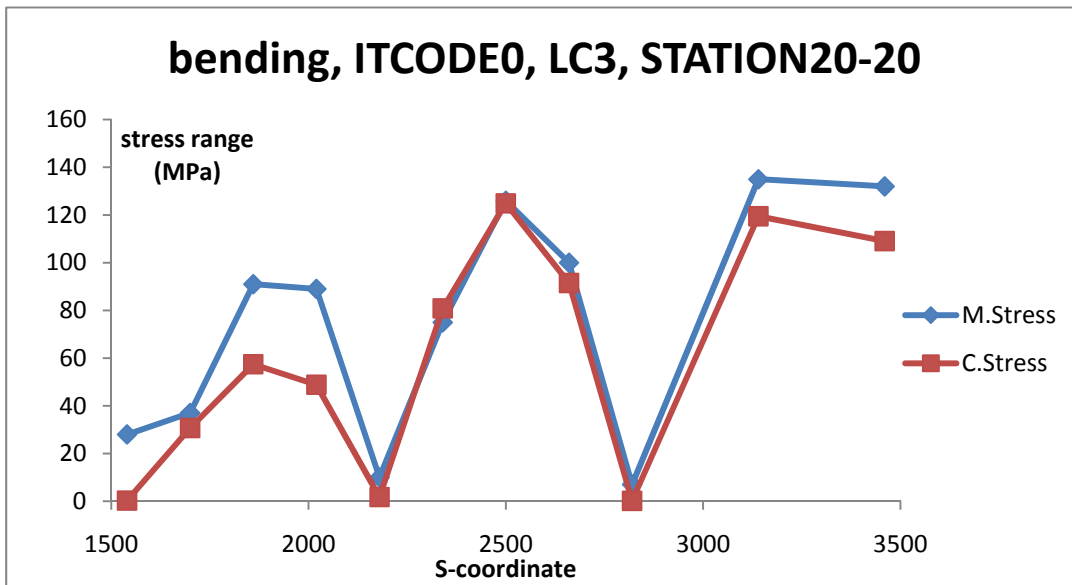
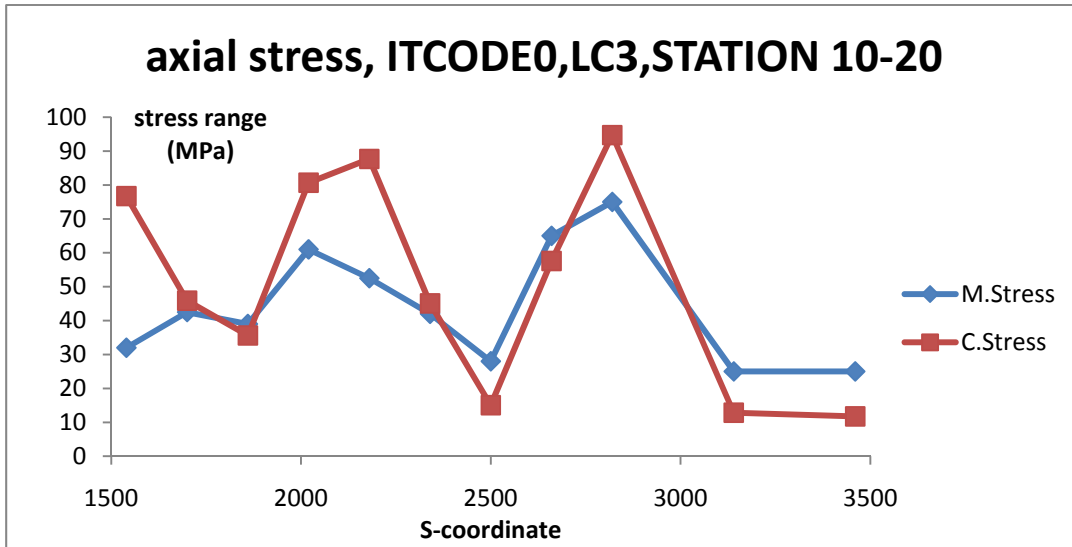


Figure 6.9, COMPARISION, LC3, ITCODE 0, stations 10-20



LC3—ITCODE 31—station 1-9

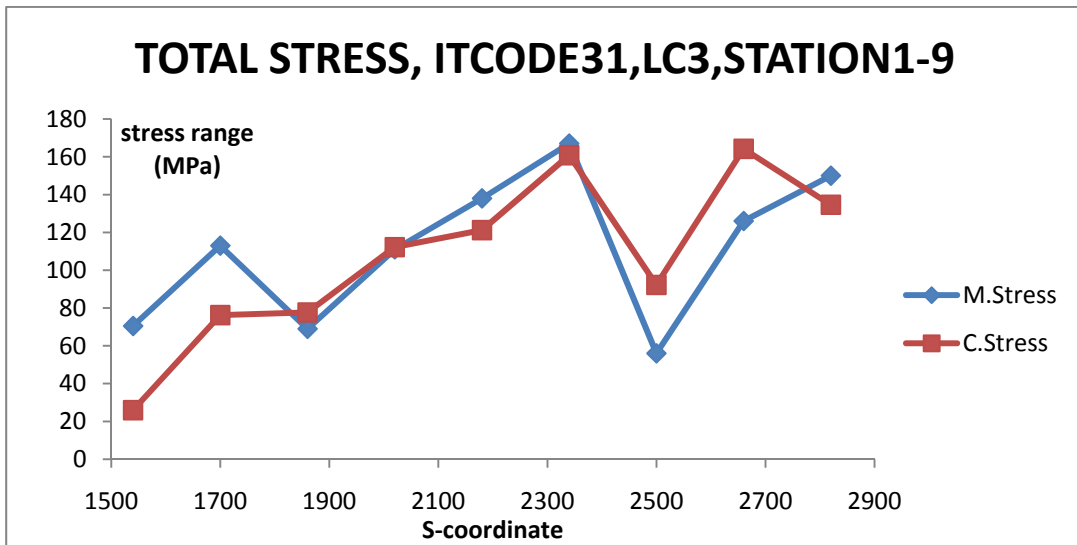
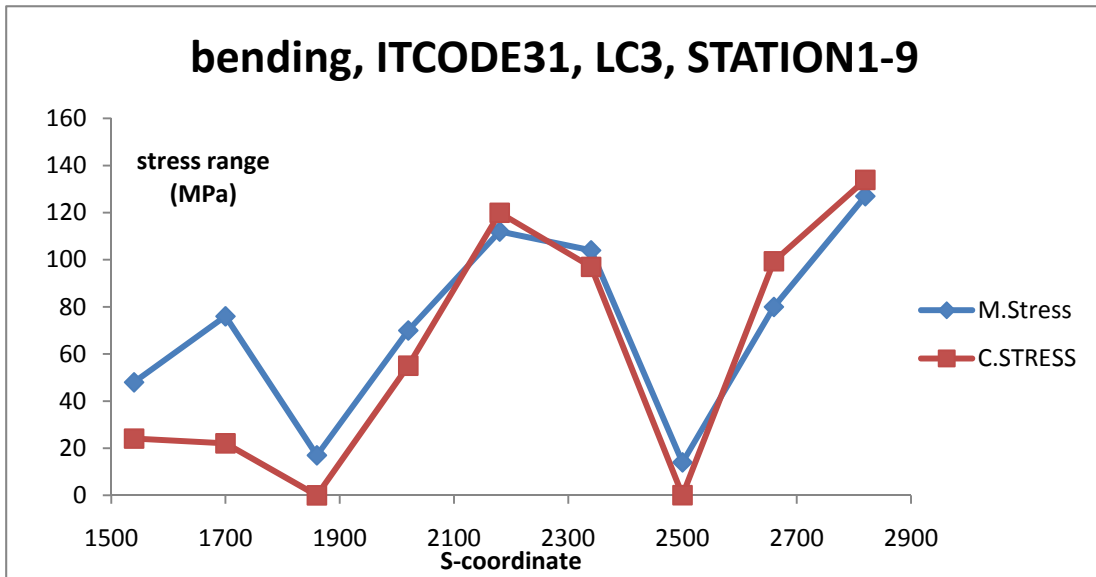
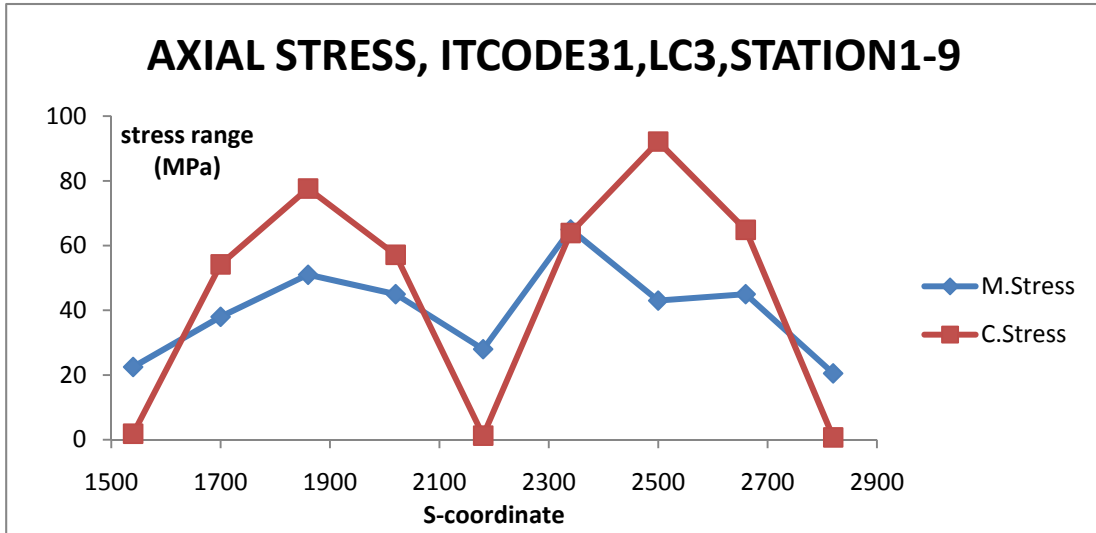


Figure 6.10, COMPARISON, LC3, ITCODE 31, stations 1-9



LC3—icode 31—station 10-20

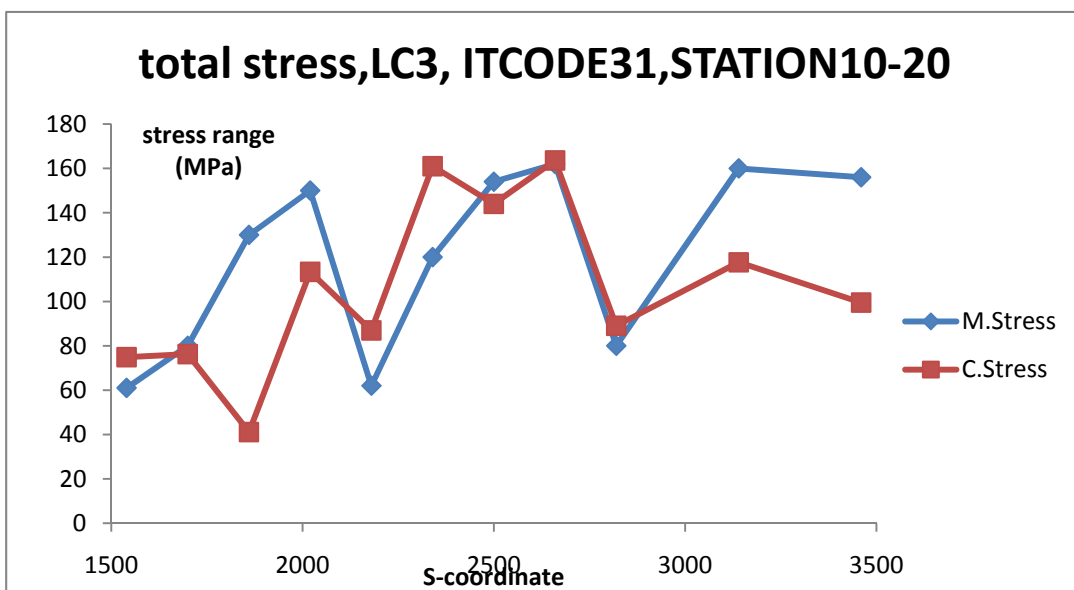
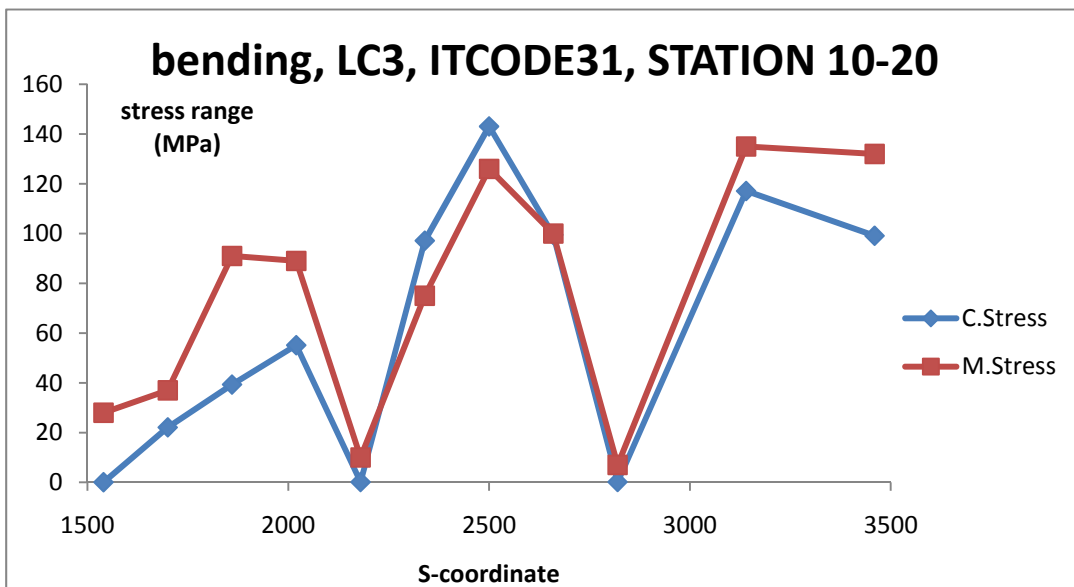
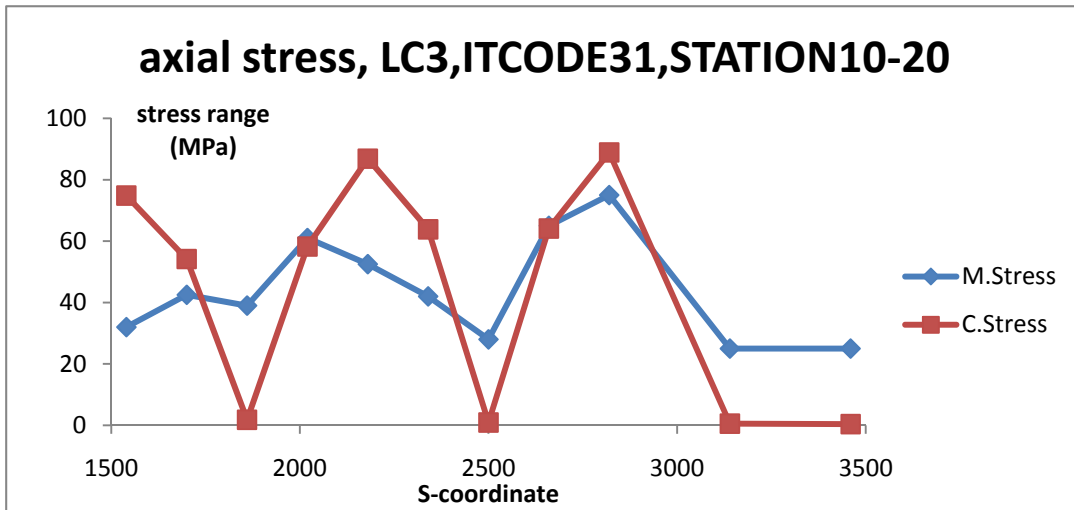


Figure 6.11, COMPARISION, LC3, ITCODE 31, stations 10-20

6.2 Correlation studies

In this section, the correlation studies about the fatigue damage on tensile aemour layer are carried out. We focus on the relationship between fatigue damage and E-modulus of bending stiffener, and the relationship between fatigue damage and GAP. The GAP refers to the distance between bending stiffener and flexible pipe.

6.2.1 Correlation between E-modulus of bending stiffener and fatigue damage

The original E-modulus of bending stiffener is used as a reference. 20 groups of E-modulus values are chosen. They are 40%, 60%, 80%, 120%, 140%, 160%, 180%, 200%, 220%, 240%, 260%, 280%, 300%, 320%, 340%, 360%, 380%, 400%, 420% and 440% of original E-modulus we are using in section 4.2.2. Figure 6.12 shows their strain- stress curves.

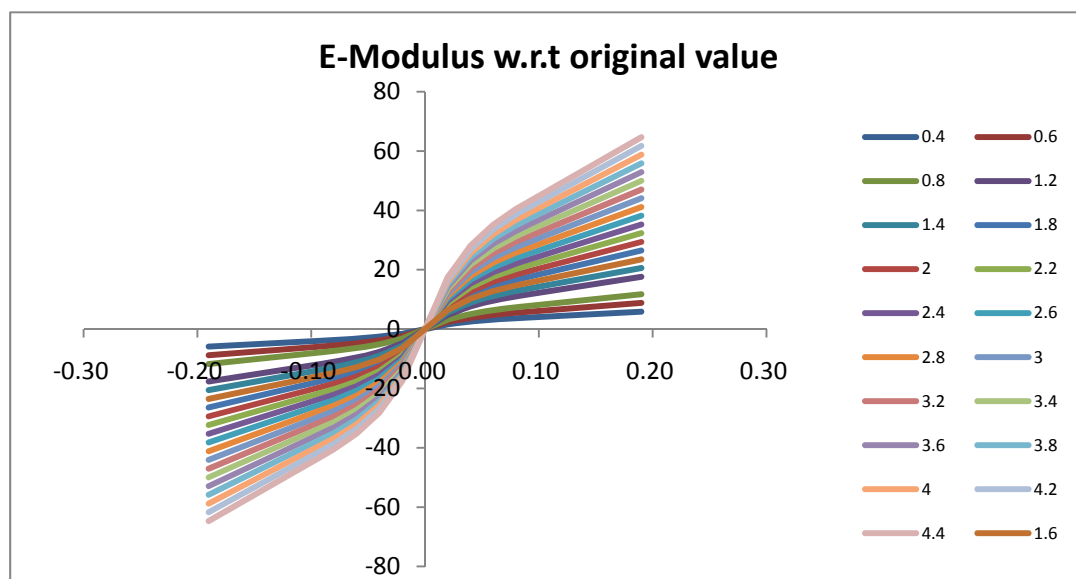


Figure 6.12, E-modulus for correlation studies

For each E-modulus value, the BFLEX calculations on LC1 and LC2 are finished. Then the fatigue damage values of each tensile layer armour are available. The damage results are summarized in figure 6.13 to figure 6.16.

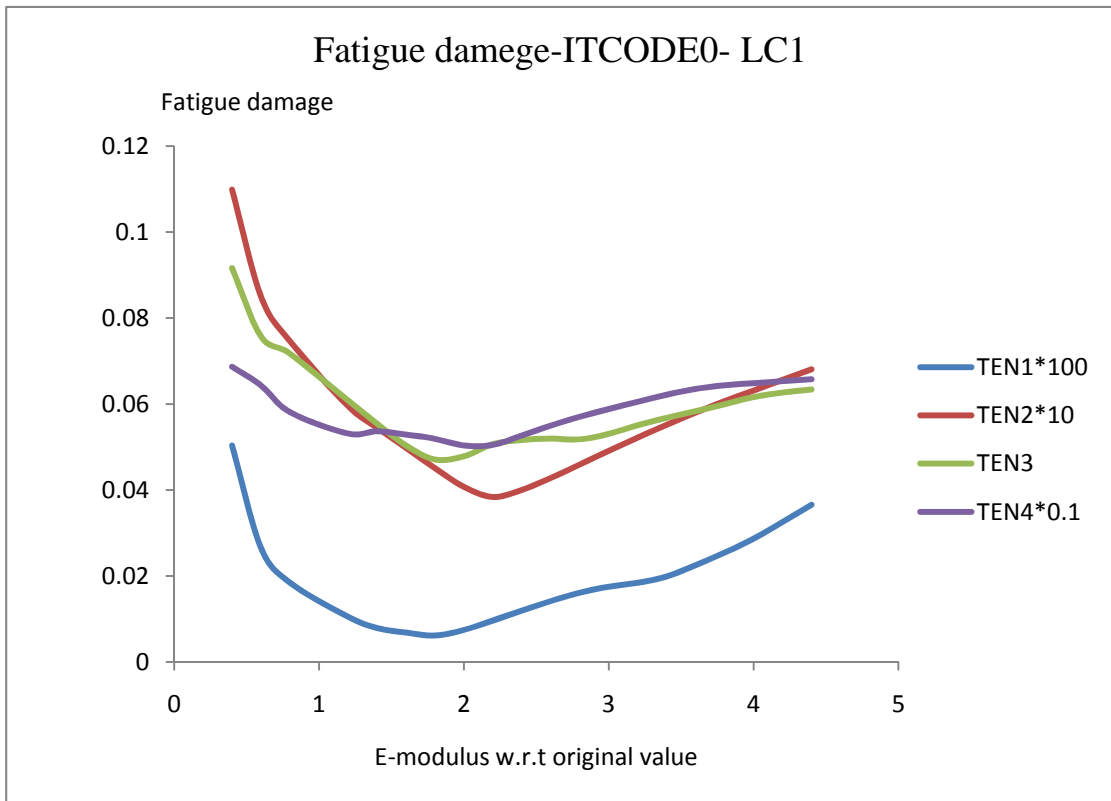


Figure 6.13, correlation studies on E-modulus, LC1, ITCODE0

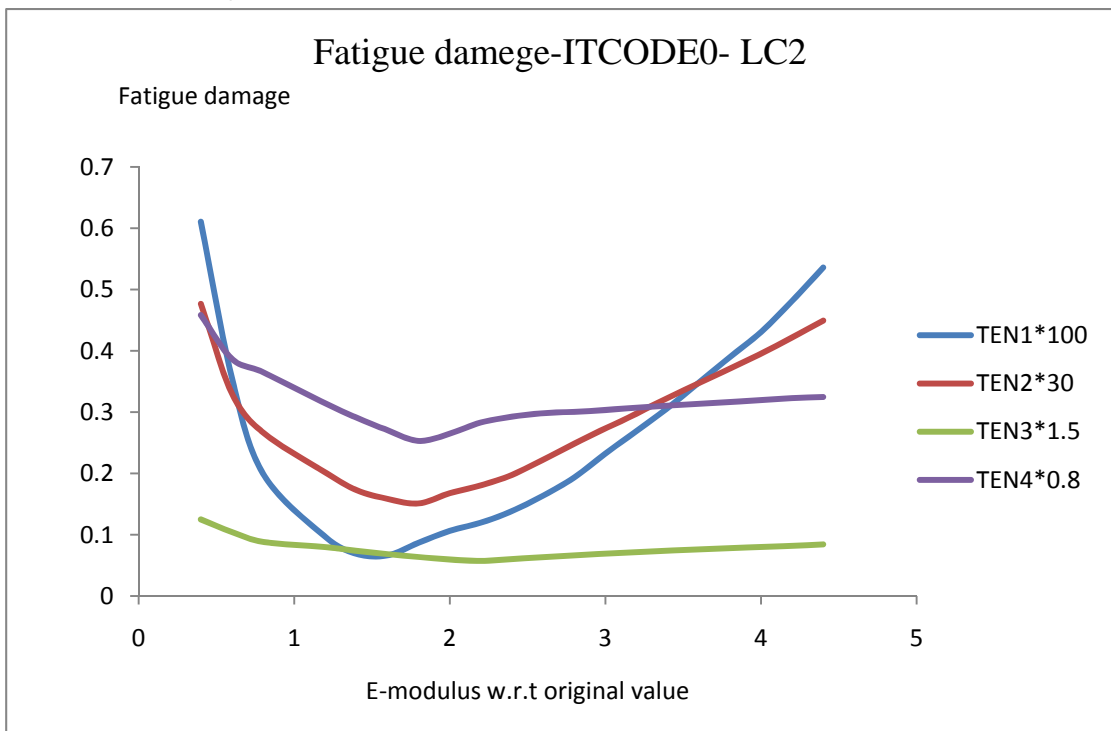


Figure 6.14, correlation studies on E-modulus, LC2, ITCODE0

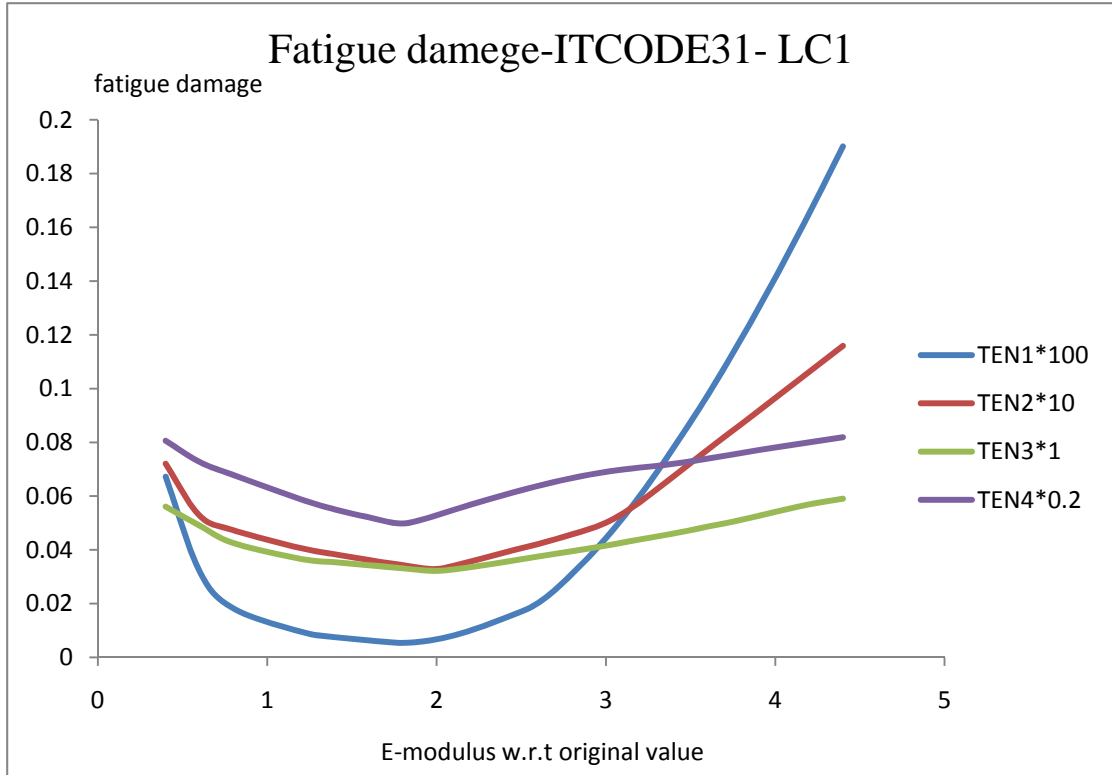


Figure 6.15, correlation studies on E-modulus, LC1, ITCODE31

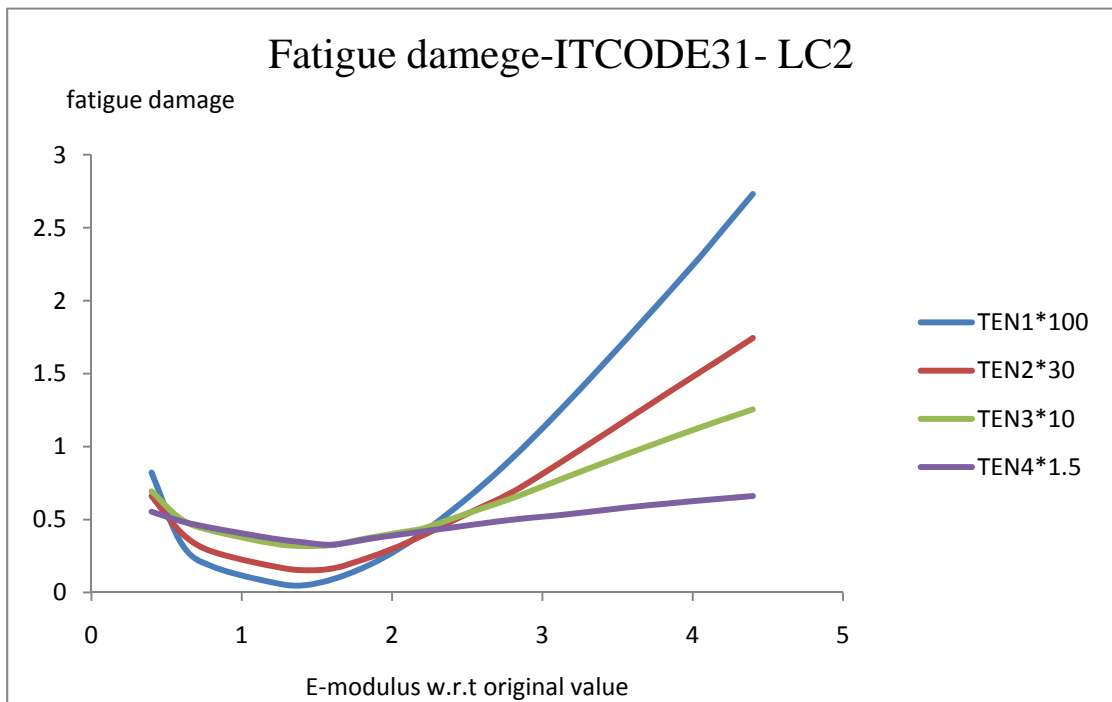


Figure 6.16, correlation studies on E-modulus, LC2, ITCODE31

In figure 6.13- figure 6.16, in order to display the fatigue- modulus relationship for each tensile armour layer in a same plot, the fatigue damage is multiplied with a certain value. That because the fatigue damage of outer layer is much smaller, compared with that of innermost tensile armour layer.

It is obvious to see that, the fatigue damage of each tensile armour layer will decrease first, and then increase, after the E-modulus reaches a certain value. It is very easy to explain this phenomenon. The function of bending stiffener is to reduce the curvature of flexible pipe. When the E-modulus is too small, the bending stiffener nearly does not work, that is why a high value of fatigue damage is observed, when the E-modulus is low. At the same time, if the E-modulus of bending stiffener is too high, that means the stiffness of bending stiffener is very high. This would increase the interaction between bending stiffener and flexible pipe. As a result of this, the flexible pipe components will be subjected to more loading. High fatigue damage is indispensable.

6.2.2 Correlation studies between Gap and fatigue damage.

In this section, the correlation studies between gap and fatigue damage of tensile layer is carried out. The parameter that is used to measure the gap between bending stiffener and flexible pipe is radius of CONTACT elements, RD (see user manual of BFLEX 2010, section 2.19.3, page 55). The radius of CONTACT elements is a parameter that is used to judge whether contact happens between flexible pipe and bending stiffener. When RD is smaller, there exists a big gap between bending stiffener and flexible pipe. Then an R with a high value means the gap is smaller and the contact happens more easily.

Figure 6.17 show the relationship between RD and fatigue damage for each tensile armour layer. The horizontal axis represents RD. The diameter of CORE element group is 400, and the inner diameter of bending stiffener is 407. In this correlation studies, BFLEX models with 6 different values for CONTACT diameter are analyzed. The result is shown in figure 6.17. It is very easy to see, in our range of RD, the fatigue damage is increasing, with the increasing of Rd. The increasing of R is identical to the decreasing of gap between bending stiffener and flexible pipe.

The correlation curve between gap and fatigue damage of tensile armour layer should be similar to the curve shown in figure 6.18. For a small gap, the interaction between bending stiffener and flexible pipe is strong. This results more fatigue loading on the tensile armour layers. For a high value of gap, this means that the bending stiffener does not work properly. The function of bending stiffener is not overall displayer. This will cause a high value of fatigue damage.

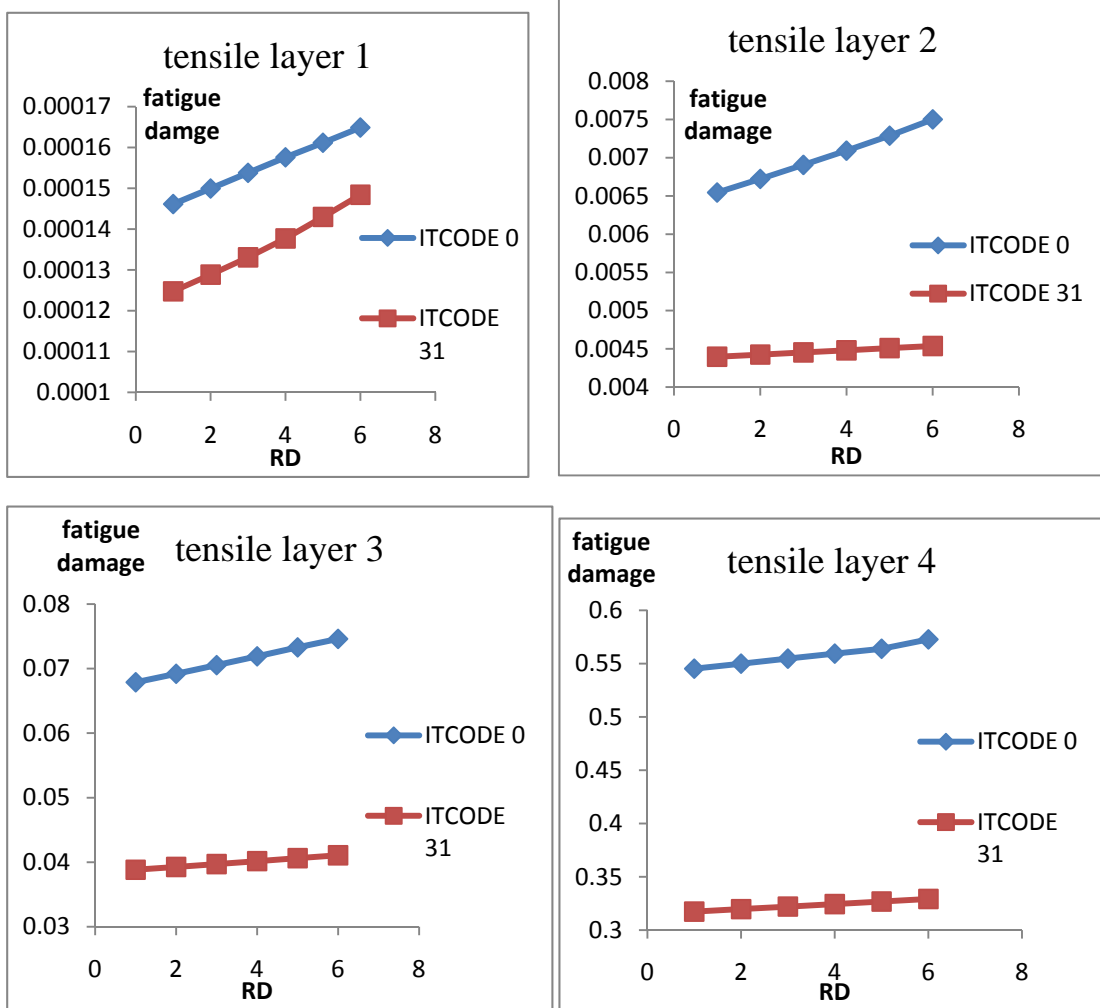


Figure 6.17, correlation studies on RD, LC1

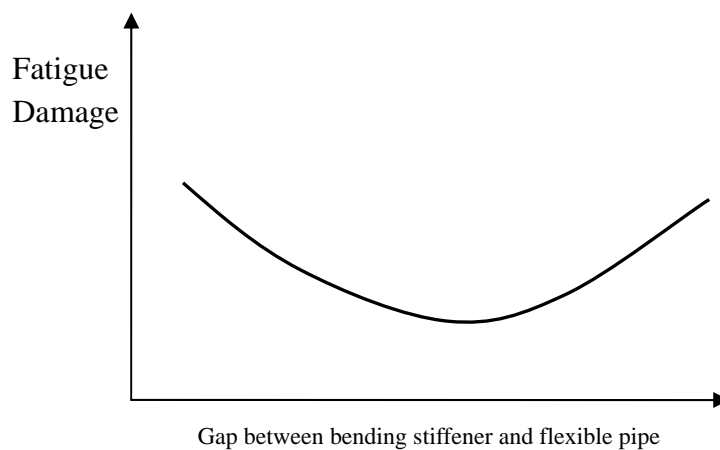


Figure 6.18, the ideal relationship between fatigue damage and GAP

6.3 Conclusions

For the correlation relationship between E-modulus of bending stiffener and fatigue damage on tensile armour layer

The figure 6.13 to figure 6.16 displays a good relationship between E-modulus and fatigue damage. This fits with our understanding about the bending stiffener. According to the calculation results, a specified value of E-modulus of bending stiffener could make the tensile armour layers be subjected to the least fatigue damage. And it is recommended to finish this design work with BFLEX2010. It is not very difficult to understand this principle. When the E-modulus is low, this is identical with the condition in which the bending stiffener is too soft. The bending stiffener could not reduce the curvature along the flexible pipe, when it is subjected to various loading. Then the condition, in which E-modulus is high, means the bending stiffener is too rigid. This would result a strong interaction between bending stiffener and flexible pipe. The loading on tensile armour layers is relatively large, which results in severe fatigue damage.

For the correlation relationship between RD and fatigue damage on tensile armour layer

Figure 6.17 should only display part of the relationship between RD and fatigue damage. RD controls the gap between bending stiffener and flexible pipe. As RD is increasing, the GAP between bending stiffener and flexible pipe would decrease. There should exist a specific value for RD, to make the fatigue damage on tensile armour layer at a minimum value. For this problem, further research is needed.

Appendix1. BFLEX input file, ITCODE0, LC1

```

#input file for itcode=0
HEAD BFLEX2010-ITCODE0 LC1, by Minghao Chen
#The Unity is mm, Newton, and second.
#-----
# Control data
#          maxit ndim isolvr npoint ipri   conr   gacc   iproc
CONTROL   100   3     2     16    11    1.e-5   9.81   stressfree
DYNCONT   1     0.0   0.09  -0.05
#MAXIT is the maximum number of iteration at each time step!!
#          T      DT   DTVI   DT0   TYPE   steptype  ITERCO  ITCRIT  MAXIT  MAXDIV  CONR
TIMECO    2.0    1.0   1.0   201.0  STATIC  auto     none    all    50     7     1e-5
TIMECO    400.0  1.0  10.0   201.0  STATIC  auto     GO-ON   all    20     5     1e-5
#
#-----
#tensile layer is modelled very very completely...
#They are core, 4 tensile layers, bending stiffener, contact and the virtual rigid pipe.
#Nocoor input
#          no          x      y      z
Nocoor Coordinates 1001      0      0      0
                    1300   14950  0      0

Nocoor Coordinates 2001   1800      0      0
                    2056   4550   0      0

Nocoor Coordinates 3001      0      0      0
                    3060   2950  0      0

Nocoor Coordinates 4001   14950  0      0
                    4040   16900 0      0
#-----
#          no      x0      y0      z0      b1      b2      b3      R      node      xcor      theta
Nocoor Polar  0.0    0.0    0.0    0.0    0.0    0.0    160.815  10001  10300  0.0    0
                                                    14950  -89.7743

#          n      ninc      dx      dtheta
Repeat 16     300      0.0      0.3927
#-----
#          no      x0      y0      z0      b1      b2      b3      R      node      xcor      theta
Nocoor Polar  0.0    0.0    0.0    0.0    0.0    0.0    168.735  20001  20300  0.0    0
                                                    14950   85.5605

#          n      ninc      dx      dtheta
Repeat 16     300      0.0      0.3927
#-----
#          no      x0      y0      z0      b1      b2      b3      R      node      xcor      theta

```

```

Nocoor Polar 0.0 0.0 0.0 0.0 0.0 176.655 30001 0.0 0
                                     30300 14950 -76.1996
#      n  ninc      dx      dtheta
Repeat 16      300      0.0      0.3927
#-----
#      no      x0      y0      z0      b1      b2      b3      R      node      xcor      theta
Nocoor Polar 0.0 0.0 0.0 0.0 0.0 0.0 184.575 40001 0.0 0
                                     40300 14950 72.9299
#      n  ninc      dx      dtheta
Repeat 16      300      0.0      0.3927

Visres Integration 1 Sigma-xx-ax sigma-xx
#-----
# Elcon  input

# The core-----
#
#      group      elty      material  no      n1      n2
Elcon  core      pipe52      mypipe  10001  1001  1002
#      n      elinc  nodinc
Repeat 299      1      1
#-----
# The bend stiffener-----
#      group      elty      crossname  elid      n1      n2
Elcon  bendstiffener pipe52      mybendstiffener 60001  2001  2002
#      n      elinc  nodinc
Repeat 55      1      1
#-----
# contact between pipe and bending stiffener
#      group      elty      crossname  elid      n1      n2
Elcon  bscontact  cont130      bscontmat1 70001  1037
#      n      elinc  nodinc
Repeat 55      1      1
#-----
# virtual rigid pipe-----
# rigid pipeline as a reference, here myrigidpipe is the name for the manufacturing material
#      group      elty      material  elid      n1      n2
Elcon  rigidpipe  pipe31      myrigidpipe 80001  3001  3002
#      n      elinc  nodinc
Repeat 59      1      1
#-----
# Tensile Layers
# Tensile Layer 1-----
#      group      elty      flexcrossname  no      n1      n2      n3      n4
Elcon  tenslayer1  hshear352      mypipe      20001  1001  1002  10001  10002
                                     20016  1001  1002  14501  14502
#      n      elinc  nodinc
Repeat 299      16      1
#-----
# Tensile Layer 2-----
#      group      elty      flexcrossname  no      n1      n2      n3      n4

```

```

Elcon tenslayer2 hshear352 mypipe      30001 1001 1002 20001 20002
      30016 1001 1002 24501 24502
#      n  elinc  nodinc
Repeat 299 16      1
#-----
# Tensile Layer 3-----
#      group      elty  flexcrossname      no  n1  n2  n3  n4
Elcon  tenslayer3 hshear352 mypipe      40001 1001 1002 30001 30002
      40016 1001 1002 34501 34502
#      n  elinc  nodinc
Repeat 299 16      1
#-----
# Tensile Layer 4-----
#      group      elty  flexcrossname      no  n1  n2  n3  n4
Elcon  tenslayer4 hshear352 mypipe      50001 1001 1002 40001 40002
      50016 1001 1002 44501 44502
#      n  elinc  nodinc
Repeat 299 16      1
# the right side rigid pipe
Elcon  rightpipe  pipe31      myrigidpipe 90001 4001 4002
#      n  elinc  nodinc
Repeat 39 1      1
#-----
# Orient input
#
# The core-----
#      no      x  y  z
Elorient Coordinates 10001 0 1e3 0
      10299 0 1e3 0
#the bending stiffener-----
#      no      x  y  z
Elorient Coordinates 60001 0 1e3 0
      60055 0 1e3 0
#contact elements group-----
Elorient Eulerangle 70001 0 0 0
      70055 0 0 0
# rigid pipeline group-----
#      no      x  y  z
Elorient Coordinates 80001 0 1e3 0
      80059 0 1e3 0
# Tensile Layer 1-----
#      no      x  y  z
Elorient Coordinates 20001 0 1e3 0
      20016 0 1e3 0
repeat 299 16 0 0 0
# Tensile Layer 2-----
#      no      x  y  z
Elorient Coordinates 30001 0 1e3 0

```

```

30016 0 1e3 0
repeat 299 16 0 0 0
# Tensile Layer 3-----
#          no      x      y      z
Elorient Coordinates 40001 0 1e3 0
                    40016 0 1e3 0
repeat 299 16 0 0 0
#          no      x      y      z
# Tensile Layer 4-----
Elorient Coordinates 50001 0 1e3 0
                    50016 0 1e3 0
repeat 299 16 0 0 0

# right side rigid pipeline group
#          no      x      y      z
Elorient Coordinates 90001 0 1e3 0
                    90039 0 1e3 0

#-----
#          groupn      mname      sname      isl      isn      TX      TY      TZ      MAXIT      IGAP
CONTINT bscontact core bendstiffener 60001 60055 1 10000 1 60 1
#-----
#          ELGRP      PIPE      RAD      TH      RCD/CDr      TCD/Cdt      RMADD      TMADD      MD      MS      ODP      ODW      rks
ELPROP rigidpipe pipe 200 87.5 0.8 0.1 1.0 0.1 0.5e-3 0.17e-3 487.5 487.5 0.5
#          ELGRP      PIPE      RAD      TH      RCD/CDr      TCD/Cdt      RMADD      TMADD      MD      MS      ODP      ODW      rks
ELPROP rightpipe pipe 200 87.5 0.8 0.1 1.0 0.1 0.5e-3 0.17e-3 487.5 487.5 0.5
#-----
#          name      type      diameter      inside
ELPROP bscontact bellmouth 400 1 CONTPAR1_500
#-----
# Definition of flexible pipe cross-section
#          name      type      ifric      disfac      forfac      geofac      endfac      ID      Timeini      itcode      ILAEXT      IELBFL      FIMOD      CONTDEN      NELGR      EL1GRP      EL1GRP      EL2GRP      EL3GRP
EL4GRP
CROSSECTION MYPIPE FLEXCROSS 1 10000.0 10.0 0.0 1.01 228.6 2.0 0 20 80 0 0.8e-6 5 core tenslayer1 tenslayer2 tenslayer3 tenslayer4
#          CTYPE      TH      matname      FRIC      LAYANG      RNUM      TEMP      nlmat      CCODE      CFATFL      AREA      IT      INY      IKS      WIDTH
CARC 7.00 steel 0.15 88.062 1 0.0 none CARCOSSq NONE 0.00 0.000e+00 0.000e+00 0.000e+00 0.00
THER 3.99 PVDF 0.15 0.000 0 0.0 none NONE NONE 0.00 0.000e+00 0.000e+00 0.000e+00 0.00
THER 12.00 PVDF 0.15 0.000 0 0.0 none NONE NONE 0.00 0.000e+00 0.000e+00 0.000e+00 0.00
THER 1.02 PVDFc 0.15 0.000 0 0.0 none NONE NONE 0.00 0.000e+00 0.000e+00 0.000e+00 0.00
ZETA 12.00 carbon_steel 0.25 88.868 1 0.0 none MYZETAq FiZ 0.00 0.000e+00 0.000e+00 0.000e+00 0.00
SPIR 5.99 carbon_steel 0.15 88.868 1 0.0 none MYSPIRAq FiZ 0.00 0.000e+00 0.000e+00 0.000e+00 0.00
THER 1.52 PA11 0.15 0.000 0 0.0 none NONE NONE 0.00 0.000e+00 0.000e+00 0.000e+00 0.00
TENS 5.99 carbon_steel 0.15 -44.000 54 0.0 none TENSILEq FIT 0.00 0.000e+00 0.000e+00 0.000e+00 0.00
THER 0.41 PA11 0.15 0.000 0 0.0 none NONE NONE 0.00 0.000e+00 0.000e+00 0.000e+00 0.00
THER 1.52 PA11 0.15 0.000 0 0.0 none NONE NONE 0.00 0.000e+00 0.000e+00 0.000e+00 0.00
TENS 5.99 carbon_steel 0.15 44.000 57 0.0 none TENSILEq FIT 0.00 0.000e+00 0.000e+00 0.000e+00 0.00
THER 0.41 PA11 0.15 0.000 0 0.0 none NONE NONE 0.00 0.000e+00 0.000e+00 0.000e+00 0.00
THER 1.52 PA11 0.15 0.000 0 0.0 none NONE NONE 0.00 0.000e+00 0.000e+00 0.000e+00 0.00

```


TENS	5.99	carbon_steel	0.15	-42.000	61	0.0	none	TENSILEq	FiT	0.00	0.000e+00	0.000e+00	0.000e+00	0.00
THER	0.41	PA11	0.15	0.000	0	0.0	none	NONE	NONE	0.00	0.000e+00	0.000e+00	0.000e+00	0.00
THER	1.52	PA11	0.15	0.000	0	0.0	none	NONE	NONE	0.00	0.000e+00	0.000e+00	0.000e+00	0.00
TENS	5.99	carbon_steel	0.15	42.000	64	0.0	none	TENSILEq	FiT	0.00	0.000e+00	0.000e+00	0.000e+00	0.00
THER	0.41	PA11	0.15	0.000	0	0.0	none	NONE	NONE	0.00	0.000e+00	0.000e+00	0.000e+00	0.00
THER	0.41	PA11	0.15	0.000	0	0.0	none	NONE	NONE	0.00	0.000e+00	0.000e+00	0.000e+00	0.00
THER	12.00	PA11	0.15	0.000	0	0.0	none	NONE	NONE	0.00	0.000e+00	0.000e+00	0.000e+00	0.00

#CROSS-SECTION BOUNDARY DATA

#	NAME	type	X0	Y0	CCURV	P1	P2	P3	P4	NINTER	ICODE		
CROSSGEOM	CARC-CARCOSSq			BFLEX	0	0	S	5.05	180.00	0.0	1.4	5	2
				S		3.50	90.00	0.0	1.4	5	0		
				S		15.45	0.00	0.0	1.4	5	0		
				S		7.00	270.00	0.0	1.4	5	0		
				S		15.45	0.00	0.0	1.4	5	0		
				S		3.50	90.00	0.0	1.4	5	0		
				S		5.05	180.00	0.0	1.4	5	2		
CROSSGEOM	ZETA-MYZETAq			BFLEX	0	0	CI	90.0000	187.5000	1.5000	0.0000	10	0
				S		4.4172	97.5000	0.0000	0.0000	10	0		
				CI		187.5000	330.0000	1.5000	0.0000	10	2		
				S		1.9386	240.0000	0.0000	0.0000	10	0		
				CO		150.0000	90.0000	1.5000	0.0000	10	0		
				S		1.6524	180.0000	0.0000	0.0000	10	3		
				CO		90.0000	10.0000	2.4000	0.0000	10	0		
				S		3.8922	100.0000	0.0000	0.0000	10	0		
				CI		190.0000	270.0000	2.4000	0.0000	10	0		
				S		12.6004	180.0000	0.0000	0.0000	30	1		
				CI		270.0000	367.5000	1.5000	0.0000	10	0		
				S		4.4172	277.5000	0.0000	0.0000	10	0		
				CI		7.5000	150.0000	1.5000	0.0000	10	2		
				S		1.9386	60.0000	0.0000	0.0000	10	0		
				CO		330.0000	270.0000	1.5000	0.0000	10	0		
				S		1.6524	0.0000	0.0000	0.0000	10	3		
				CO		270.0000	190.0000	2.4000	0.0000	10	0		
				S		3.8922	280.0000	0.0000	0.0000	10	0		
				CI		10.0000	90.0000	2.4000	0.0000	10	0		
				S		12.6004	0.0000	0.0000	0.0000	30	1		
CROSSGEOM	TENS-TENSILEq			BFLEX	0	0	S	12.0	0.0	0.0	0.0	10	0
				S	5.99	90.0	0.0	0.0	10	0			
				S	12.0	180.0	0.0	0.0	10	1			
				S	5.99	270.0	0.0	0.0	10	0			
CROSSGEOM	SPIR-MYSPIRAq			BFLEX	0	0	S	5.99	90.0	0	0	10	0
				S	16.0	180.0	0	0	10	2			
				S	5.99	270.0	0	0	10	0			
				S	16.0	0.0	0	0	10	1			

```

#-----
# BENDING STIFFENER
#          name          type      local  global  id   od   no_th  rks   imno_i  imno_o  mat_bend
CROSECTION MYBENDSTIFFENER  NLBENDSTIFF      1      2001  407  447   10   0.1    0.1    mat_bend  mat_bend
              52      2052  407  447   10   0.1    mat_bend  mat_bend
              56      2056  407  447   10   0.1    mat_bend  mat_bend
#-----
# Boundary condition data
#      Loc      node      dir
BONCON GLOBAL 3060      1
BONCON GLOBAL 3060      2
BONCON GLOBAL 3060      3
BONCON GLOBAL 3060      4
BONCON GLOBAL 3060      6

BONCON GLOBAL 4040      2
BONCON GLOBAL 4040      3
BONCON GLOBAL 4040      4
BONCON GLOBAL 4040      6

BONCON GLOBAL 1002 2 REPEAT 298 1
BONCON GLOBAL 2002 2 REPEAT 55 1

CONSTR CONEQ GLOBAL 1300 1 0.0 4001  1  1
CONSTR CONEQ GLOBAL 1300 2 0.0 4001  2  1
CONSTR CONEQ GLOBAL 1300 3 0.0 4001  3  1
CONSTR CONEQ GLOBAL 1300 4 0.0 4001  4  1
CONSTR CONEQ GLOBAL 1300 5 0.0 4001  5  1
CONSTR CONEQ GLOBAL 1300 6 0.0 4001  6  1

BONCON LOCAL 10001 1
REPEAT 16 300
BONCON LOCAL 20001 1
REPEAT 16 300
BONCON LOCAL 30001 1
REPEAT 16 300
BONCON LOCAL 40001 1
REPEAT 16 300

BONCON LOCAL 10300 1
REPEAT 16 300
BONCON LOCAL 20300 1
REPEAT 16 300
BONCON LOCAL 30300 1
REPEAT 16 300
BONCON LOCAL 40300 1
REPEAT 16 300

#-----
CONSTR CONEQ GLOBAL 1001 1 0.0 3001  1  1
CONSTR CONEQ GLOBAL 1001 2 0.0 3001  2  1

```

```

CONSTR CONEQ GLOBAL 1001 3 0.0 3001 3 1
CONSTR CONEQ GLOBAL 1001 4 0.0 3001 4 1
CONSTR CONEQ GLOBAL 1001 5 0.0 3001 5 1
CONSTR CONEQ GLOBAL 1001 6 0.0 3001 6 1

CONSTR CONEQ GLOBAL 2001 1 0.0 3037 1 1
CONSTR CONEQ GLOBAL 2001 2 0.0 3037 2 1
CONSTR CONEQ GLOBAL 2001 3 0.0 3037 3 1
CONSTR CONEQ GLOBAL 2001 4 0.0 3037 4 1
CONSTR CONEQ GLOBAL 2001 5 0.0 3037 5 1
CONSTR CONEQ GLOBAL 2001 6 0.0 3037 6 1
#-----
# Constraint input
CONSTR PDISP GLOBAL 3060 5 -0.1309 100
#-----
# Cload input
#
# hist dir no1 r1 no2 r2 n m
CLOAD 200 1 4040 725000
#-----
#external pressure and gravity loading
# PRESHIST GRAVHIST
PELOAD 400 600
#-----
#internal pressure load
# HIST ELNR1 P1 ELNR2 P2
PILOAD 500 10001 47.5 10299 47.5
#PILOAD 500 80001 0 80059 0
#-----

# History data
# pdisp
#100, at 2 sec, we still have load factor=0.0
THIST 100 0 0.0
1 0.0
2 0.0
3 0.0
100 1.0
300 -1.0
400 0.0

# cload
#200, at 1.0 sec, load factor has reached to 1.0
THIST 200 0 0.0
1 1.0
20 1.0

# ext pressure
THIST 300 0 0.0
1.0 1.0
20 1.0

# gravity
THIST 400 0 0.0

```

```

2 0.0
5 0.0
20 0.0
# internal pressure
THIST 500 0 0.0
1 1.0
20 1.0
# gravity
THIST 600 0 0.0
1 0.0
3 0.0
6 1.0
400 1.0
#-----
# Material data
# name type poiss density talfa tecond heatc eps sigma
MATERIAL mat_bend hyperelastic 0.3 0 11.7e-6 2.0 50 -0.19 -14.7
-0.09 -9.7
-0.08 -9.2
-0.07 -8.6
-0.06 -8.0
-0.05 -7.2
-0.04 -6.4
-0.03 -5.2
-0.02 -4.0
-0.01 -2.0
0.01 2.0
0.02 4.0
0.03 5.2
0.04 6.4
0.05 7.2
0.06 8.0
0.07 8.6
0.08 9.2
0.09 9.7
0.19 14.7
#-----
# name type poiss density talfa tecond heatc EM GM trans-EM
MATERIAL PVDF elastic 0.45 1.76998e-6 1 1 1 1516.9 523.07 1516.9
MATERIAL PVDFc elastic 0.45 1.01e-6 1 1 1 1516.9 523.07 1515.9
MATERIAL PA11 elastic 0.45 1.03809e-6 1 1 1 55.2 19.03 55.2
MATERIAL steel elastic 0.3 7.82874e-6 1 1 1 2.1e5 80769 2.1e5
MATERIAL carbon_steel elastic 0.3 7.82874e-6 1 1 1 2.1e5 80769 2.1e5
#-----
# material name linear Poiss Tlefa tecond Haetc Beta EA EIY EIZ GIT EM GM DENSITY ETRANS
MATERIAL myrigidpipe linear 0.3 0.1 0.1 1 0 2.23e11 1.84e15 1.84e15 1e15 2.1e5 8e4 1 2.1e5
#-----

```

```
#materials for the contact element
# name type rmyx rmyz xmat ymat zmat
MATERIAL bscontmat1 isocontact 0.20 bellx bellz
# name type alfa eps sig
MATERIAL bellx epcurve 1 0 0
1.0 1
1000 20
#
MATERIAL belly epcurve 1 0 0
1 1
1000 900
#
MATERIAL bellz hycurve -1000 -1e5
-0.01 -0.5
0.0
1000 1e5
```

Appendix 2. BFLEX input file, LC1, ITCODE 31

```
#input file for itcode=31
#we will use the sandwich model
HEAD BFLEX2010-ITCODE31 LC1, by Minghao Chen
#The Unity is mm, Newton, and second.
#-----
# Control data
# maxit ndim isolvr npoint ipri conr gacc iproc
CONTROL 100 3 2 16 11 1.e-5 9.81 stressfree
DYNCONT 1 0.0 0.09 -0.05
# T DT DTVI DT0 TYPE steptype ITERCO ITCRIT MAXIT MAXDIV CONR
TIMECO 2.0 1.0 1.0 201.0 STATIC auto none all 50 7 1e-5
TIMECO 400.0 1.0 10.0 201.0 STATIC auto GO-ON all 20 5 1e-5
#-----
#Nocoor input
# no x y z
Nocoor Coordinates 1001 0 0 0
1300 14950 0 0
Nocoor Coordinates 2001 1800 0 0
2056 4550 0 0
Nocoor Coordinates 3001 0 0 0
3060 2950 0 0
Nocoor Coordinates 4001 14950 0 0
4040 16900 0 0
#
```

Visres Integration 1 Sigma-xx-ax sigma-xx

```
#-----
# The core
#
#      group      elty      material no      n1      n2
Elcon  core      pipe52  mypipe  10001  1001  1002
#      n      elinc  nodinc
Repeat 299      1      1
#
# The bend stiffener
#      group      elty      crossname      elid      n1      n2
Elcon  bendstiffener pipe52  mybendstiffener 60001  2001  2002
#      n      elinc  nodinc
Repeat 55      1      1
#
# Tensile Layers
#      group      elty      crossname      elid      n1      n2
Elcon  tensilelayer1 pipe52  mypipe  20001  1001  1002
#      n      elinc  nodinc
Repeat 299      1      1
# Tensile Layers
#      group      elty      crossname      elid      n1      n2
Elcon  tensilelayer2 pipe52  mypipe  30001  1001  1002
#      n      elinc  nodinc
Repeat 299      1      1
# Tensile Layers
#      group      elty      crossname      elid      n1      n2
Elcon  tensilelayer3 pipe52  mypipe  40001  1001  1002
#      n      elinc  nodinc
Repeat 299      1      1
# Tensile Layers
#      group      elty      crossname      elid      n1      n2
Elcon  tensilelayer4 pipe52  mypipe  50001  1001  1002
#      n      elinc  nodinc
Repeat 299      1      1
#
# contact between pipe and bending stiffener
#      group      elty      crossname      elid      n1      n2
Elcon  bscontact  cont130  bscontmat1  70001  1037
#      n      elinc  nodinc
Repeat 55      1      1
#
# rigid pipeline as a reference, hrrere myrigidpipe is the name for the manufacturing material
#      group      elty      material      elid      n1      n2
Elcon  rigidpipe  pipe31  myrigidpipe  80001  3001  3002
#      n      elinc  nodinc
Repeat 59      1      1
# the right side rigid pipe
Elcon  rightpipe  pipe31  myrigidpipe  90001  4001  4002
#      n      elinc  nodinc
Repeat 39      1      1
```

```

#-----
# Orient input
# The core
#
# no      x      y      z
Elorient Coordinates 10001 0 1e3 0
                    10299 0 1e3 0
#the bending stiffener
#
# no      x      y      z
Elorient Coordinates 60001 0 1e3 0
                    60055 0 1e3 0
# Tensile Layer 1
#
# no      x      y      z
Elorient Coordinates 20001 0 1e3 0
                    20299 0 1e3 0
# Tensile Layer 2
#
# no      x      y      z
Elorient Coordinates 30001 0 1e3 0
                    30299 0 1e3 0
# Tensile Layer 3
#
# no      x      y      z
Elorient Coordinates 40001 0 1e3 0
                    40299 0 1e3 0
# Tensile Layer 4
#
# no      x      y      z
Elorient Coordinates 50001 0 1e3 0
                    50299 0 1e3 0
#contact elements group
Elorient Eulerangle 70001 0 0 0
                    70055 0 0 0
# rigid pipeline group
#
# no      x      y      z
Elorient Coordinates 80001 0 1e3 0
                    80059 0 1e3 0
# right side rigid pipeline group
#
# no      x      y      z
Elorient Coordinates 90001 0 1e3 0
                    90039 0 1e3 0
#-----
#      groupn      mname      sname      is1      isn      TX      TY      TZ      MAXIT      IGAP
CONTINT bscontact core bendstiffener 60001 60055 1 10000 1 60 1
#-----
#      ELGRP      PIPE      RAD      TH      RCD/CDr      TCD/Cdt      RMADD      TMADD      MD      MS      ODP      ODW      rks
ELPROP rigidpipe pipe 200 87.5 0.8 0.1 1.0 0.1 0.5e-3 0.17e-3 487.5 487.5 0.5
#-----
#      ELGRP      PIPE      RAD      TH      RCD/CDr      TCD/Cdt      RMADD      TMADD      MD      MS      ODP      ODW      rks
ELPROP rightpipe pipe 200 87.5 0.8 0.1 1.0 0.1 0.5e-3 0.17e-3 487.5 487.5 0.5
#
# name type diameter inside
ELPROP bscontact bellmouth 400 1 CONTPAR1_500
#
# name type ifric disfac forfac geofac endfac ID Timeini itcode ILAEXT IELBFL FIMOD CONTDEN NELGR EL1GRP EL1GRP EL2GRP EL3GRP
EL4GRP
CROSECTION MYPIPE FLEXCROSS 1 10000.0 10.0 0.0 1.01 228.6 2.0 31 20 80 0 0.8e-6 5 core tensilelayer1 tensilelayer2 tensilelayer3

```

tensilelayer4

#	CTYPE	TH	matname	FRIC	LAYANG	RNUM	TEMP	nlmat	CCODE	CFATFL	AREA	IT	INY	IKS	WIDTH
	CARC	7.00	steel	0.15	88.062	1	0.0	none	CARCOSSq	NONE	0.00	0.000e+00	0.000e+00	0.000e+00	0.00
	THER	3.99	PVDF	0.15	0.000	0	0.0	none	NONE	NONE	0.00	0.000e+00	0.000e+00	0.000e+00	0.00
	THER	12.00	PVDF	0.15	0.000	0	0.0	none	NONE	NONE	0.00	0.000e+00	0.000e+00	0.000e+00	0.00
	THER	1.02	PVDFc	0.15	0.000	0	0.0	none	NONE	NONE	0.00	0.000e+00	0.000e+00	0.000e+00	0.00
	ZETA	12.00	carbon_steel	0.25	88.868	1	0.0	none	MYZETAq	FiZ	0.00	0.000e+00	0.000e+00	0.000e+00	0.00
	SPIR	5.99	carbon_steel	0.15	88.868	1	0.0	none	MYSPIRAq	FiZ	0.00	0.000e+00	0.000e+00	0.000e+00	0.00
	THER	1.52	PA11	0.15	0.000	0	0.0	none	NONE	NONE	0.00	0.000e+00	0.000e+00	0.000e+00	0.00
	TENS	5.99	carbon_steel	0.15	-44.000	54	0.0	none	TENSILEq	FiT	0.00	0.000e+00	0.000e+00	0.000e+00	0.00
	THER	0.41	PA11	0.15	0.000	0	0.0	none	NONE	NONE	0.00	0.000e+00	0.000e+00	0.000e+00	0.00
	THER	1.52	PA11	0.15	0.000	0	0.0	none	NONE	NONE	0.00	0.000e+00	0.000e+00	0.000e+00	0.00
	TENS	5.99	carbon_steel	0.15	44.000	57	0.0	none	TENSILEq	FiT	0.00	0.000e+00	0.000e+00	0.000e+00	0.00
	THER	0.41	PA11	0.15	0.000	0	0.0	none	NONE	NONE	0.00	0.000e+00	0.000e+00	0.000e+00	0.00
	THER	1.52	PA11	0.15	0.000	0	0.0	none	NONE	NONE	0.00	0.000e+00	0.000e+00	0.000e+00	0.00
	TENS	5.99	carbon_steel	0.15	-42.000	61	0.0	none	TENSILEq	FiT	0.00	0.000e+00	0.000e+00	0.000e+00	0.00
	THER	0.41	PA11	0.15	0.000	0	0.0	none	NONE	NONE	0.00	0.000e+00	0.000e+00	0.000e+00	0.00
	THER	1.52	PA11	0.15	0.000	0	0.0	none	NONE	NONE	0.00	0.000e+00	0.000e+00	0.000e+00	0.00
	TENS	5.99	carbon_steel	0.15	42.000	64	0.0	none	TENSILEq	FiT	0.00	0.000e+00	0.000e+00	0.000e+00	0.00
	THER	0.41	PA11	0.15	0.000	0	0.0	none	NONE	NONE	0.00	0.000e+00	0.000e+00	0.000e+00	0.00
	THER	0.41	PA11	0.15	0.000	0	0.0	none	NONE	NONE	0.00	0.000e+00	0.000e+00	0.000e+00	0.00
	THER	12.00	PA11	0.15	0.000	0	0.0	none	NONE	NONE	0.00	0.000e+00	0.000e+00	0.000e+00	0.00

#CROSS-SECTION BOUNDARY DATA

#	NAME	type	X0	Y0	CCURV	P1	P2	P3	P4	NINTER	ICODE	
CROSSGEOM	CARC-CARCOSSq				0	0	5.05	180.00	0.0	1.4	5	2
		S			3.50	90.00	0.0	1.4	5	0		
		S			15.45	0.00	0.0	1.4	5	0		
		S			7.00	270.00	0.0	1.4	5	0		
		S			15.45	0.00	0.0	1.4	5	0		
		S			3.50	90.00	0.0	1.4	5	0		
		S			5.05	180.00	0.0	1.4	5	2		
CROSSGEOM	ZETA-MYZETAq				0	0	90.0000	187.5000	1.5000	0.0000	10	0
		S			4.4172	97.5000	0.0000	0.0000	10	0		
		CI			187.5000	330.0000	1.5000	0.0000	10	2		
		S			1.9386	240.0000	0.0000	0.0000	10	0		
		CO			150.0000	90.0000	1.5000	0.0000	10	0		
		S			1.6524	180.0000	0.0000	0.0000	10	3		
		CO			90.0000	10.0000	2.4000	0.0000	10	0		
		S			3.8922	100.0000	0.0000	0.0000	10	0		
		CI			190.0000	270.0000	2.4000	0.0000	10	0		
		S			12.6004	180.0000	0.0000	0.0000	30	1		
		CI			270.0000	367.5000	1.5000	0.0000	10	0		
		S			4.4172	277.5000	0.0000	0.0000	10	0		
		CI			7.5000	150.0000	1.5000	0.0000	10	2		
		S			1.9386	60.0000	0.0000	0.0000	10	0		
		CO			330.0000	270.0000	1.5000	0.0000	10	0		
		S			1.6524	0.0000	0.0000	0.0000	10	3		
		CO			270.0000	190.0000	2.4000	0.0000	10	0		


```

                S      3.8922  280.0000  0.0000  0.0000  10  0
                CI     10.0000   90.0000  2.4000  0.0000  10  0
                S      12.6004   0.0000  0.0000  0.0000  30  1

CROSSGEOM TENS-TENSILEq  BFLEX  0  0  S 12.0    0.0    0.0  0.0  10  0
                        S 5.99   90.0    0.0  0.0  10  0
                        S 12.0   180.0    0.0  0.0  10  1
                        S 5.99   270.0    0.0  0.0  10  0
CROSSGEOM SPIR-MYSPIRAq  BFLEX  0  0  S 5.99    90.0    0  0  10  0
                        S 16.0   180.0    0  0  10  2
                        S 5.99   270.0    0  0  10  0
                        S 16.0    0.0    0  0  10  1

#-----#
# BENDING STIFFENER
#
# name type local global id od no_th rks imno_i imno_o mat_bend
CROSSECTION MYBENDSTIFFENER NLBENDSTIFF 1 2001 407 800 10 0.1 mat_bend mat_bend
#-----#
# Boundary condition data
# Loc node dir
BONCON GLOBAL 3060 1
BONCON GLOBAL 3060 2
BONCON GLOBAL 3060 3
BONCON GLOBAL 3060 4
BONCON GLOBAL 3060 6

BONCON GLOBAL 4040 2
BONCON GLOBAL 4040 3
BONCON GLOBAL 4040 4
BONCON GLOBAL 4040 6
BONCON GLOBAL 1002 2 REPEAT 298 1
BONCON GLOBAL 2002 2 REPEAT 55 1

CONSTR CONEQ GLOBAL 1300 1 0.0 4001 1 1
CONSTR CONEQ GLOBAL 1300 2 0.0 4001 2 1
CONSTR CONEQ GLOBAL 1300 3 0.0 4001 3 1
CONSTR CONEQ GLOBAL 1300 4 0.0 4001 4 1
CONSTR CONEQ GLOBAL 1300 5 0.0 4001 5 1
CONSTR CONEQ GLOBAL 1300 6 0.0 4001 6 1
#Here we use the CONSTR-Constraints to relate core with virtual pipe
CONSTR CONEQ GLOBAL 1001 1 0.0 3001 1 1
CONSTR CONEQ GLOBAL 1001 2 0.0 3001 2 1
CONSTR CONEQ GLOBAL 1001 3 0.0 3001 3 1
CONSTR CONEQ GLOBAL 1001 4 0.0 3001 4 1
CONSTR CONEQ GLOBAL 1001 5 0.0 3001 5 1
CONSTR CONEQ GLOBAL 1001 6 0.0 3001 6 1
#here we use the CONSTR-Constraints to relate bending stiffener with virtual
CONSTR CONEQ GLOBAL 2001 1 0.0 3037 1 1
CONSTR CONEQ GLOBAL 2001 2 0.0 3037 2 1
CONSTR CONEQ GLOBAL 2001 3 0.0 3037 3 1

```

```

CONSTR CONEQ GLOBAL 2001 4 0.0 3037 4 1
CONSTR CONEQ GLOBAL 2001 5 0.0 3037 5 1
CONSTR CONEQ GLOBAL 2001 6 0.0 3037 6 1
#-----
# Constraint input
CONSTR PDISP GLOBAL 3060 5 -0.1309 100
#-----
# Cload input
# hist dir no1 r1 no2 r2 n m
CLOAD 200 1 4040 725000
#-----
#external pressure and gravity loading
# PRESHIST GRAVHIST
PELOAD 400 600
#-----
#internal pressure load
# HIST ELNR1 P1 ELNR2 P2
PILOAD 500 10001 47.5 10299 47.5
#PILOAD 500 80001 0 80059 0
#-----
# History data
#100, at 2 sec, we still have load factor=0.0
THIST 100 0 0.0
1 0.0
2 0.0
3 0.001
100 1.0
300 -1.0
400 0.0
#200, at 1.0 sec, load factor has reached to 1.0
THIST 200 0 0.0
1 1.0
20 1.0
#at 2 sec, it is still 0.0, but then begin to rise.
THIST 300 0 0.0
1.0 1.0
20 1.0
THIST 400 0 0.0
2 0.0
5 0.0
20 0.0
THIST 500 0 0.0
1 1.0
20 1.0
THIST 600 0 0.0
1 0.0
3 0.0
6 1.0
400 1.0
#-----
MATERIAL mat_bend hyperelastic 0.3 0 11.7e-6 2.0 50 -0.19 -14.7

```

-0.09 -9.7
 -0.08 -9.2
 -0.07 -8.6
 -0.06 -8.0
 -0.05 -7.2
 -0.04 -6.4
 -0.03 -5.2
 -0.02 -4.0
 -0.01 -2.0
 0.01 2.0
 0.02 4.0
 0.03 5.2
 0.04 6.4
 0.05 7.2
 0.06 8.0
 0.07 8.6
 0.08 9.2
 0.09 9.7
 0.19 14.7

```

#-----
#          name          type  poiss  density  talfa tecond  heatc  EM      GM      trans-EM
MATERIAL  PVDF          elastic  0.45  1.76998e-6  1  1  1  1516.9  523.07  1516.9
MATERIAL  PVDFc          elastic  0.45  1.01e-6  1  1  1  1516.9  523.07  1515.9

MATERIAL  PA11          elastic  0.45  1.03809e-6  1  1  1  55.2  19.03  55.2

MATERIAL  steel          elastic  0.3  7.82874e-6  1  1  1  2.1e5  80769  2.1e5

MATERIAL  carbon_steel    elastic  0.3  7.82874e-6  1  1  1  2.1e5  80769  2.1e5
#          material name  linear  Poiss  Tlefa  tecond  Haetc Beta  EA  EIY  EIZ  GIT  EM  GM  DENSITY  ETRANS
MATERIAL  myrigidpipe    linear  0.3  0.1  0.1  1  0  2.23e11  1.84e15  1.84e15  1e15  2.1e5  8e4  1  2.1e5
#-----
#materials for the contact element
#          name          type  rmyx  rmyz  xmat  ymat  zmat
MATERIAL  bscontmatl  isocontact  0.20  bellx  bellz
#          name          type  alfa  eps  sig
MATERIAL  bellx          epcurve  1  0  0
          1.0  1
          1000  20
MATERIAL  belly          epcurve  1  0  0
          1  1
          1000  900
MATERIAL  bellz          hycurve  -1000 -1e5
          -0.01 -0.5
          0  0
          1000 1e5
  
```

Reference

- [1.] Stig Berge, Svein Sævik, Nina Langhelle, Tore Holmås, Oddvar I. Eide (2001): *Recent Developments in qualification and design of Flexible Risers*, OMAE 2001-3340
- [2.] Stig Berge, Terje Glomsaker (2004): *Robuster Material Selection (RMS) in the – Offshore Industry Flexible risers*, MARINTEK REPORT
- [3.] Svein Sævik, *BFLEX2010- Theory Manual*, MARINTEK REPORT
- [4.] Berge, S., Engseth, A., Fylling, I., Larsen, C.M, Leira, B.J., Nygaasd, I. and Olufsen A. (1992): *Handbook on Design and Operation of Flexible Pipes*, SINTEF REPORT
- [5.] Moan, Torgeir (2003), *Finite element modeling and analysis of marine structures*, Department of Marine Technology, Norwegian University of Science and Technology., Trondheim 2003
- [6.] Yong Bai, Qiang Bai (2005), *Subsea pipelines and Risers*, Elsevier
- [7.] Svein Sævik, *BFLEX 2010 Version 3.0.5 User Manual*, MARINTEK
- [8.] Svein Sævik, *BFLEX 2010 Version 3.0.5 Test Manual*, MARINTEK